Studies on Bio-geochemistry, Bio-optical Properties and Satellite Validation of Coastal Waters of South Eastern Arabian Sea

Thesis submitted to

Cochin University of Science and Technology

in partial fulfilment of the requirements

for the degree of

Doctor of Philosophy

In Marine science

Under the Faculty of Marine Sciences

By

Shaju S. S.

Reg.No. 3586

CENTRAL INSTITUTE OF FISHERIES TECHNOLOGY

CIFT JUNCTION, MATSYAPURI P.O.

COCHIN 682 029

March 2015

Studies on Bio-Geochemistry, Bio-Optical Properties and Satellite Validation of Coastal Waters of South Eastern Arabian Sea

Ph.D. thesis under faculty of marine sciences

Author

Shaju S.S.
Research student
Fishing technology Division
Central Institute of Fisheries Technology (CIFT)
Cochin 682 029
shaju.peringammala@gmail.com

Supervising Guide

Dr. B. Meenakumari
Principal Scientist & Deputy Director general (Fisheries),
Indian Council of Agricultural Research,
Krishi anusandan bhavan-II,
PUSA,
NewDelhi 110 012
meenakumarib@gmail.com

Co-guide

Dr. Muhamed Ashraf P.
Senior scientist
Fishing technology Division
Central institute of Fisheries technology (CIFT)
Cochin 682 029
ashrafp2008@gmail.com

March 2015

डा. (श्रीमती) बि. मीनाकुमारी
उप महानिदेशक (मात्स्यिकी)
Dr. (Ms) B. Meenakumari
DEPUTY DIRECTOR GENERAL (Fisheries)

भारतीय कृषि अनुसंधान परिषद
कृषि अनुसंधान भवन-II, पूसा, नई दिल्ली 110 012
INDIAN COUNCIL OF AGRICULTURAL RESEARCH
KRISHI ANUSANDHAN BHAWAN-II, PUSA, NEW DELHI 110 012

Certificate

This is to certify that this thesis titled **'Studies on Bio-geochemistry, Bio-optical Properties and Satellite Validation of Coastal Waters of South Eastern Arabian Sea'** is an authentic record of research work carried out by Mr. Shaju, S. S., M.Sc., under my guidance and supervision in Fishing Technology Division of Central Institute of Fisheries Technology, Cochin, in partial fulfillment of the requirements for the degree of Doctor of Philosophy and that no part thereof has previously formed the basis for award of any degree, diploma, associateship, fellowship or any other similar titles of this or any other University or Institution

Cochin-29
March, 2015

Dr. B. Meenakumari
Supervising Guide

Telephone 2666845, 2666846, 2666847, 2666848, 2668145
2666763, 2666764, 2666765, 2666766
2668576, 2668577, 2668578, 2668579, 2668580

www.cift.res.in
Fax : 0091-484-2668212
E-mail : enk_ciftaris@sancharnet.in
cift@ciftmail.org

केन्द्रीय मात्स्यकी प्रौद्योगिकी संस्थान
CENTRAL INSTITUTE OF FISHERIES TECHNOLOGY
भारतीय कृषि अनुसंधान परिषद
(Indian Council of Agricultural Research)
सिफ्ट जंक्शन, मत्स्यपुरी पी. ओ., कोच्चिन - 682 029
CIFT Junction, Matsyapuri P.O., Cochin - 682 029

Dr. Muhamed Ashraf P
Senior Scientist

Certificate

This is to certify that this thesis titled **'Studies on Bio-geochemistry, Bio-optical Properties and Satellite Validation of Coastal Waters of South Eastern Arabian Sea'** is an authentic record of research work carried out by Mr. Shaju, S. S., M.Sc., under my co-guidance and joint supervision in Fishing Technology Division of Central Institute of Fisheries Technology, Cochin, in partial fulfillment of the requirements for the degree of Doctor of Philosophy and that no part thereof has previously formed the basis for award of any degree, diploma, associateship, fellowship or any other similar titles of this or any other University or Institution

Cochin-29
March, 2015

Dr. Muhamed Ashraf P
Co-Guide

डा. (श्रीमती) बि. मीनाकुमारी
उप महानिदेशक (मात्स्यिकी)
Dr. (Ms) B. Meenakumari
DEPUTY DIRECTOR GENERAL (Fisheries)

भारतीय कृषि अनुसंधान परिषद
कृषि अनुसंधान भवन-II, पूसा, नई दिल्ली 110 012
INDIAN COUNCIL OF AGRICULTURAL RESEARCH
KRISHI ANUSANDHAN BHAWAN-II, PUSA, NEW DELHI 110 012

Certificate

This is to certify that all the relevant corrections and modifications suggested by the audience during the pre-synopsis Seminar and recommended by the Doctoral Committee of the candidate has been incorporated in the thesis

Cochin-29
March, 2015

Dr. B. Meenakumari
Supervising Guide

Declaration

*I hereby declare that the thesis entitled "**Studies on Bio-Geochemistry, Bio-Optical Properties and Satellite Validation of Coastal Waters of South Eastern Arabian Sea**" is an authentic record of the research work carried out by me under the guidance and supervision of Dr. B. Meenakumari, Principal Scientist & Deputy Director general (Fisheries), Indian Council of Agricultural Research, Krishi anusandan bhavan-II, PUSA, Newdelhi 110 012, and no part of this has previously formed the basis of the award of any degree, diploma, associateship, fellowship or any other similar title or recognition.*

Kochi-16
March , 2015

Shaju S. S.

Dedicated to my achan, amma, and lechu

Acknowledgement

I would like to take this opportunity to thank all the persons who have made it possible for me to commence and complete this enormous task. I would like to acknowledge and commend them for their efforts, cooperation and collaboration that have worked towards the successes of this study.

I am deeply grateful to my supervising guide, Dr. B. Meenakumari , for patiently taking me through this difficult task of ocean research. I express my deep and sincere gratitude to my guide for conceptualisation and implementation of this research topic, in addition to his peerless guidance and motivation all the way through my doctoral research.

I am thankful to my co-guide Dr. Muhamed Ashraf P., for his valuable suggestions and encouragement during my work.

This work would not have been possible without the substantial financial support provided in the form of Research Fellowship for the project entitled 'In-situ time series measurements of Bio-optical parameters off Kochi', under SATCORE, Indian National centre for Ocean Information Services, Ministry of Earth Sciences, Government of India, Hydrabad. I express my profound sense of gratitude to Dr. Satesh Shenoi, Director, INCOIS, for his benevolent support during this period. I extend my special gratitude towards Dr. T. Srinivasakumar, INCOIS for the satellite data and the facility he provided at INCOIS.

I am grateful to Dr. T.K. Srinivasa Gopal and Dr. C.N. Ravisankar for providing facilities for the research work at CIFT.

I am also grateful to Dr. Leela Edvin, HOD, FT Division, CIFT for her support and encouragement.

I do not have words to acknowledge Dr. Aneesh Lotliker and Dr. Sanjiba Kumar Baliarsingh for their help and encouragement through the course of my research. I specially thank Dr. Aneesh Lotlikar for the patience and encouragement he given to me. I have immense pleasure to express my sincere thanks to Prof. (Dr.) Trevor Platt and Dr.

(Mrs.) Shubha Sathyendranath, Plymouth Marine laboratory, Canada for sharing their knowledge, and valuable lectures during the POGO training programme.

I am grateful to Dr. M.R. Boopendranath, Dr. Sali N Thomas, Dr. Pravin Puthra, Dr. Madhu V.R , Dr. C.N. Joshi and other scientist and technical staffs of the CIFT for their unrestricted support and help.

I thank all the boat staffs of commercial trawlers Bharathdarsan, Mosa and CIFT vessel Sagar Sakthi, for their unrestricted support, courage and food they provided during each cruises. I especially thank Vincent and (Late) Sebastian for the arrangements and help they rendered to me for the cruises.

I am grateful to Minu P. for her help that she rendered throughout my research work. I owe special thanks to my colleagues, Mr. Renju ravi, Vipin P.M, Jose Fernandez, Aneesh Kumar, Paresh Khanolkar, Libin Baby, Archana G, Muhamed Azrudin, Dr. Usha Bhagerathan and Dr. Gipson for their unstinted support all through the course of this research work.

The numerous, laborious and tedious field trips in the past five years became an enjoyable experience and beautiful memory because of Dhiju Das P.H., Sathosh kumar, Ragesh N., Dr. Nishad perur, and Manu K.P.

I would like to thank Dr. Anilkumar vijayan, CMLRE for the help and encouragement for the analysis of absorption data.

I thankfully acknowledge all teaching and nonteaching staff members of Department of Chemical oceanography, School of Marine sciences, CUSAT, for their encouragement and co-operation.

I would like to thank my father, mother, wife, son, sisters, father-in law, mother-in law, Brother-in-laws, and cousins for their support, patience, and for their continued inspiration over the years.

Shaju S. S.

Contents

Chapter 1

INTRODUCTION

1.1. General Introduction

Ocean covers approximately 71% of earth's surface. It contains about 25% of the total planetary vegetation, with much of this restricted to coastal region. We depend on the ocean for food, transportation, minerals and recreation. Physical processes related to the global energy and water cycles, and the associated biological and chemical processes are crucial to the understanding of climate (IPCC Climate Change 1995). In upwelling systems, biogeochemical cycle plays an important role in supporting and determining the level of oceanic primary production (PP). Small changes in biogeochemical conditions results in major changes in biogeochemical pathways and ultimately in the trophic structure of food webs (Fréon et al., 2009). Among these bio-geochemical cycles, the oceanic carbon cycle is of particular importance, and its understanding has been a major goal in oceanographic research (Barber and Hilting, 2002 and Stocker et al.,

2001).The most developed areas in earth are concentrated within the coastal zones. The rapid modernization, change in carbon budget dynamics, ocean primary productivity, biological richness of ocean especially in the coastal area and its effect on the environment is the main concern to scientific community. Although many research activities have been carried out in the world ocean, its understanding of ocean stills stands incomplete due to limited *in-situ* observations. The advantage of satellites is that, it provides consistent, repetitive and wide-area synoptic coverage which in turn radically changed the nature of oceanographic understanding along with in-situ observations (Longhurst et al 1995).

The structure of the physical and chemical environment is commonly expressed in terms of water quality parameters such as temperature, salinity, dissolved oxygen, nutrients, metal concentration, pigments etc. Hydrogeochemical factors can influence the colour, odour, taste, temperature and degree of mineralisation of water derived from surface runoff, underground springs etc. (Clark and Snyder, 1970). Studies on the distributional and biogeochemical characteristics of nutrients in coastal waters can provide satisfactory assessment on the bioavailability of various nutrients. In situ methods employed for water quality assessment can consume much time and there are constraints too. Only a limited number of sampling points can be performed, making it difficult to capture the range and variability of coastal processes and constituents. In addition, the mixing between fresh and oceanic water creates complex physico-chemical and biological processes that are difficult to understand, causing the existing measurement methodologies to have

significant logistical, technical, and economic challenges and constraints. The challeges with the coastal ocean colour remote sensing is the accuracy and reliability of the retrieval algorithms. With this background, coastal optics have been the topic of numerous studies (Devred et al., 2011; Babin et al., 2003) highlighting the necessity of bio-optical measurements at regional scale. Current ocean-colour remote sensing, limited by algorithms and sensor configurations, are mainly focused on the retrieval of Chlorophyll *a* (Letelier and Abbott 1996, O'Reilly et al., 1998). The use of optical properties of water and bio-optical model parameterizations remains challenging for the coastal waters (Siegel et al., 2002). Hence it is very important to understand the optical properties, especially the absorption properties of the substances present.

1.2. Ocean colour

Satellite sensors provide the most effective means for frequent, synoptic, water quality observations over large areas (Miller et al. 2005). Ocean colour imagery is increasingly used as a tool to complete data sets collected by traditional means (Hellweger et al. 2004; Gohin et al. 2008). Colour of the ocean contains latent information on the abundance of the marine microflora- phytoplankton. Ocean-colour remote sensing was conceived primarily as a method for producing synoptic fields of phytoplankton biomass indexed as chlorophyll. The technique exploits the absorption of light by the pigments. Phytoplankton in the water is invisible to the naked eye at close quarters, but has huge collective impact visible from space. The ocean colour means the energy resolved to the spectral radiance. In other words the colour of the ocean is determined by the interactions of light

with water. When light hits the surface of water, the radiation can be absorbed, transmitted, scattered, or reflected in differing intensities. Water components can be determined based on the spectral appearance. A major product of ocean-colour remote sensing is distribution of chlorophyll concentration, the most fundamental property of the ocean ecosystem. Ocean colour contains a wealth of information, with many present and potential applications by providing the interface between the physical forcing field (light) and the biological building blocks (phytoplankton pigments).

Ocean colour data works as the basis for computation of regional and basin scale estimates of primary production. Relationships between reflectance ratios and chlorophyll concentrations depend on phytoplankton species composition. The measurement of phytoplankton abundance across wide scales can be most effectively achieved by satellite remote sensing, where the spectral composition of radiance leaving the ocean surface is measured by satellite-born multispectral sensors. This is used to obtain estimates of near proxy for phytoplankton abundance. It is used as a general tool for extrapolation to large horizontal scale of sparse measurements of ecophysical rates. Typology of seasonality in pelagic ecosystem can be studied using ocean colour data. It can also be used for the study of feedbacks between pelagic microbiota and mixed layer physics. It has wide applications in fisheries sector too, like identification of potential fisheries zone (PFZ) in Indian coastal waters. The List of the current ocean colour remote sensors is given in the table 1.1. Also the list of the historical ocean colour remote sensors is given in the table 1.2. The list of scheduled ocean colour remote sensors is given in the table 1.3.

Table1.1 List of the current ocean colour remote sensors in alphabetical order

Sensor	Agency	Satellite	Launch Date	Swath (Km)	Spatial Resolution (Km)	Bands	Spectral Coverage (NM)	Orbit
COCTS CZI	CNSA (China)	HY-1B (China)	11-Apr-07	2400 500	1100 250	10 4	402 - 12,500 433 - 695	Polar
GOCI	KARI/ KIOST (South Korea)	COMS	26-Jun-10	2500	500	8	400 - 865	Geostationary
HICO	ONR, DOD and NASA	JEM-EF Int. Space Stn.	18 Sept. 2009	50 km Selected coastal scenes	100	124	380 - 1000	51.6°, 15.8 orbits p/d
MERSI	CNSA (China)	FY-3A (China)	27-May-08	2400	250/1000	20	402-2155	Polar
MERSI	CNSA (China)	FY-3B (China)	5-Nov-10	2400	250/1000	20	402-2155	Polar
MERSI	CNSA (China)	FY-3C (China)	23-Sep-13	2400	250/1000	20	402-2155	Polar
MODIS-Aqua	NASA (USA)	Aqua (EOS-PM1)	4-May-02	2330	250/500/1000	36	405-14,385	Polar
MODIS-Terra	NASA (USA)	Terra (EOS-AM1)	18 Dec. 1999	2330	250/500/1000	36	405-14,385	Polar
OCM-2	ISRO (India)	Oceansat-2 (India)	23 Sept. 2009	1420	360/4000	8	400 - 900	Polar
VIIRS	NOAA (USA)	SuomiNPP	28 Oct. 2011	3000	375 / 750	22	402 - 11,800	Polar

Source http://www.ioccg.org/sensors_ioccg.html

Table1.2 List of the Historical ocean colour remote sensors in alphabetical order

Sensor	Agency	Satellite	Operating Dates	Swath (Km)	Spatial Resolution (m)	Bands	Spectral Coverage(nm)	ORBIT
CZCS	NASA (USA)	Nimbus-7 (USA)	24/10/78 - 22/6/86	1556	825	6	433-12500	Polar
CMODIS	CNSA (China)	SZ-3 (China)	25/3/02 - 15/9/02	650-700	400	34	403-12,500	Polar
COCTS CZI	CNSA (China)	HY-1A (China)	15/5/02 - 1/4/04	1400 500	1100 250	10 4	402-12,500 420-890	Polar
GLI	NASDA (Japan)	ADEOS-II (Japan)	14/12/02 - 24/10/03	1600	250/1000	36	375-12,500	Polar
MERIS	ESA (Europe)	ENVISAT (Europe)	1/3/02 - 9/5/12	1150	300/1200	15	412-1050	Polar
MOS	DLR (Germany)	IRS P3 (India)	21/3/96 - 31/5/04	200	500	18	408-1600	Polar
OCI	NEC (Japan)	ROCSAT-1 (Taiwan)	27/01/99 - 16/6/04	690	825	6	433-12,500	Polar
OCM	ISRO (India)	IRS-P4 (India)	26/5/99 - 8/8/10	1420	360/4000	8	402-885	Polar
OCTS	NASDA (Japan)	ADEOS (Japan)	17/8/96 - 29/6/97	1400	700	12	402-12,500	Polar
OSMI	KARI (Korea)	KOMPSAT-1 /Arirang-1(Korea)	20/12/99 - 31/1/08	800	850	6	400-900	Polar
POLDER	CNES (France)	ADEOS (Japan)	17/8/96 - 29/6/97	2400	6 km	9	443-910	Polar
POLDER-2	CNES (France)	ADEOS-II (Japan)	14/12/02 - 24/10/03	2400	6000	9	443-910	Polar
POLDER-3	CNES (France)	Parasol	Dec 2004 - Dec 2013	2100	6000	9	443-1020	Polar
SeaWiFS	NASA (USA)	OrbView-2 (USA)	01/08/97 - 14/02/11	2806	1100	8	402-885	Polar

Source http://www.ioccg.org/sensors_ioccg.html

Table 1.3 List of the Scheduled ocean colour remote sensors in alphabetical order

Sensor	Agency	Satellite	Scheduled Launch	Swath (Km)	Spatial Resolution (M)	# of Bands	Spectral Coverage (NM)	Orbit
OLCI	ESA/ EUMETSAT	Sentinel 3A	Jun-15	1270	300/1200	21	400 - 1020	Polar
COCTS CZI	CNSA (China)	HY-1C/D (China)	2015	2900 1000	1100 250	10 10	402 - 12,500 433 -885	Polar
SGLI	JAXA (Japan)	GCOM-C	2016	1150 - 1400	250/1000	19	375 - 12,500	Polar
HSI	DLR (Germany)	EnMAP	2017	30	30	242	420 - 2450	Polar
VIIRS	NOAA /NASA (USA)	JPSS-1	2017	3000	370 / 740	22	402 - 11,800	Polar
OLCI	ESA/ EUMETSAT	Sentinel-3B	2017	1265	260	21	390 - 1040	Polar
COCTS CZI	CNSA (China)	HY-1E/F (China)	2017	2900 1000	1100 250	10 4	402 - 12,500 433 - 885	Polar
Multi-spectral Optical Camera	INPE / CONAE	SABIA-MAR	2018	200/2200	200/1100	16	380 - 11,800	Polar
GOCI-II	KARI/KIOST (South Korea)	GeoKompsat 2B	2018	1200 x 1500 TBD	250/1000	13	412 - 1240 TBD	Geostationary
OCI	NASA	PACE	2018	*	*	*	*	Polar
OES	NASA	ACE	>2020	TBD	1000	26	350-2135	Polar
Coastal Ocean Color Imaging Spec (Name TBD)	NASA	GEO-CAPE	>2022	TBD	250 - 375	155 TBD	340-2160	Geostationary
VSWIR and TIR Instruments	NASA	HYSPIRI	>2022	145	60	10 nm contiguous bands	380 - 2500	LEO, Sun Sync.

Source http://www.ioccg.org/sensors_ioccg.html

1.2.1. Coastal Zone Color Scanner (CZCS)

The Coastal Zone Color Scanner (CZCS) was the first instrument devoted to the measurement of ocean color and flown on a spacecraftNimbus-7, which was launched on October 24th, 1978. The spacecraft was in a Sun-synchronous orbit, with an inclination of 104.9 degrees, and a nominal altitude of 955 km. It had an equatorial crossing time of noon, in an ascending orbit.

CZCS had six spectral bands, four of which were used primarily for ocean color. These were of a 20 nanometer bandwidth centered at 443, 520, 550, and 670 nm. (http://oceancolor.gsfc.nasa.gov).

1.2.2. Ocean Color and Temperature Scanner (OCTS)

On August 17, 1996, the Japanese Space Agency (NASDA - National Space Development Agency) launched the Advanced Earth Observing Satellite (ADEOS). ADEOS was in a descending, Sun synchronous orbit with a nominal equatorial crossing time of 10:30 AM. Among the instruments carried aboard the ADEOS spacecraft was the Ocean Color and Temperature Scanner (OCTS). OCTS is an optical radiometer with eight calibrated bands in the VIS/NIR. OCTS had a swath width of approximately 1400 km, and a nominal nadir resolution of 700 m. The instrument operated at three tilt states (20 degrees aft, nadir and 20 degrees fore), similar to the SeaWiFS.

1.2.3. Sea-viewing Wide Field-of-view Sensor (SeaWiFS)

The purpose of the Sea-viewing Wide Field-of-view Sensor (SeaWiFS) is to provide quantitative data on global ocean bio-optical properties to the Earth science community. The Sea Star spacecraft, developed by Orbital Sciences Corporation, carried the SeaWiFS instrument and was launched to the low Earth orbit on board an extended Pegasus launch vehicle on August 1, 1997. Instrument bands of SeaWiFS in the visible region is given in the table 1.4.

Table 1.4 Instrument Bands of Sea WiFS in the visible region

Band	Wavelength
1	402-422 nm
2	433- 453 nm
3	480-500 nm
4	500-520nm
5	545-565nm
6	660-680nm
7	745-785nm

Source http://oceancolor.gsfc.nasa.gov/SeaWiFS/SEASTAR/SPACECRAFT.html

The purpose of SeaWiFS was to examine oceanic factors that affect global change and to assess the ocean's role in the global carbon cycle, as well as other biogeochemical cycles, through a comprehensive research programme. The atmospheric correction algorithms for processing SeaWiFS data included a number of improvements over the CZCS algorithms. Data sets from field studies have been collected to validate these improvements.

1.2.4. Moderate Resolution Imaging Spectro-radiometer (MODIS)

MODIS is a key instrument aboard the Terra (EOS AM) and Aqua (EOS PM) satellites. The MODIS-Terra was launched on December 18, 1999, and Aqua on May 4, 2002.Terra's orbit around the Earth is timed so that it passes from north to south across the equator in the morning, while Aqua passes south to north over the equator in the afternoon. It is having a spatial resolution of 1km in ocean colour application. The instrument bands of MODIS in visible region is given in the table 1.5.

Table 1.5 Instrument Bands of MODIS in visible region

Band	Wavelength
1	405 – 420 nm
2	438 - 448 nm
3	483 - 493 nm
4	526 - 536 nm
5	546 - 556 nm
6	662 - 672 nm
7	673 - 683 nm
8	743 - 753 nm

Source http://modis.gsfc.nasa.gov/about/specifications.php

1.2.5. Medium-Spectral Resolution, Imaging Spectrometer (MERIS)

MERIS was a programmable, medium-spectral resolution, imaging spectrometer operating in the solar reflective spectral range in which, fifteen spectral bands can be selected by ground command. MERIS operated in a Spatial Resolution of 1040m x 1200 m in ocean, 260m x 300m in Land & coast with 15 Waveband in VIS-NIR.

1.2.6. Oceansat 2 (OCM 2)

India's Polar Satellite Launch Vehicle, PSLV-C14, in its 16th Mission launched 958 kg Oceansat-2 and six nano-satellites into a 720 km intended Sun Synchronous Polar Orbit (SSPO) on September 23, 2009. This satellite carrier carry three payloads Ocean Color Monitor (OCM), Ku-band Pencil Beam Scatterometer and Radio Occultation Sounder for Atmosphere (ROSA). This satellite would carry three payloads, Ocean Color Monitor (OCM) has eight spectral bands from the visible to near infrared (0.4-0.9 microns). Oceansat-2 is having 7 bands in the visible region. The instrument band of OCM 2 in visible region is given in the table 1.6.

Table 1.6. Instrument Bands of OCM 2 in visible region

Band	Wavelength
1	404-424 nm
2	431-451 nm
3	476-496 nm
4	500-520 nm
5	546-566 nm
6	610-630 nm
7	725-755 nm

Source (http://www.ioccg.org/sensors/OCEANSAT_2.pdf)

Oceansat-2 is having Local Area Coverage (LAC) with 360m resolution and Global Area Coverage (GAC) with 4 km resolution.

1.3. Optical Active Substance (OAS)

The OAS in the natural environment, can be classified into two, dissolved and particulate. The matter that is having a size less than 0.22 µm is termed as dissolved and above this size is termed as particulate matter (Blough and Del Vecehio, 2002). The optically active constituent of dissolved fraction mainly consists of fulvic and humic acid and is referred as Coloured Dissolved Organic Matter (CDOM) (Coble, 1996). The composition of suspended matter is very complex and can be divided into organic and inorganic. The organic fraction includes phytoplankton containing chlorophyll a, as major fraction with its accessory pigments. The inorganic component includes sediment and non-living particles. Apart from these, water molecule also produces a considerable amount of absorption and scattering. Pure water absorbs wavelengths in the interval 400–500 nm at low rates, but absorption rate increases strongly with increasing wavelength in the interval 500–700 nm (Pope and Fry, 1997). CDOM in seawater has a decreasing rate of absorption with increasing wavelength, while phytoplankton absorbs most strongly in the bands 400–500 and 650–700 nm. Absorption coefficients for pure water, a_w, for phytoplankton corresponding to chlorophyll a concentration of 1 mg m^{-3}, a_{OP}, and for CDOM corresponding to $a_{cdom}(350)$ is given in the figure 1.1.

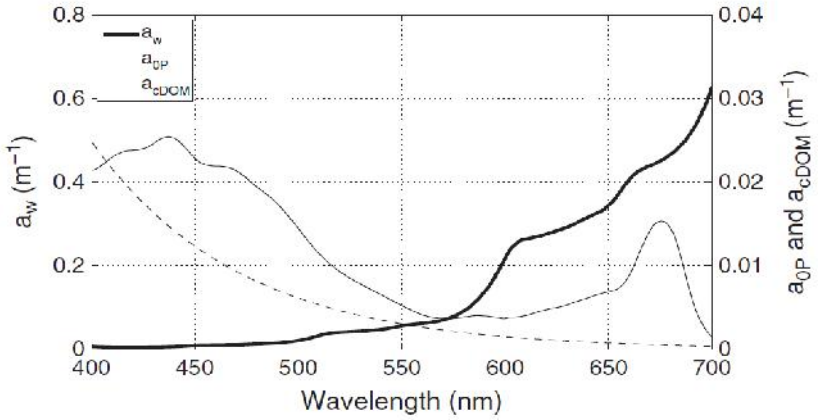

Fig1.1. Absorption coefficients for pure water, a_w, for phytoplankton corresponding to chlorophyll a concentration of 1 mg m^{-3}, a_{0P}, and for CDOM corresponding to $a_{cdom}(350)=0.05$ m^{-1}. (Source Mueller et al 2003)

1.4. Optical classification of sea water

Classification of ocean waters into Case 1 and 2 is based on the relative contributions of optically-relevant constituents to the bulk optical properties of the sea. The case classification based on the relative contribution of optically active substances (OAS) such as phytoplankton, Coloured Dissolved Organic Matter (CDOM) commonly known as yellow substance and suspended sediment is given in the figure 1.2.

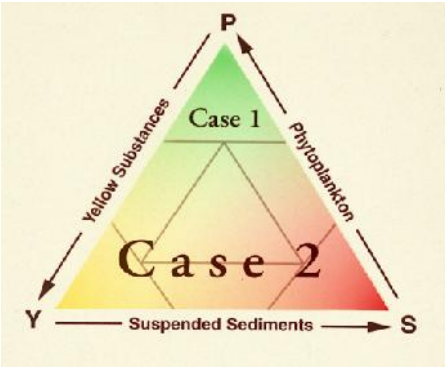

Figure 1.2. Case classification of Optically Active Substance (OAS) based on the relative contribution of the components (IOCCG2000).

1.5. Radiative Transfer Theory (RT)

The transfer of radiation through the atmosphere to the sea, inside it, back to surface, through atmosphere and finally to the sensor of the satellite is termed as radiative transfer (RT). In other words, it is the propagation of radiation through an absorbing and scattering medium. When solar radiation passes through the atmosphere, it undergoes attenuation (scattering and absorption). Scattering is by means of air molecules (Rayleigh scattering), and aerosols (Mie scattering), while absorption take place by gaseous molecules (Gordon 1978). Radiation reaching the sea surface is partly reflected/refracted at the intermediate layer of the atmosphere and at the sea surface (sun glint), while certain amount of radiation is transmitted through the water column. The transmitted radiation is either absorbed and /or scattered by the OAS present in it. The amount of energy emerging from the sea depends on the optical properties of OAS. By assuming a single scattering albedo, RT between sun, atmosphere and water medium was formulated by Gordon (1978) as

$$L_T(\lambda)=tL_w(\lambda) + TL_g(\lambda) + L_p(\lambda)$$

Where L_T is the total radiance received by the sensor, L_w is the radiance leaving the water coloumn (water leaving radiance), L_g is the radiance reflected at the sea surface (sunglint radiance), L_p is the total atmospheric path radiance, which is the sum of aerosol and rayleigh radiance ($L_a + L_r$), T is the direct transmittance of atmosphere due to non-uniform angular distribution and is associated with sun glitter. t is the difference transmittance associated with water leaving radiance. T_d is the diffuse transmission coefficient at wavelength (λ).

1.6. Ocean colour component Retrieval algorithms

The aim of ocean colour remote sensing is to remotely estimate the concentrations of seawater constituents, such as dissolved organic matter,

suspended sediments, and particularly, chlorophyll a (chl-a) in the surface layer (Clarke et al. 1970, Clarke and snyder 1970), based on the water-leaving radiance. The overall accuracy of retrieved water leaving radiance and constituents depends on the performance of the atmospheric correction and in-water algorithms. The water colour interpretation can be approached with different methods (Gordon and Morel 1983).

Table 1.7. Chl-aalgorithms for different sensors with maximum ratio value

Sensor	Equation	Maximum ratio value (*R*)
MODIS/OC3M	Chl a $=10^{(0.2830-2.753R\ ^\wedge 1.457R^\wedge 2-\ 0.659\ R^\wedge 3\ 1.403R^\wedge 4)}$	Rrs(443;490)/Rrs(550)
MERIS OC4E	Chl a $=10^{\ (0.368-\ 2.814R+\ 1.456R^\wedge 2-\ 0.768R^\wedge 3-1.292R^\wedge 4)}$	Rrs(443;490;510)/Rrs(560)
SeaWiFS/OC4v4	Chl a $=10^{\ (0.366-3.067R+\ 1.930R^\wedge 2+\ 0.649R^\wedge 3-1.532R^\wedge 4)}$	Rrs(443;490;510)/Rrs(555)

1.6.1. Empirical algorithms

Empirical algorithms are the establishment of statistical relationships between the water-leaving radiance (Lw) and the concentration of the water constituents (e.g. Chl-a, Total suspended matter and Coloured Dissolved Organic Matter). Empirical algorithms establish a relationship between optical properties and the concentration of constituents present in the water. These relationships are made based upon in situ measurements of the OAS and simultaneous measurement of the radiance or reflectance at different wavelengths using hyperspectral or multispectral radiometers. For example, the most common relationship to estimate chl-a, makes use of the band ratio, where ratio of radiance or reflectance values between different wavelengths is regressed against chl-a concentration. The presence of phytoplankton decreases the reflectance in the blue region of the visible spectrum, while it does not significantly affect the reflectance in the green region. Hence, ratios of two reflectance values at different wave bands are used as a way to deal with the variability and the uncertainty affecting the absolute reflectance and water-leaving radiance values (O'Reilly et al., 1998,

IOOCG 2000). In Case 2 waters, for algorithms based on one ratio, estimation of chl-a is with relatively low accuracy, so multiple band ratios are used to include a wider range of variability (Hoge and Swift 1986).

1.6.2. Analytical Algorithms

Analytical algorithms involve the determination of concentration of optical substances, by solving the radiative transfer equation (Gordon 1978). This is a complex and difficult method to implement. When the analytical approach requires approximations or calibrations with empirical coefficients (Carder et al. 1999), the epithet "semi" is used.

1.6.3. Semi analytical

Semi analytical or semi empirical method lies in between the first two methods. In general, this approach uses models to provide values of reflectance ratios based on inherent optical properties (Gordon and Morel 1983; Gordon et al. 1988; Morel and Maritorena 2001). The radiative transfer equation is introduced in the empirical relationships, providing the spectral shape of IOPs of phytoplankton, particulate and dissolved water constituents. They have the advantage of considering the physical and biological causes of the colour variation of the ocean. This approach has been used by numerous models to estimate water constituents in case 1 and case 2 waters (Gordon et al. 1988; Carder et al. 1999; Morel and Maritorena 2001; Gitelson et al. 2008).The list of different algorithms and its details on radiometric quantity, number of bands and band ratio details is given in the table 1.8.

Table 1.8. List of different algorithms and its details on radiometric quantity, number of bands and band ratio details

Algorithm Name	Radiometric quantity [nLw/Rrs]	No. of Bands	Band-Ratio
Empirical ocean color algorithms:			
OC1a	Rrs	2	[490 / 555]
OC1b	Rrs	2	[490 / 555]
OC1c	Rrs	2	[490 / 555]
OC1d	Rrs	2	[490 / 555]
OC2a	Rrs	2	[412 / 555]
OC2b	Rrs	2	[443 / 555]
OC2d	Rrs	2	[510 / 555]
OC2	Rrs	2	[443 / 555]
OC2v2	Rrs	2	[490 / 555]
OC2v4	Rrs	2	[490 / 555]
OC3d	Rrs	3	[443; 490 / 555]
OC4	Rrs	4	[443; 490; 510 / 555]
OC4v4	**Rrs**	**4**	**[443; 490; 510 / 555]**
AikC	nLw	2	[490 / 555]
AikP	nLw	2	[490 / 555]
OCTSC	nLw	3	[490; 520; 565 / 555]
Pldr	Rrs	2	[443; 565 / 555]
CalCOFI-1	Rrs	2	[490 / 555]
CalCOFI-2	Rrs	2	[490 / 555]
CalCOFI-3	Rrs	3	[490; 510 / 555]
CalCOFI-4	Rrs	4	[412; 443; 510 / 555]
Morel-1	Rrs	2	[443 / 555]
Morel-2	Rrs	2	[490 / 555]
Morel-3	Rrs	2	[443 / 555]
Morel-4	Rrs	2	[490 / 555]
Semi-analytical ocean color algorithms:			
Semi-Clark	NA	NA	NA
Semi-Carder	NA	NA	NA
Semi-gsm01	NA	NA	NA

1.6.4. Neural network

In order to cope with the complexity of case 2 waters, the use of neural network modeling has recently been introduced. One technique that may be used to solve the inverse problem in hydro-optical remote sensing is the use of a neural network (NN) approach, which involves the inversion of the

relationship between reflectance in different spectral bands, and the concentrations of multiple types of water constituents. For this purpose, the neural network is used as a multiple non-linear regression technique, and is thus related to the simpler case of a linear regression.

1.7. Aim and Objectives of the study

In situ methods used for water quality assessment have both physical and time constraints. Just a limited number of sampling points can be performed due to this, making it difficult to capture the range and variability of coastal processes and constituents. In addition, the mixing between fresh and oceanic water creates complex physical, chemical and biological environment that are difficult to understand, causing the existing measurement methodologies to have significant logistical, technical, and economic challenges and constraints.

Remote sensing of ocean colour makes it possible to acquire information on the distribution of chlorophyll and other constituents over large areas of the oceans in short periods. There are many potential applications of ocean colour data. Satellite-derived products are a key data source to study the distribution pattern of organisms and nutrients (Guillaud et al. 2008) and fishery research (Pillai and Nair 2010; Solanki et al. 2001. Also, the study of spatial and temporal variability of phytoplankton blooms, red tide identification or harmful algal blooms monitoring (Sarangi et al. 2001; Sarangi et al. 2004; Sarangi et al. 2005; Bhagirathan et al., 2014), river plume or upwelling assessments (Doxaran et al. 2002; Sravanthi et al. 2013), global productivity analyses (Platt et al. 1988; Sathyendranath et al. 1995; IOCCG2006) and oil spill detection (Maianti et al. 2014). For remote sensing to be accurate in the complex coastal waters, it has to be validated with the in

situ measured values. In this thesis an attempt to study, measure and validate the complex waters with the help of satellite data has been done.

Monitoring of coastal ecosystem health of Arabian Sea in a synoptic way requires an intense, extensive and continuous monitoring of the water quality indicators. Phytoplankton determined from chl-a concentration, is considered as an indicator of the state of the coastal ecosystems. Currently, satellite sensors provide the most effective means for frequent, synoptic, water-quality observations over large areas and represent a potential tool to effectively assess chl-a concentration over coastal and oceanic waters; however, algorithms designed to estimate chl-a at global scales have been shown to be less accurate in Case 2 waters, due to the presence of water constituents other than phytoplankton which do not co-vary with the phytoplankton. The constituents of Arabian Sea coastal waters are region-specific because of the inherent variability of these optically-active substances affected by factors such as riverine input (e.g. suspended matter type and grain size, CDOM) and phytoplankton composition associated with seasonal changes.

The following hypothesis is set as a basis to achieve this. The use of regionally parameterized algorithms will improve the estimation of chl-a in coastal areas, and lead to a more comprehensive assessment of the water quality. It will lead to an improved characterisation of the variability of chl-a within the Arabian coastal waters, especially the southeastern part.

The main objectives of this thesis are

- To study the spatial and temporal variability of hydrogeochemical factors and its effect on chlorophyll *a* concentration in the study area between 2008 and 2012.

- To study the inherent optical properties of the coastal waters at different regions of South Eastern Arabian Sea (SEAS).
- To study the apparent optical properties of the coastal waters at different regions of SEAS.
- Validation of satellite derived chlorophyll *a* and remote sensing reflectance applied with different atmospheric correction scheme with *in situ* data of coastal waters of SEAS.

References

Babin, M., Stramski, D., Ferrari, G.M., Claustre, H., Bricaud, A., Obolensky, G., and Hoepffner, N. 2003. Variations in the light absorption coefficients of phytoplankton, non algal particles, and dissolved organic matter in coastal waters around Europe. Journal of Geophysical Research. 108(C7): 3211.

Barber, R.T., and A.K. Hilting. 2002. History of the study of plankton productivity. P.J.LeB. Williams, D.N. Thomas, C. Reynolds (Eds.), Phytoplankton productivity: Carbon assimilation in marine and freshwater ecosystems, Blackwell Science, Oxford, pp. 16–43.

Bhagirathan, U., S.S. Shaju, N. Ragesh, B. Meenakumari, and P. Muhamed Ashraf. 2014. Observation bio-optical properties of a phytoplankton bloom in coastal waters off Cochin during the onset of southwest monsoon. Indian journal of Geo-marine Sciences. 43(2): 289-296.

Blough, N. L., and R. Del Vecchio. 2002. Chromophoric DOM in the coastal environment, p. 509–546. In D. Hansell and C. A. Carlson [eds.], Biogeochemistry of marine dissolved organic matter. Academic.

Carder, K. L., F. R. Chen, Z. P. Lee, S. K. Hawes, and D. Kamykowski. 1999. Semi-analytic Moderate-Resolution Imaging Spectrometer algorithms for chlorophyll a and absorption with bio-optical domains based on nitrate-depletion temperatures. Journal of Geophysical Research. 104: 5403-5421.

Clark, S. M., and Snyder, Jr. 1970. Limnological study of Lower Columbia river, 1967-68.V.S. Fish and Wildlife Service, Special Scientific Report Fisheries No.610 : 14.

Clarke, G.L., G. C. Ewing, and C. J. Lorenzen. 1970. Spectra of backscattered light from the sea obtained from aircraft as a measure of chlorophyll concentration. Science 167: 11-19.

Coble, P.G., 1996. Characterization of marine and terrestrial DOM in seawater using excitation-emission matrix spectroscopy. Marine Chemistry 52: 325-346.

Devred, E., Sathyendranath, S., Stuart, V., and Platt, T. 2011. A three component classification of phytoplankton absorption spectra: Application to ocean-color data. Remote Sensing of Environment 115: 2255–2266.

Doxaran, D., J.M. Froidefond, S. Lavender, and P. Castaing. 2002. Spectral signature of highly turbid waters Application with SPOT data to quantify suspended particulate matter concentrations. Remote Sensing of Environment 81: 149 - 161.

Fréon, P., M. Barange, and J. Aristegui. 2009. Eastern boundary upwelling ecosystems: integrative and comparative approaches. Progress in Oceanography. 83: 1–14.

Gitelson, A. A., G. Dall'Olmo, W. Moses, D. Rundquist, T. Barrow, T. Fisher, D. Gurlin, and J. Holz. 2008. A simple semi-analytical model for remote estimation of chlorophyll-a in turbid waters: Validation. Remote Sensing of Environment. 112: 3582-3593.

Gohin, F., B. Saulquin, H. Oger-Jeanneret, L. Lozac'h, L. Lampert, A. Lefebvre, P. Riou, and F. Bruchon. 2008. Towards a better assessment of the ecological status of coastal waters using satellite-derived chlorophyll-a concentrations. Remote Sensing of Environment. 112: 3329-3340.

Gordon, H. R. 1978. Removal of atmospheric effects from satellite imagery of the oceans. Applied Optics. 17(10): 1631-1636.

Gordon, H. R., and A. Y. Morel. 1983. Remote assessment of ocean color for interpretation of satellite visible imagery: A review. Lecture Notes on Coastal and Estuarine Study. 4: 1-114.

Gordon, H. R., O. B. Brown, R. H. Evans, J. W. Brown, R. C. Smith, K. S. Baker, and D. K. Clark. 1988. A semi-analytic radiance model of ocean colour. Journal of Geophysical Research. 93: 10909-10924.

Guillaud, J. F., A. Aminot, D. Delmas, F. Gohin, M. Lunven, C. Labry, and A. Herbland. 2008. Seasonal variation of riverine nutrient inputs in the northern Bay of Biscay (France), and patterns of marine phytoplankton response. Journal of Marine Systems. 72: 309-319.

Hellweger, F.L., P. Schlossera, U. Lalla, J.K. Weisselc. 2004. Use of satellite imagery for water quality studies in New York Harbor. Estuarine, Coastal and Shelf Science. 61: 437–448

Hoge, F. E., and R. N. Swift. 1986. Chlorophyll pigment concentration using spectral curvature algorithms: an evaluation of present and proposed satellite ocean color sensor bands. Applied Optics. 25: 3677.

IOCCG. 2000. Remote Sensing of Ocean Colour in Coastal, and Other Optically-Complex, Waters. In S. Sathyendranath [ed.], Reports of the International Ocean Colour Coordinating Group 3.

IOCCG. 2006. Remote Sensing of Inherent Optical Properties: Fundamentals, Tests of Algorithms, and Applications, p. 126. In R. Arnone, M. Babin, A.H. Barnard, E. Boss, J.P. Cannizzaro, K.L. Carder, F.R.Chen, E. Devred, R. Doerffer, K. Du, F. Hoge, O.V. Kopelevich, T. Platt, A.

Poteau, C. Roesler, and S. Sathyendranath [eds.], Reports of the International Ocean Colour Coordinating Group 5.

IPCCClimate Change 1995: The Science of Climate Change J.T. Houghton, L.G.M. Filho, B.A. Callandar, N. Harris, A. Kattenberg, K Maskell (Eds.), Contribution of Working Group 1 to the Second Assessment Report of the Intergovernmental Panel on Climate Change, Cambridge University Press, New York (1996), p. 572.

Letelier, R. M., Abbott, M. R., 1996. An analysis of chlorophyll fluorescence algorithms for the moderate resolution imaging spectrometer (MODIS). Remote Sensing of Environment. 58: 215-223.

Longhurst, A.R., S. Sathyendranath, T. Platt, C. Caverhill. 1995. An estimate of global primary production in the ocean from satellite radiometer data. Journal of Plankton Research. 17 (6): 1245–1271.

Maianti, P., Rusmini, M., Tortini, R., Via, G. D., Frassy, F., Marchesi, A., Nodari, F. R., Gianinetto, M. 2014. Monitoring large oil slick dynamics with moderate resolution multispectral satellite data. Natural Hazards. DOI 10.1007/s11069-014-1084-9.

Miller, K. G., M. A. Kominz, J. V. Browning, J. D. Wright, G. S. Mountain, M. E. Katz, P. J. Sugarman, B. S. Cramer, N. Christie-Blick, S. F. Pekar. 2005. The Phanerozoic Record of Global Sea-Level Change. Science. 310: 1293. DOI 10.1126/science.1116412.

Mueller, J. L., G. S. Fargion and C. R. McClain (Eds.). 2003. Ocean Optics Protocols For Satellite Ocean Color Sensor Validation, Revision 4, Volume IV: Inherent Optical Properties: Instruments, Characterizations, Field Measurements and Data Analysis Protocols. NASA/TM-2003-211621/Rev4-Vol.IV.

Morel, A., and S. Maritorena. 2001. Bio-optical properties of oceanic waters: A reappraisal. Journal of Geophysical Research. 106: 7163-7180.

O'Reilly, J.E., Maritorena, S., Mitchell, B. G., Siegel, D.A., Carder, K.L., Garver, S.A., Kahru, M., McClain, C. 1998. Ocean color chlorophyll algorithms for SeaWiFS. Journal of Geophysical Research. 103.

Pillai, V.N., Nair, P. G. 2010.Potential fishing zone (PFZ) advisories-Are they beneficial to the coastal fisher folk? A case study along Kerala coast, South India. Biological Forum-An International Journal. 2(2): 46-55.

Platt, T., S. Sathyendranath, C. M. Caverhill, and M. R. Lewis. 1988. Ocean primary production and available light: further algorithms for remote sensing. Deep Sea Research Part A. Oceanographic Research Papers 35: 855-879.

Pope, R.M., Fry, E.S., 1997. Absorption spectrum (380–700 nm) of pure water. II. Integrating cavity measurements. Applied Optics. 36 (33): 8710-8723.

Sarangi, R.K., P. Chauhan, S.R. Nayak. 2005. Inter- annual variability of phytoplankton bloom in the northern Arabian Sea during winter monsoon period (February to March) using IRS-P4 OCM data. Indian Journal of Geo-Marine Sciences. 34(2): 163-173.

Sarangi, R.K.P. Chauhan, S.R. Nayak. 2001. Phytoplankton bloom monitoring in the offshore water of Northern Arabian Sea using IRS-P4 OCM satellite data. Indian Journal of Geo-Marine Sciences. 30(4): 214-221.

Sarangi, R.K.P. Chauhan, S.R. Nayak. 2004. Detection and monitoring of Trichodesmium blooms in the coastal waters off Saurashtra coast, India using IRS-P4 OCM data. Current Science. 86: 12-25.

Sathyendranath, S., A. Longhurst, C. M. Caverhill, and T. Platt. 1995. Regionally and seasonally differentiated primary production in the North Atlantic. Deep-Sea Research I. 42: 1773-1802.

Siegel, D.A., Maritorena, S., Nelson, N.B., Hansell, D.A., Lorenzi Kayser, M. 2002. Global ocean distribution and dynamics of colored dissolved and detrital organic materials. Journal of Geophysical Research. 107(C12): 3228 doi: 10.1029/2001JC000965.

Solanki, H.U, Dwivedi, R.M, Nayak, S.R, Jadeja, J.V, Thaker, D.B, Dave, H.B. and Patel, M.I. 2001 (a). Application of Ocean colour monitor chlorophyll and AVHRR SST for fishery forecast. Preliminary Validation results off Gujarat coast, north coast of India. Indian Journal of Geo-Marine Sciences. 30: 132-138.

Sravanthi, N., I. V. Ramana, P. Yunus Ali, M. Ashraf, M. M. Ali, and A.C. Narayana. 2013. An Algorithm for Estimating Suspended Sediment Concentrations in the Coastal Waters of India using Remotely Sensed Reflectance and its Application to Coastal Environments International Journal of Environmental Research. 7(4): 841-850. ISSN: 1735-6865.

Stocker, T.F., G.K.C. Clarke, H. Le Treut, R.S. Lindzen, V.P. Meleshko, R.K. Mugara, T.N. Palmer, R.T. Pierrehumbert, P.J. Sellers, K.E. Trenberth, J. Willebrand. 2001. Physical Climate processes and Feedbacks. J.T. Houghton, Y. Ding, D.J. Griggs, M. Noguer, P.J. van der Linden, X. Dai, K. Maskell, C.A. Johnson (Eds.), Climate Change 2001: The Scientific Basis. Contribution of Working Group I to the Third Assessment Report of the Intergovernmental Panel on Climate Change. Cambridge University Press, Cambridge, pp. 419–470.

Chapter 2

MATERIALS AND METHODS

2.1. Description of study area

Kochi (formerly known as Cochin) is a part of the Greater Cochin region and the largest urban agglomeration in the Indian state of Kerala with a population of 2.2 million as per Census 2011. Its area consists of Corporation of Kochi (Cochin), 9 municipalities, 14 Panchayaths and parts of 4 Panchayaths. Since the majority of the human population lives within 60 km of the coast, the quality of coastal waters and estuaries is increasingly threatened by anthropogenic activities, such as population growth, urbanization, maritime traffic, over fishing, leaching of fertilizers from the land, phytoplankton blooms, untreated industrial discharge, oil pollution and tourism, among others. The Kochi backwaters form a complex network of shallow brackish water body (256 km^2) with a tidal amplitude of ≤1.0 m running parallel to the southwest coast of India (9°30′ and 10°10′N, 76°10′ and 76°30′E), with two permanent openings to the South Eastern Arabian Sea (SEAS) and receives fresh water in an amount of 2.0×10^{10} m^3 $year^{-1}$ (Qasim, 2003). Six rivers discharge about 2,91,010 m^3 $year^{-1}$ of fresh water (Srinivas et al., 2003) and 3,29,106 tons $year^{-1}$ of sediment flux from its catchments (Thomson, 2002) to the SEAS. These coastal waters are a unique region occupying the well-known mud banks, which are store houses of primary nutrients, attracting immense fishery during the southwest monsoon (Varma and Kurup 1969; Sylas 1984; Mathew et al. 1995; Balachandran 2004).

The annual rain fall is about 3.2 m, varying considerably from year to year. The development of anthropogenic activities produces discharges that pollute and weaken the coastal ecosystems, and increases the vulnerability of these environments.

Table 2.1. Average monthly river discharge rate (Mm^3) to the Cochin backwaters (Revichandran et al. 2011)

Month	Rivers							
	Muvattupuzha	Chalakudy	Periyar	Meenachil	Pamba	Achankovil	Manimala	Average
January	179.49	25.76	93.75	5.19	63.56	9.59	5.46	54.69
February	157.36	16.02	81.15	1.21	38.57	4.56	4.66	43.36
March	172.50	17.03	90.71	5.25	42.65	3.55	3.15	47.84
April	179.06	17.81	116.95	34.20	68.87	13.16	22.44	64.64
May	230.23	40.13	169.32	48.68	155.40	31.45	67.00	106.03
June	694.65	259.08	990.66	273.46	673.09	199.63	356.72	492.47
July	984.52	543.21	1,654.09	312.30	836.50	247.06	400.67	711.19
August	809.34	471.27	1,500.37	286.75	677.47	203.62	305.37	607.74
September	460.90	223.72	814.82	169.39	480.64	152.61	202.39	357.78
October	540.80	173.77	684.87	166.93	563.97	199.16	260.44	369.99
November	399.60	109.60	440.88	172.30	356.79	158.09	158.65	256.56
December	220.64	41.52	157.71	37.31	113.45	30.13	29.22	90.00
Total	5,029.11	1,938.92	6,795.29	1,512.97	4,070.96	1,252.61	1,816.15	3,202.29

There are three seasons prevailing in the estuary; monsoon (June–September), post-monsoon (October–January) and pre-monsoon (February–May). More than 70% of annual rain fall occurs during the monsoon period resulting in heavy fresh water discharge to the estuary. During monsoon, the estuary is virtually converted into a freshwater basin even in the areas around bar mouth and frequently develops stratification resulting in less dense river water at surface and high dense seawater at the bottom layers. In post-monsoon season, the discharge from river gradually diminishes and tidal influence gains momentum. In pre-monsoon season, the river discharge is at its minimum and sea water influence is in maximum, and homogeneity exists in the water column (Menon et al., 2000).

Winds in this region are stronger (8- 10 m/s) north easterlies during post monsoon (October – January) and pre monsoon (February – May), while it is south westerly during monsoon (June – September). The current direction is from south to north during November – January, and it reverses in February with strong north to south currents from May to October (Shirodkar et al., 2009). The onset of south west monsoon occurs in late May and early June and continues through October. From November to February, the coast is influenced by lighter, drier northeast winds. The upwelling period (June to October) of southwest monsoon is associated with algal blooms and the favourable productivity factors support large fisheries along the west coast, which contributes 60% to the total fish catches along the Indian coast (Naqvi et al., 2000).

The area has a strong monsoonal influence resulting in seasonal changes in hydrographic conditions influenced by river water discharge and surface circulation. During Pre-monsoon (February-May) wind induced upwelling along with a northward undercurrent and a southward surface flow associated with strong vertical mixing is observed off Kochi waters (Prasad and Ikeda 2001). Upwelling process supported by the southerly current is also observed along the coastal waters during monsoon season (Joshi and Rao, 2012). After monsoon season, the hydrographic parameters change causing very strong fresh water discharge from backwaters (Srinivas and Dinesh Kumar, 2006).During the monsoon period, the nutrient values of the coastal waters increases and surface salinity and water temperature falls down, detrital load increases and consequently light penetration diminishes. These rapid changes often lead to very high production at primary and secondary levels(Madhupratap et al., 1990).During the transition period of monsoon to post monsoon season, the freshwater containing- high levels of

nutrients are transported through the Kochi inlet or barmouth, thus making a significant contribution to the nutrient budget of the coastal waters. At certain locations during southwest monsoon period seasonal phytoplankton blooms (Srinivas and kumar, 2006) were also observed.

At the height of the monsoon, a large volume of fresh water discharges through the bar-mouth into the sea, lowering salinities near the shore and river runoff is controlled by short term variations rather than long term variations. (DarbyShyre, 1967).

Like most of the major estuarine and coastal systems of the world, the Kochi estuary has also been increasingly affected by anthropogenic activities such as intertidal land reclamation, effluent discharges, expansion for harbour development and dredging activities and urbanization (Gopalan et al., 1983; Menon et al., 2000). Kochi estuary has also received a high influx of anthropogenic nutrients, heavy metals and organic matter from increased agricultural activities, domestic sewage inputs, industrial effluents and marine fish farming, during the last two decades (Qasim, 2003; Balachandran et al., 2005; Thomson, 2002; Martin et al., 2008, 2010).

2.2. Sampling

The selection of stations was based on bathymetry, and they were scattered equally on either side of the backwater outlet. The surface water samples were collected using a 2.5 l Hydro-Bios Niskin plastic water sampler. Prior to sampling, the sampler and the sampling bottles was acid washed with 1N HCl. Sample bottles were rinsed two times with the environmental sample and then the sample was collected using commercial fishing trawlers *Bharath Darsan* and *Mosa* and CIFT Fishing vessel *Sagar Sakthi*. Location of sampling points of three transects.

Table 2.2. Details of sampling sites selected for the study.

Transect	Station name	Description	Latitude	Longitude	Depth (m)
T1	S1	Barmouth	09.969 °	76.255 °	10
T2	S2	10m station southern part of the barmouth	09.906 °	76.208 °	10
	S4	10m station at the western part of the barmouth	09.957 °	76.168 °	10
	S7	10m station at the Northern part of the barmouth	10.040 °	76.153 °	10
	S8	10m station at the Northern part of the barmouth	09.993 °	76.153 °	10
T3	S3	20m station at the southern part of the barmouth	09.905 °	76.157 °	20
	S5	20m station at the Northern part of the barmouth	10.000 °	76.101 °	20
	S6	20m station at the Northern part of the barmouth	10.040 °	76.093 °	20

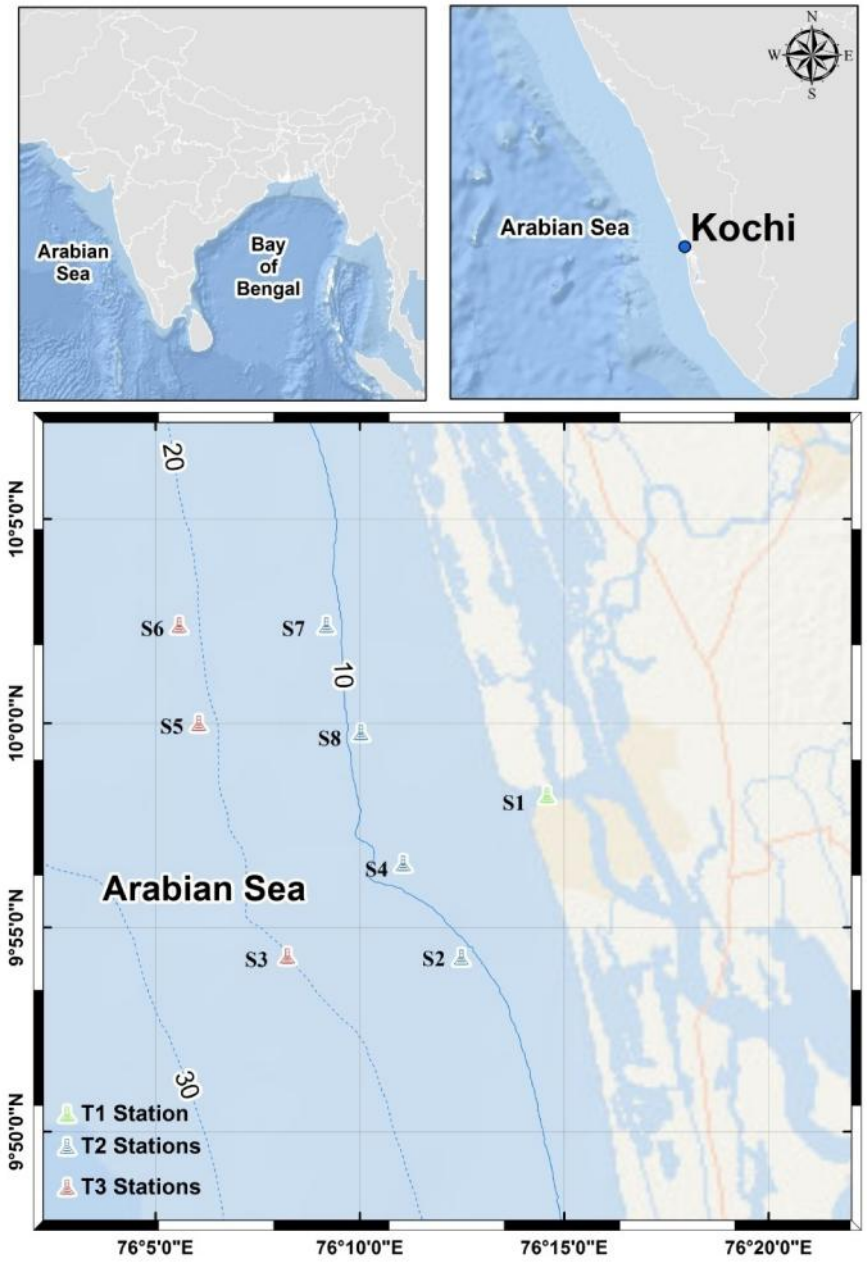

Figure 2.1. Map of study area showing location of the sampling

2.3. Analytical Methodology

2.3.1. Sea Surface Temperature (SST)

SST data is collected from the MODIS aqua data from the NASA website, http://oceancolor.gsfc.nasa.gov/.

2.3.2. Rainfall Data

Rain fall data was collected from the Indian metrological department using the new high spatial resolution (0.25X0.25 degree) long period (1901-2013) daily gridded rainfall data set over India (Pai et al. 2014).

2.3.3. Current Data

Current data is collected from the NCEP/NCAR Reanalysis 1 project using a state-of-the-art analysis/forecast system. The data was done at 8 times daily in the model, because the inputs available in that era were available at 3Z, 9Z, 15Z, and 21Z, whereas the 4x daily data has been available at 0Z, 6Z, 12Z, and 18Z. These latter times were forecasted and the combined result for this early era is 8x daily. The local ingestion process took only the 0Z, 6Z, 12Z, and 18Z forecasted values, and thus only those were used to make the daily time series and monthly means here. These variables are averages of instantaneous values at the 4 reference times; 0,6,12 and 18z over the averaging period (month) (Kalnay et al.1996). This is used to study the changes in the current pattern of the study area.

2.3.4. pH (Hydrogen ion concentration)

pH was measured using Eutech Instruments(PC 2700). The pH meter was calibrated with National Institute of Standards and Technology (NIST) standards of certified values of pH corresponding to 4, 7 and 10.

2.3.5. Salinity

Salinity was measured by Mohr-Knudson method (Grasshoff et al. 1983).

2.3.6. Turbidity

Turbidity was measured using Micro100 IR – turbidity meter and regular calibration was done with National Institute of Standards and Technology (NIST) standards. Three standards with certified turbidity values 0.02 NTU, 10 NTU and 100 NTU were used for the calibration.

2.3.7. Dissolved Oxygen

Dissolved oxygen (DO) was estimated according to Winkler's titration method (Grasshoff et al. 1983).

2.3.8. Determination of Nutrients in Seawater

Nutrients (Nitrite, phosphate and silicate) were estimated spectrophotometrically as per standard methods (Grasshoff, 1983). The method of nitrite determination depends on reaction with an aromatic amine, sulphanilamide, which is then coupled with n-(1-naphthyl) – ethylene diamine dihydrochloride, to form an azo dye. The absorbance of the dye is measured spectrophotometrically at 543 nm. Phosphate in seawater is allowed to react with acid Ammonium molybdate, forming a phosphomolybdate complex, which is reduced by ascorbic acid, in presence of antimonyl ions (to accelerate to reaction) to a blue coloured complex containing 1: 1 atomic ratio of phosphate and antimonyl ions. The blue colour formedby the reaction was measured at 880nm using a 1cm cell (cuvette). To avoid interference by silicate the pH is kept below 1.The seawater sample is allowed to react with molybdate under conditions, which result in the formation of silicomolybdate,

phosphomolybdate and arsenomolybdate complexes. A reducing solution, containing ascorbic acid and oxalic acid is then added which reduces the silicomolybdate complex to give a blue reduction compound and simultaneously decomposes any phosphomolybdate so that interference from phosphate and arsenate is eliminated. The intensity was measured at 810 nm.

2.3.9. Chlorophyll a

Chl-a was measured using a field fluorometer (model: 10-AU; Turner designs, Sunnyvale, CA, USA) following the Welschmeyer method (Welschmeyer 1992). Between 0.1 and 1.0l of water were filtered onto 25 mm glass fibre filters (GFF) using a vacuum pressure of less than 200 mm Hg and extracted overnight in 90% acetone. The samples were then centrifuged for 10–20 min at 2000 rpm and the raw fluorescence given as digital volts was converted to chl-a concentrations using calibration curves from chl-a standards (Sigma-Aldrich Company Ltd., St. Louis, MO, USA).

2.3.10. Analysis of Total Suspended Matter (TSM)

Seawater samples are collected, in clean polyethylene bottles from undisturbed or temporarily disrupted area. A known amount of water was filtered a through a pre-washed, pre-dried at 103-105 ºC, 0.45 µm millipore filter paper. It was then rinsed, dried and reweighed with at least 7 digits of precision to calculate the correct TSM in mg/L.

TSM was then Calculated by using the equation given below as per Strickland and Parsons, 1972

$$TSM(mg/L) = \big((A - B)\ X\ 1000\big)/C$$

where

A = final dried weight of the filter (in milligrams = mg)
B = Initial weight of the filter (in milligrams = mg)
C = Volume of water filtered (in Litres)

2.3.11. Spectrophotometric Analysis of CDOM Optical Properties

CDOM samples were collected in 100 ml amber glass bottles that had been rinsed three times with sample water before filling. Water samples were filtered onboard through 0.2 μm GF/F filters. 0.4 ml of 0.5 M $HgCl_2$ was then added to 200 ml of sample to avoid any bacterial degradation.

The sample was then preserved at low temperature until analysis in the laboratory. The sample transparency was measured using an UV/VIS spectrophotometer over the spectral range 400to 700 nm with an interval of 1 nm against milli-Q water as blank. The spectral absorption coefficient was calculated by normalizing with respect to 440 nm (Kowalczuk and Kaczmark,1996). Remote sensing studies in which the competition of CDOM with phytoplankton pigments in absorption in the blue is important often employ 440 nm (Carder et al., 1989; Bowers et al.2000) and this wavelength was chosen here for the same reason.

$$a_{CDOM}(\lambda) = aCDOM\ (440)\ \exp\ [-s\ (\lambda - 440)]\ [m^{-1}]$$

Where, aCDOM (440) is the absorption measured at 440 nm and s is the slope coefficient which was calculated as the slope of the curve resulted by plotting logarithm of aCDOM against wavelength (λ). The magnitude of a_{CDOM} (440) gives the concentration while the spectral slope(s) indicates its composition (Stedmon and Markager, 2003). The absorption coefficients were then corrected for backscattering of small particles and colloids, which pass through filters

(Green and Blough, 1994).

$$aCDOM\_corr\ (\lambda) = aCDOM\ (\lambda) - aCDOM\ (700) * (\lambda/700)\ [m^{-1}]$$

2.3.12. Analysis of Spectral Absorption Coefficient of Phytoplankton

Seawater samples (2-5 liters) were collected and transferred, to polyethylene filtration bottles. The filtration bottles and caps are rinsed at least three times with the sample before filling. After filling, the contents are filtered under low vacuum (<25 hPa) through in-line 25 mm whatman GF/F filters. All filtration procedures are done under subdued light conditions. After the sample is filtered, each filter is transferred to a pre washed and dried filter case. The light absorption spectrum of phytoplankton can be measured by the quantitative filter technique (QFT) method (Mitchell, 1990). The absorption spectra of total particulate matter relative to a blank filter saturated with sea water were recorded in the wavelength range 350-750nm at a resolution of 1 nm with a double-beam spectrophotometer equipped with an integrating sphere. For each of the measured spectra, the optical density obtained at 750 nm was subtracted from that of all other wavelengths. Optical density of the total suspended matter was corrected for the path length amplification (β effect) and converted into light absorption coefficients by the total particulate matter and detrital matter (ap(λ) and ad(λ) respectively) according to Cleveland and Weidemann (1993) Kyewalyanga et al., (1998) as follows.

$$a_p(\lambda) = \frac{2.303\ OD_s(\lambda)}{v/s}$$

$$OD_S(\lambda) = 0.378OD_f(\lambda) + 0.523\ [OD_f(\lambda)]^2$$

Where $OD_S(\lambda)$ is the optical density of total suspended particulate matter, v is the filtration volume (m^3) and s is the filtration area (m^2).

Following the measurement of the total particulate absorption spectrum, the filters were extracted in 100% methanol following the procedure of Kishino et al. (1985) and then saturated with filtered seawater. Following

this extraction, the absorption of the filters relative to blank filters also treated with methanol and re-saturated with filtered seawater was determined in the spectrophotometer. These spectra represent absorption by non-methanol extractable detrital

$$a\ (\lambda) = \frac{2.303\ OD_s(\lambda)}{v/s}$$

Where ODs (λ) is calculated using the same equation as above. The term vand s stands for the filtration volume (m^3) and filtration area (m^2) respectively.

An estimate of phytoplankton component of the total particulate absorption (aph(λ)) was then determined by subtracting ad(λ) from ap(λ) (Kishino et al., 1985)

$$a_{ph}(\lambda) = a_p(\lambda) - a\ (\lambda)$$

The chlorophyll-specific light absorption coefficients of phytoplankton (a*ph(λ)) were obtained by dividing (a_{ph}(λ)) by the Chl-a concentration.

2.3.13. Phytoplankton Numerical Density

Water samples were collected for identifying phytoplankton taxonomy and stored in high-density polyethylene bottles and preserved using buffered formalin. Leica Generic DMIL inverted microscope with phase contrast was used to estimate phytoplankton diversity and abundance using standard keys of identification (Tomas 1997).

2.3.14. Derivative Analysis

The fourth derivative of the ap(λ) and aph(λ) was calculated by applying a 41 point fourth degree polynomial smoothing and then differentiating using the Savitzky-Golay method (Savitzky, Golay1964). The polynomial smoothing was applied because differentiation tends to amplify the

effects of high frequency noise in the spectra (Aguirre- Gomes et al. 2001). The procedure was carried out using Microcal Origin 8.0 scientific analysis software. Peaks in the fourth derivative curves were selected using the peak finder tool in the software.

2.3.15. Remote Sensing Reflectance

Remote-sensing reflectance (Rrs) in hyperspectral bands were measured using a Satlantic^{TM} hyperspectal radiometer (HyperOCRII). This instrument contains 256 optical channels between 350 and 800 nm that measure downwelling surface irradiance (ES) and profiles of downwelling irradiance (Ed) and upwelling radiance (Lu). The radiometers were deployed away from the vessel to avoid ship-induced perturbations and shading (Fargion and Mueller 2000). The data were recorded using SatView^{TM} software and processed with Prosoft ^{TM} software. When the tilt of the sensor was more than 5° and profiling velocity was more than 0.7 m s^{-1}, the data were discarded to ensure a high quality for the measurements. The Rrs (λ) was then calculated from

$$Rrs(\lambda) = \frac{\left(Lw(\lambda, 0^{+})\right)}{\left(Ed(\lambda, 0^{+})\right)}$$

where Ed(λ, 0^{+}) is the above-surface downwelling spectral irradiance (W m^{-2} nm^{-1}) and Lw(λ, 0^{+}) is the water-leaving radiance (Wm^{-2} nm^{-1} sr^{-1}). Standard ocean optics protocols (Fargion and Mueller 2000) were used in the computation of water-leaving radiance (Lw).

2.3.16. Satellite Data Processing

Moderate Resolution Imaging Spectroradiometer on Aqua satellite (MODIS-Aqua) level-0 data, corresponding to the days of in situ data, were acquired from GSFCNASA (http://oceancolor.gsfc.nasa.gov). The data were

processed from Level 0 to Level 2 using the Sea Viewing Wide Field of view Sensor (SeaWiFS) Data Analysis System (SeaDAS) software with two atmospheric correction schemes. The two atmospheric correction schemes chosen were: (1) multi-scattering with two-band model selection NIR correction (hereafter referred to as A1) (Siegel et al. 2000); and (2) multi-scattering with Management Unit of the North Sea Mathematical Models (MUMM) correction and MUMM NIR calculation (hereafter referred to as A2) (Ruddick et al 2000). The first atmospheric correction scheme was used as a default for MODIS-Aqua data and the default bio-optical algorithm (OC3M) was used for the retrieval of chl-a. The satellite match-up data for chl-a and Rrs at wavelengths 412, 443, 469, 488, 531, 555, 645, 667, and 678 nm were extracted from a 3 × 3 pixel box (Bailey and Werdell 2006). Subsequently the quality of the match-up data was assessed according to Ocean Optics Protocols (Fargion and Mueller 2000) and 13 match-up points were selected for validation based on spatial criteria with satellite pixel corresponding to *in situ* location and temporal criteria used is ± 3 hours of satellite overpass.

2.3.17. Statistical Analysis

ANOVA (one way) was used to evaluate the spatial and temporal distribution of the parameters in the study area. Spearman's correlation analysis and principal component analysis (SPSS, 15.0) were used for the statistical analysis.

References

Aguirre-Goméz, R., Weeks, A. R., and Boxall, S. R. 2001. The identification of phytoplankton pigments from absorption spectra. International Journal of Remote Sensing. 22(2 & 3): 315 - 338.

Bailey, S. W., and P. J. Werdell. 2006. A Multi-Sensor Approach for the On-Orbit Validation of Ocean Color Satellite Data Products. Remote Sensing of Environment. 102: 12−23.doi:10.1016/j.rse.2006.01.015.

Balachandran, K. K. 2004. Does subterranean flow initiate mud banks off the southwest coast of India? Estuarine, Coastal and Shelf Science. 59: 589–598.

Balachandran, K. K., Lalu, Raj, C. M., Nair, M., Joseph, T., Sheeba, P., and Venugopal, P. 2005. Heavy metal accumulation in a flow restricted, tropical estuary. Estuarine, Coastal and Shelf Science. 65: 361–370.

Bowers, D. G., Harker, G. E. L., Smith, P. S. D., Tett, P. 2000: Optical properties of a region of freshwater influence (the Clyde Sea). Estuarine Coastal and Shelf Science. 50: 717 – 726.

Carder, K. L., Steward, R. G., Harvey, G. R., Ortner, P. B. 1989: Marine humic and fulvicacids: their effects on remote sensing of ocean chlorophyll. Limnology and Oceanography. 34: 168 – 81.

Cleveland, J. S., and Weidemann, A. D. 1993: Quantifying absorption by aquatic particles: A multiple scattering correction for glass-fiber filters. Limnology and Oceanography. 3: 1321-1327.

Darbyshyre, M. 1967. The surface waters off the coast of Kerala, southwest India. Deep Sea Research. 14: 295-320.

Fargion, G. S., and J. L. Mueller. 2000. Ocean Optics Protocols for Satellite Ocean Color Sensor Validation, 184pp Greenbelt, MA: NASA Goddard Space Flight Center. Revision 2, NASA/TM–2001-209955.

Gopalan, U. K., Vengayil, D. T., Varma, U. P., and Kutty, K. M. 1988.The shrinking backwaters of Kerala. Journal of Marine Biological Association of India. 25(1 & 2): 131–141.

Grasshoff, K., Ehrhardt, M., Krembling, K. 1983. Methods of Seawater Analysis. New York: Verlag Chemie

Green, S., and Blough, N. 1994: Optical absorption and fluorescence properties of chomophoric dissolved organic matter in the natural waters. Limnology and Oceanography. 39: 1903 – 1916.

Joshi, M. And A.D. Rao. 2012. Response of southwest monsoon winds on shelf circulation off Kerala Coast. India Continental Shelf Research. 32: 62–70.

Kalnay, E., M. Kanamitsu, R. Kistler, W. Collins, D. Deaven, L. Gandin, M. Iredell, S. Saha, G. White, J. Woollen, Y. Zhu, M. Chelliah, W. Ebsuzaki, W. Higgins, J. Janowiak, K. C. Mo, C. Ropelewski, J. Wang, A. Leetma, R. Reynolds, R. Jenne, D. Joseph, 1996. The NCEP/NCAR 40-year reanalysis project, Bull. Amer. Meteor. Soc., 77, 437–470.

Kishino, M., Takahashi, M., Okami, N and Ichimura, S. 1985. Estimation of the spectral absorption coefficients of phytoplankton in the sea. Bulletin of Marine Science. 37: 634-642.

Kowalczuk, P., Kaczmark, S. 1996: Analysis of temporal and spatial variability of Yellow Substance absorption in the southern Baltic. Oceanologia. 3 – 32.

Kyewalyanga, M.N., Platt, T., Sathyendranath, S., Lutz, V.A., and Stuart, V. 1998. Seasonal variations in physiological parameters of phytoplankton across the North Atlantic. Journal of Plankton Research. 20: l7- 42.

Madhupratap, M., Nair, S.R.S., Haridas, P., Padmavati, G. 1990. Response of zooplankton to physical changes in the environment: coastal upwelling along central west coast of India. Journal of coastal research. 6: 413-426

Martin, G.D., Muraleedharan, K.R., Vijay, J.G., Rejomon, G., Madhu, N.V., Shivaprasad, A. 2010. Formation of anoxia and denitrification in the bottom waters of a tropical estuary, southwest coast of India. Biogeoscience Discussion. 7:1751–1782.

Mathew, J., Mytheenkhan, B., and Kurian, N. P. 1995. Mud banks of the southwest coast of India. II. Wave–mud interactions. Journal of Coastal Research. 11(1): 179–187.

Martin, G.D., Vijay, J.G., Laluraj, C.M., Madhu, N.V., Joseph, T., Nair, M., 2008. Fresh water influence on nutrient stoichiometry in a tropical estuary, southwest coast of India. Applied Ecology and Environmental Research. 6: 57–64.

Menon, N.N., Balchand, A.N., Menon, N.R. 2000. Hydrobiology of the Cochin backwater system – a review. Hydrobiologia. 430: 149–183.

Mitchell, B.G. 1990: Algorithms for determining the absorption coefficient of aquatic particulates using the quantitative filter technique (QFT). Soc. Photo-Opt. Instr. Eng. Ocean Optics. X: 137-148.

Naqvi, S. W. A., Jayakumar, D. A., Narvekar, P. V., Naik, H., Sarma, V. V. S., De Souza W., Joseph, S., George, M. D. 2000. Increased marine production of N_2O due to intensifying anoxia on the Indian continental shelf. Nature. 408: 346 – 349

Pai, D. S., Latha, Sridhar, Rajeevan, M., Sreejith, O. P., Satbhai, N.S., and Mukhopadyay, B. 2014. Development of a new high spatial resolution (0.25° × 0.25°) Long Period (1901-2010)daily gridded rainfall data set over India and its comparison with existing data sets over the region. MAUSAM. 65 (1): 1-18.

Prasad, T.G and Ikeda, M. 2001: Spring evolution of Arabian Sea High in the Indian Ocean. Journal of Geophysical Research.106 (C11): 31085- 31098

Qasim, S.Z., 2003. Indian Estuaries. Allied publication Pvt. Ltd. Heriedia Marg, Ballard estate, Mumbai, p. 259.

Revichandran, C., Srinivas, K., Muraleedharan, K. R., Rafeeq, M., Amaravayal, S., Vijayakumar, K., et al. 2011. Environmental set-up and tidal propagation in a tropical estuary with dual connection to the sea (SW Coast of India).Environmental Earth Sciences. doi: 10.1007/s12665-011-1309-0.

Ruddick, K. G., F. Ovidio, and M. Rijkeboer. 2000. Atmospheric Correction of Seawifs Imagery for Turbid Coastal and Inland Waters. Applied Optics. 39: 897–912. doi:10.1364/AO.39.000897.

Savitzky, A., and Golay, M.J.E. 1964. Smoothing and differentiation of data by simplified least squares procedures. Analytical Chemistry. 36: 1627 - 1639.

Shirodkar, P. V., Mesquita, A., Pradhan, U. K., Verlekar, X. N., Babu, M. T., Vethamony, P. 2009. Factors controlling physico-chemical characteristics in the coastal waters off Mangalore – A multivariate approach. Environment Research. 109: 245–257

Siegel, D. A., M. Wang, S. Maritorena, and W. Robinson. 2000. Atmospheric Correction of Satellite Ocean Color Imagery: The Black Pixel Assumption. Applied Optics. 39: 3582−3591. doi:10.1364/ AO.39.003582.

Srinivas, K., Revichandran, C., Maheswaran, P.A., M. Asharaf, T.T., Murukesh, N., 2003. Propagation of tides in the Cochin estuarine system, southwest coast of India. Indian Journal of Geo- Mar Science. 32 (1): 14–24.

Srinivas, K., DineshKumar, P.K. 2006. Atmospheric forcing on the seasonal variability of sea level at Cochin, southwest coast of India. Continental Shelf Research. 26: 1113–1133.

Stedmon, C. A., and Markager, S. 2003: Behaviour of the optical properties of coloured dissolved organic matter under conservative mixing. Estuarine, Coastal and Shelf Science.57: 1 – 7.

Strickland J. D. H and Parsons T. R. 1972: A practical handbook of seawater analysis. Journal of Fisheries Research. Bd. Canada, 167, 311pp.

Sylas, E. G. 1984. Mudbanks of Kerala–Karnataka – Need for an integrated study: Mudbanks of Kerala Coast. Central Marine Fisheries Research Institute Bulletin. 31: 1–74

Thomson, K.T., 2002. Economic and Social Issues of Biodiversity Loss in Cochin Backwaters. Technical Report. Cochin University of Science and Technology. Cochin, India, pp. 51–82.

Tomas, C R. 1997. Identifying marine phytoplankton, Academic Press, New York, USA, 858

Varma, P. U., and Kurup, P. G. 1969. Formation of the Chakara (mud bank) on Kerala coast. Current Science. 38(23): 559– 560.

Welschmeyer, N.A. 1992: Flourometric analysis of chlorophyll a in the presence of chlorophyll b and phaeopigments. Limnology Oceanography. 39(8): 1985-1992.

Chapter 3

STUDIES ON BIOGEOCHEMISTRY

3.1. Introduction

Estuaries and coastal waters are characterized by strong spatial and temporal variability of physico-chemical and productivity patterns. (Cloern 2001). Coastal waters influenced by major rivers carrying substantial nutrient load provides settings to examine a broad spectrum of nutrient conditions and their relationship to biological processes. Carbon cycling in the coastal waters that connect terrestrial with oceanic systems is widely recognized to be a major component of global carbon cycles and budget (Bauer et al. 2013). The life supporting process in marine coastal ecosystems require many inorganic substances like nitrogen, phosphorous, and silicon, which are considered to be more important than others, as they play a key role in phytoplankton abundance, growth and metabolism (Raymont 1980, Grant and Gross 1996). The availability of nutrients in the euphotic zone and its subsequent chemical response is the basis of all biological properties of marine systems. It is recognized that the water quality plays an important role in selecting the size of the phytoplankton community (Malone 1980; Platt et al. 1983; Chavez 1989; Legendre and Le-Fevre 1989).

Since the Arabian Sea is under the influence of changing wind patterns associated with the summer and winter monsoons, the coastal waters of this region are significant in two ways, as the recipient of approximately 1.9×10^{10} m^3 of fresh water annually from the Cochin backwaters and as the unique region occupying the well-known mud banks, which are store houses of primary nutrients, attracting immense fishery during southwest monsoon (Balachandran 2004). The Arabian Sea is one of the most productive regions in the world and is characterized by strong seasonal oscillations in biological production. Chlorophyll-*a* (Chl-*a*) is widely considered as the proxy of phytoplankton biomass (Huot et al., 2007) and it is one of the most widely accepted methods in the study of biological production as it indicates total plant material available in the water at primary level of food chain (Weyhenmeyer et al. 1999).

The coastal areas of the tropics are productive except the turbid near river mouths, where light penetration is poor (Platt 1986). In shallow areas, the high productivity is accounted by the increased regeneration rate of nutrients due to high temperatures accelerating all bacterial processes at the bottom (Nair et al., 1973). One of the major findings of the International Indian Ocean Expedition during 1962-65 was the extremely high rates of primary production and large standing crops of phytoplankton and zooplankton along the western regions of the Arabian Sea. The values of primary production and standing crops in the central Arabian Sea are higher than the average values encountered in the world oceans (Wooster et al., 1967). The maximum production was reported nearer to the coasts, within 50 m depths and gradually decreasing seaward (Nair et al., 1973). High rate of production was also noted in the shallow waters of the coastal regions of Laccadive and Minicoy islands (Prasad and Nair, 1960).The west coast

of India experiences a time dependent wind stress due to monsoons (Pankajakshan and Rama Raju, 1987); so also the phenomenon of upwelling takes place and the presence of stratification and thermocline disappearse, due to upwelling or downwelling and the nutrient rich CDOM waters (Ramamritham and Rao, 1973; Basil, 1983) is coming to the surface. Upwelling also may be coupled with undercurrents, which move the mud deposits from deeper areas to shallow regions (Gopinathan and Qasim, 1974).

The availability of long time-series data from the global oceans at regional scale is recognized as a key element to understand the role of the oceans in modulating the behavior of the earth system. Fixed-point stations will resolve multi-disciplinary variability and processes like CO_2 uptake, biological productivity, fluxes of heat, freshwater momentum and other properties between the ocean and atmosphere, seasonal variability and both seismic and biological activity. The biological and chemical responses to natural (e.g., ENSO, IODP) events and anthropogenic perturbations are particularly important with regard to evaluating the prognostic models used in future climate projections. Coastal oceans which support large populations and economic activities, are vulnerable to critical transitions, natural or anthropogenic, can occur unexpectedly and are difficult to manage, and mitigation measures need background awareness of the ecosystems. The study of the chemical and physical forcing of the coastal environment provides background information necessary for the monitoring and understanding of the coastal oceanographic processes. Also, long term time series data has a great potential in applying the tools of modern oceanography and chemistry to unravel the geological, biological and anthropogenic coastal processes. Long-term time-series stations are invaluable for developing and testing autonomous

sensors and as focal points for process studies and satellite validation exercises. The study area draw special attention because of the occurrence of seasonal Mudbanks at certain locations, which supports large fishery during southwest monsoon period (Balachandran, 2004), and also phytoplankton blooms during the same perid (Srinivas and Dineshkumar, 2006, Usha et al 2014). The upwelling period (June to October) of southwest monsoon is associated with algal blooms and the favourable productivity factors support large fisheries along the west coast, which contributes 60% to the total fish catches along the Indian coast (Naqvi et al., 2000). The objective of this study is to evaluate the abiotic process of the south eastern Arabian sea coastal water ecosystem with respect to spatial and seasonal effect on the primary production from long term time series stations maintained in the study area.

3.2. Results

3.2.1. Inter-annual Variability in Distribution of Chlorophyll-a and Water Quality Parameters at Different Transects

The section describes the variability in distribution of chlorophyll-*a* (chl-*a*) and associated water quality parameters at annual scale for individual transects for the surface water. The inter-annual variability was described using frequency distribution plots (**Figure3.1.a and 3.1.b**). The spread of the curve depicts the variability whereas the peak shows the number of occurrences. Time-series distribution of mean chlorophyll-*a* (chl-a), sea surface temperature (SST), surface salinity, dissolved oxygen (DO), pH, turbidity, nitrite (NO2), phosphate (PO4) and silicate (Si04) corresponding to stations in transect T1, T2 and T3 are shown in **Figure. 3.2, 3.3 and 3.4** respectively with standard deviation and trend in variability.

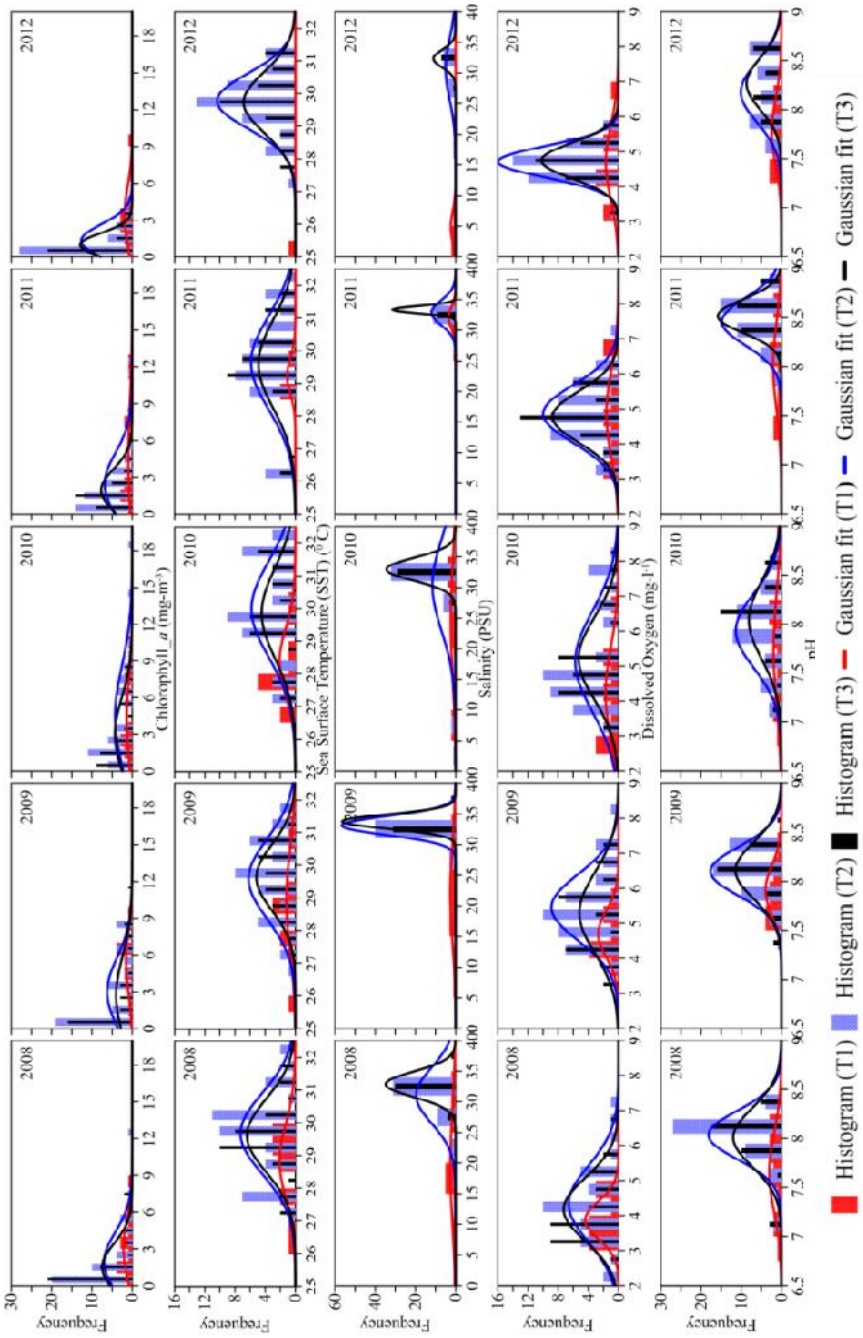

Figure 3.1.b. Histogram showing frequency distribution of chlorophyll-*a* (chl-*a*), sea surface temperature (SST), surface salinity, dissolved oxygen (DO), pH. The red bar corresponds to stations in transect T1, blue bar corresponds to stations in transect T2 and black bar corresponds to stations in transect T3. Red, blue and black lines represents the normal Gaussian distribution for the transects T1, T2 and T3 respectively

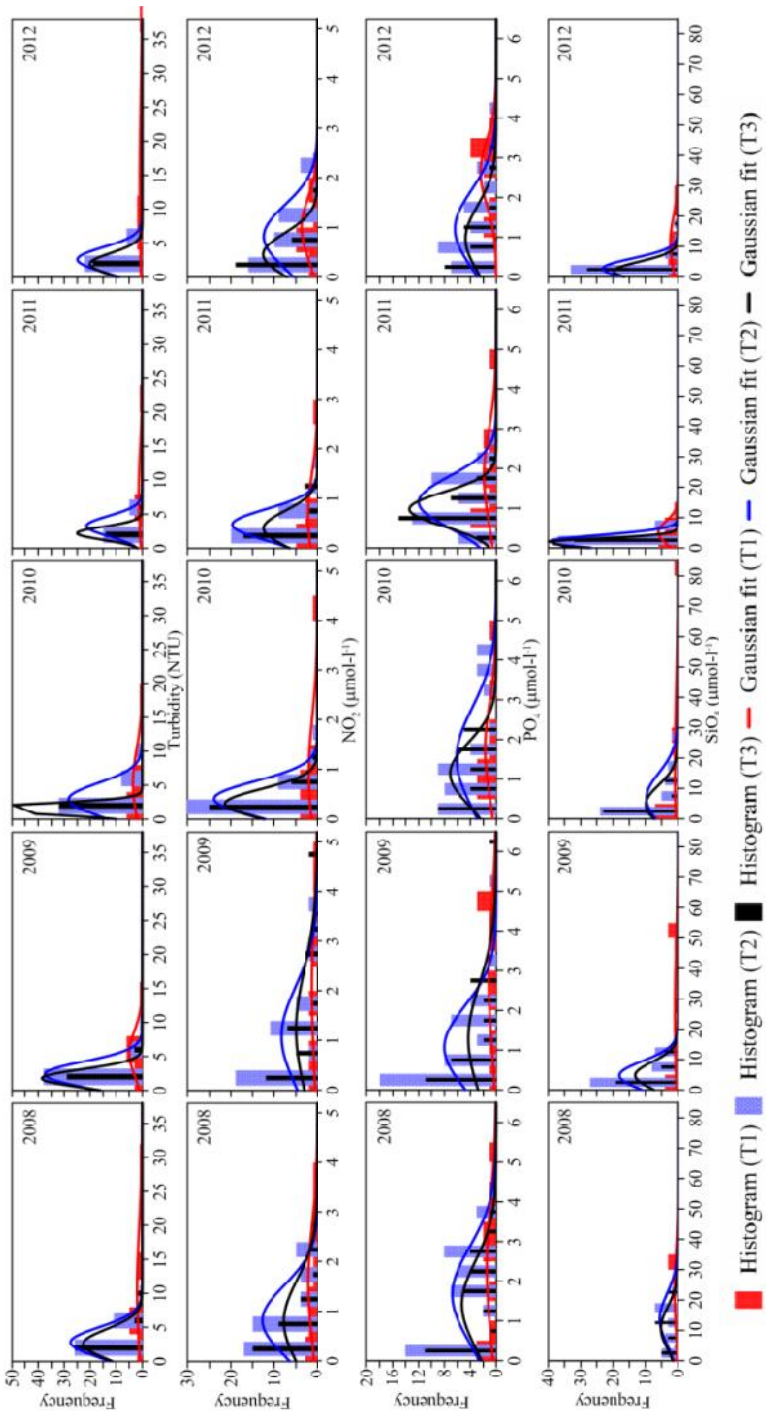

Figure 3.1.b. Histogram showing frequency distribution of turbidity, nitrite (NO_2), phosphate (PO_4) and silicate (SiO_4). The red bar corresponds to stations in transect T1, blue bar corresponds to stations in transect T2 and black bar corresponds to stations in transect T3. Red, blue and black lines represents the normal Gaussian distribution for the transects T1, T2 and T3 respectively

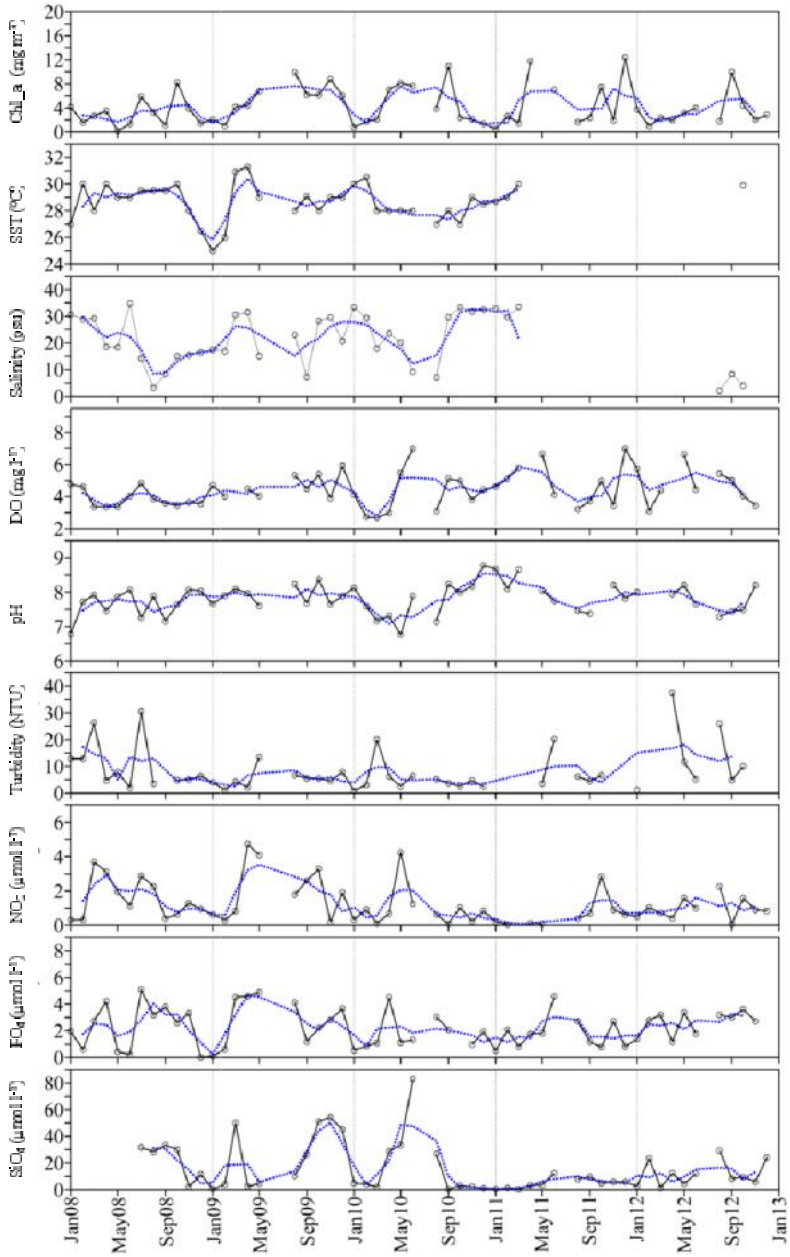

Figure 3.2. Time-series distribution of mean chlorophyll-a (chl-a), sea surface temperature (SST), surface salinity, dissolved oxygen (DO), pH, turbidity, nitrite (NO_2), phosphate (PO_4), silicate ($Si0_4$) corresponding to stations in transect T1. The dotted line represents trend in variability.

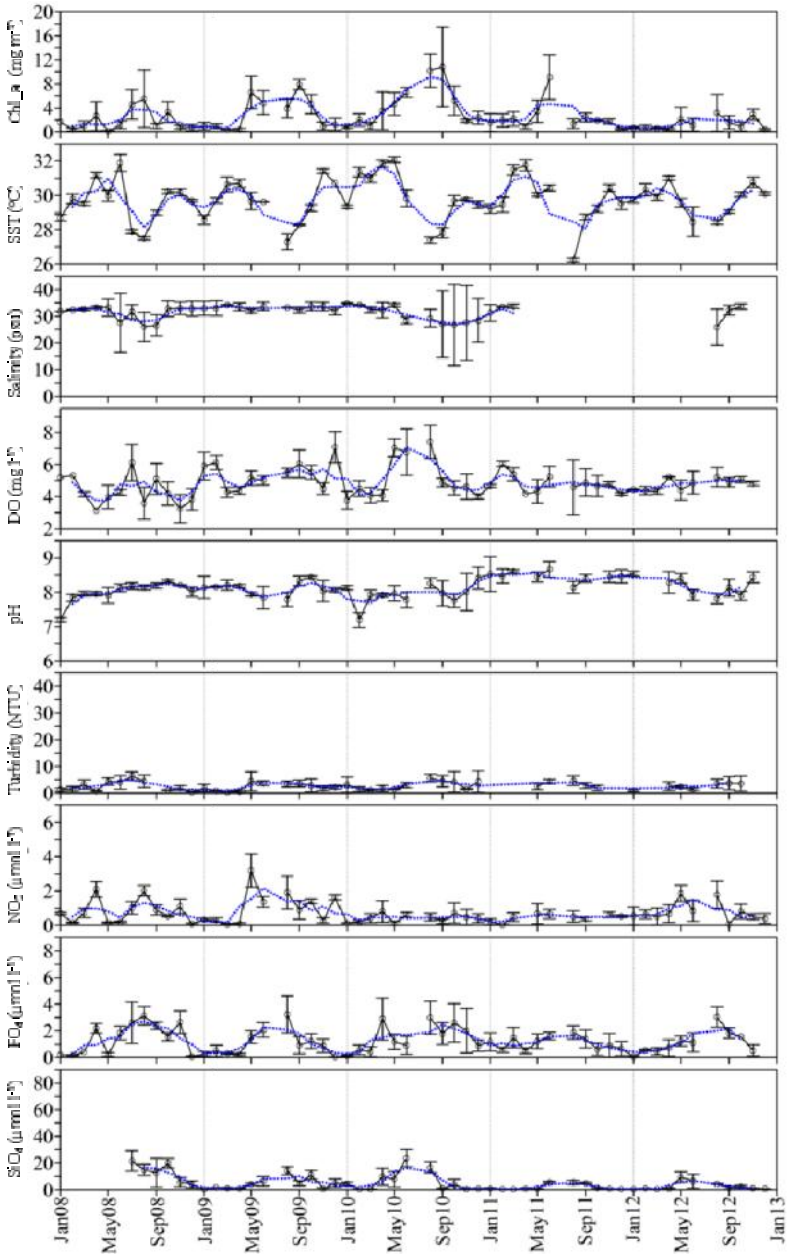

Figure 3.3: Time-series distribution of mean chlorophyll-*a* (chl-*a*), sea surface temperature (SST), surface salinity, dissolved oxygen (DO), pH, turbidity, nitrite (NO_2), phosphate (PO_4) and silicate (SiO_4) corresponding to stations in transect T2. The vertical bars represent standard deviation. The dotted line represents trend in variability.

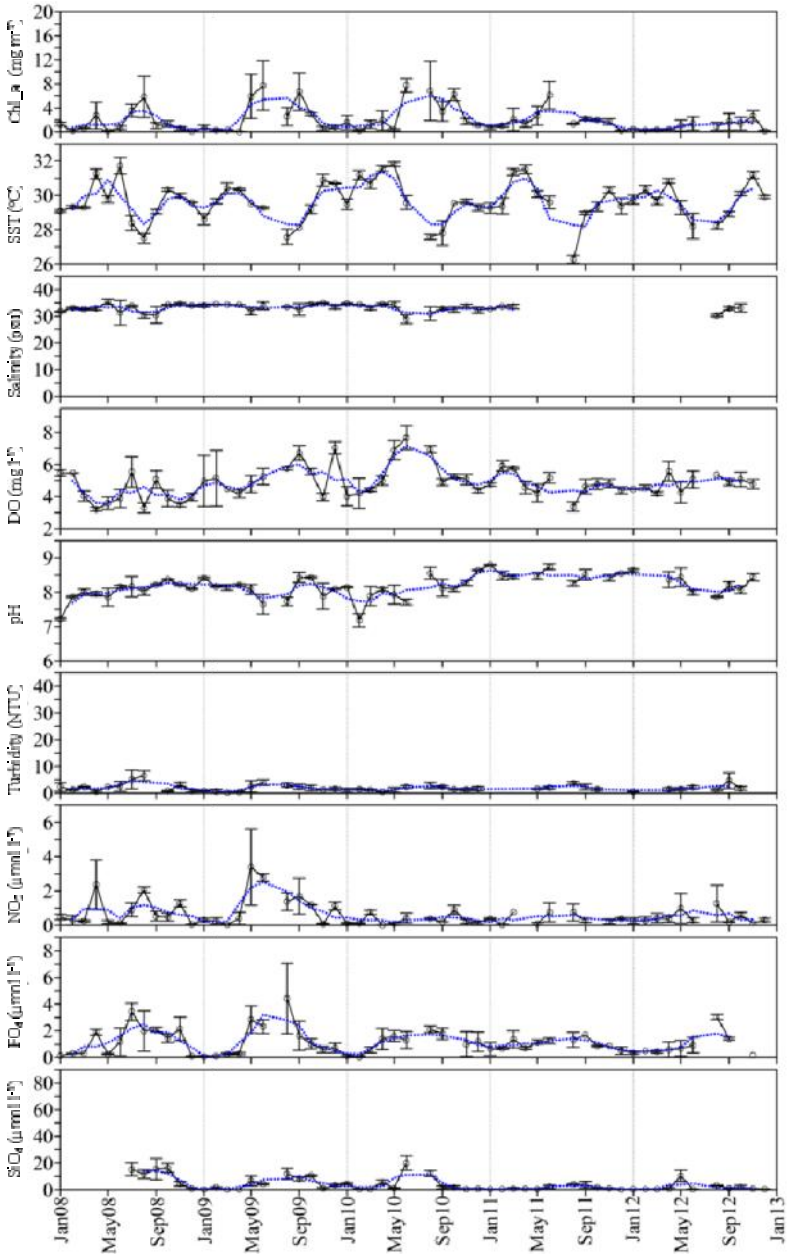

Figure 3.4: Time-series distribution of mean chlorophyll-*a* (chl-*a*), sea surface temperature (SST), surface salinity, dissolved oxygen (DO), pH, turbidity, nitrite (NO_2), phosphate (PO_4) and silicate (SiO_4) corresponding to stations in transect T3. The vertical bars represent standard deviation. The dotted line represents trend in variability.

Chl-*a* was found to be in the range of 0.17 to12.34, 0.08 to 18.33 and 0.021 to 12.42 mg m^{-3} at T1, T2 and T3 respectively. In general, it was found that stations at T1 exhibit maximum variability. However, T2 and T3 showed similar trend with marginal difference in the variability. In all the years, the peak frequency at T1 was found high in magnitude followed by T2 and T3. The Gaussian distribution showed maximum occurrence of chl-*a*, at T1, for years 2008, 2009, 2010, 2011 and 2012 between 3 to 4, 6 to 7, 2 to 3, 7 to 8 and 3 to 4 mg m^{-3} respectively. At T2, the Gaussian distribution showed peak at 0 to 1, 0 to 1, 1 to 2, 0 to 1 and 0 to 1 mg m^{-3} for the years from 2008 to 2012 respectively. At T3, the Gaussian distribution showed peak at 0 to 1, 0 to 1, 0 to 1, 1 to 2 and 0 to 1 mg m^{-3} for the same period. Among these years, maximum variability was seen in 2010 (T1: 0.786 to 10.88, T2: 0.52 to 18.33 and T3: 0.136 to 12.42) whereas the minimum was observed during the year 2012 (T1: 0.972 to 9.97, T2: 0.127 to 6.708 and T3: 0.117 to 3.33).

SST was found to in the range of 25 to 31.3°C, 26.1 to 32.3 °C and 26.05 to 32.1°C at T1, T2 and T3 respectively. In general, it was found that stations at T1 exhibit maximum variability. However, T2 and T3 showed similar trend with marginal variability. In all the years, the peak frequency at T1 was found high in magnitude followed by T2 and T3. The Gaussian distribution showed maximum occurrence of SST, at T1, for the years 2008, 2009, 2010, 2011 and 2012 between 29 to 30 °C, 28.5 to 29°C, 27.5 to 28°C, 28.5 to 29°C and 25 to 25.5°C respectively. At T2, the Gaussian distribution showed peak at 30 to 30.5°C, 29.5 to 30°C, 29.5 to 30°C, 29 to 29.5°C and 29.5 to 30°C for the years from 2008 to 2012 respectively. At T3, the Gaussian distribution showed peak at 29 to 29.5°C, 29 to 30°C, 29 to 30°C, 29 to 29.5 °C and 29.5 to 30 °C for the same period. Among these years, maximum variability was observed during the year 2010 (T1: 27 to 30.5°C, T2: 27.16 to

32.31°C and T3: 27.13 to 31.96°C) whereas the minimum was observed during the year 2012 (T2: 27.31 to 31.12°C and T3: 27.65 to 31.43°C).

Salinity was found to be in the range of 2.25 to 34.69, 3.97 to 35.72 and 26.01 to 36.1 psu at T1, T2 and T3 respectively. The highest values in the salinity were found during pre-monsoon in all the years except 2010 and 2012, during these years the salinity was high at post-monsoon season. In general, it was found that stations at T1 exhibit maximum variability. However, T2 and T3 showed similar trend with marginal variability. In all the years, the peak frequency at T1 was found to be at the high magnitude followed by T2 and T3. The Gaussian distribution showed maximum occurrence of salinity, at T1, for the year 2008, 2009, 2010, 2011 and 2012 was 15 to 20 psu, 15 to 26psu, 30 to 35psu, 30 to 35psu and 0 to 5 psu respectively. At T2, the Gaussian distribution showed peak at 31 to 34psu, for all the years from 2008 to 2012. At T3, the Gaussian distribution showed peak at 32 to 33 psu for all the years from 2008 to 2012. Between different years, maximum variability was observed during 2010 (T1: 7.15 to 33.4 psu, T2: 3.97 to 35.09 psu and T3: 27.39 to 35.0 psu) whereas the minimum was observed during the year 2012 (T2: 15.88 to 35.09 psu and T3: 29.99 to 34.27 psu).

Dissolved oxygen (DO) was found to be in the range of 2.68 to 7.0, 2.22 to 8.5 and 3.0 to 8.2 mg l^{-1}at T1, T2 and T3 respectively. In general, it was found that stations at T1 exhibit maximum variability. However, T2 and T3 showed similar trend with marginal variability. In all the years, the peak frequency at T1 was found to be at the high magnitude followed by T2 and T3. The Gaussian distribution showed maximum occurrence of DO, at T1, for the year 2008, 2009, 2010, 2011 and 2012 and was 3 to 4, 4 to 4.5, 2.5 to 3, 6.5 to 7 and 4 to 4.5mg l^{-1}respectively. At T2, the Gaussian distribution showed peak at 4 to 4.5, 5 to 5.5, 4.5, 5 and 4.5 to 5mg $l^{-1}$for the years 2008 to 2012

respectively. At T3, the Gaussian distribution showed peak at 3 to 4, 5.5 to 6, 4 to 5.5, 4.5 to 5 and 4.5 to 5 mg $l^{-1}$for the years 2008 to 2012 respectively. Between the different years, maximum variability was observed during 2010 (T1: 2.68 to 7, T2: 3.3 to 8.5 and T3: 3.18 to 8.2mg l^{-1}) whereas the minimum was observed during the year 2012 (T1: 3.09 to 6.63, T2: 3.49 to 5.91 and T3: 3.49 to 6mg l^{-1}).

pH was found to be in the range of 6.76 to 8.76, 7.01 to 8.94 and 7.07 to 8.81 at T1, T2 and T3 respectively. In general, it was found that stations at T1 exhibit maximum variability. However, T2 and T3 showed similar trend with marginal variability. In all the years, the peak frequency at T1 was found to be at the high magnitude follows by T2 and T3. The Gaussian distribution showed maximum occurrence of pH, at T1, for the year 2008, 2009, 2010, 2011 and 2012 and was 7.75 to 8.75, 7.5 to 7.75, 8 to 8.75, 8 to 8.75 and 7.25 to 7.5 respectively. At T2, the Gaussian distribution showed peak at 8 to 8.25, 8 to 8.25, 7.75 to 8, 8.5 to 8.75 and 7.5 to 7.75 for the year from 2008 to 2012 respectively. At T3, the Gaussian distribution showed peak at 8 to 8.25, 8 to 8.25, 8 to 8.25, 8.5 to 8.75 and 8 to 8.5 for the year from 2008 to 2012 respectively. Between the different years, maximum variability was seen during 2010 (T1: 6.76 to 8.78, T2: 7.01 to 8.61 and T3: 7.07 to 8.67) whereas the minimum was observed during the year 2011 (T1: 7.37 to 8.67, T2: 7.77 to 8.94 and T3: 8.17 to 8.81).

Turbidity was found to be in the range of 0.87 to 37.6, 0.15 to 9.99 and 0.097 to 8.51 NTU at T1, T2 and T3 respectively. In general, it was found that stations at T1 exhibit maximum variability. However, T2 and T3 showed similar trend with marginal variability. In all the years, the peak frequency at T1 was found to be at the high magnitude follows by T2 and T3. The Gaussian distribution showed maximum occurrence of turbidity, at T1, for the year

2008, 2009, 2010, 2011 and 2012 and was 11 to 15, 4 to 7, 0 to 4, 4 to 7 and 4 to 11 NTU respectively. At T2 and T3, the Gaussian distribution showed peak at 1 to 4 for the all the years from 2008 to 2012. Between the different years, maximum variability was seen during 2008 (T1: 2.06 to 30.5NTU, T2: 0.26 to 8.66 NTU and T3: 0.2 to 8.51NTU) whereas the minimum was observed during the year 2010(T1: 0.87 to 20NTU, T2: 0.59 to 9.99 NTU and T3: 0.097 to 3.62NTU).

Nitrite was found to be in the range of 0.037 to 4.71, 0.018 to 3.82 and 0.013 to 4.69 µmol l^{-1}at T1, T2 and T3 respectively. In general, it was found that stations at T1 exhibit maximum variability. However, T2 and T3 showed similar trend with marginal variability. In all the years, the peak frequency at T1 was found to be at the high magnitude follows by T2 and T3. The Gaussian distribution showed maximum occurrence of Nitrite, at T1, for the year 2008, 2009, 2010, 2011 and 2012 and was 0 to 0.5, 0 to 1, 0 to 1, 0 to 0.5 and 0.5 to 1µmol l^{-1} respectively. At T2 and T3, the Gaussian distribution showed peak at 0 to 0.5 for all the years from 2008 to 2012. Between the different years, maximum variability was seen during 2009 (T1: 0.17 to 4.71µmol l^{-1}, T2: 0.021 to 3.82 µmol l^{-1} and T3: 0.021 to 4.69µmol l^{-1}) whereas the minimum was observed during the year 2010 (T1: 0.089 to 4.23µmol l^{-1}, T2: 0.021 to 1.58 µmol $l^{-1}$and T3: 0.017 to 1.208µmol l^{-1}).

Phosphate was found to be in the range of 0.021 to 5.1, 0.004 to 5.21 and 0.021 to 6.3 µmol l^{-1}at T1, T2 and T3 respectively. In general, it was found that stations at T1 exhibit maximum variability. However, T2 and T3 showed similar trend with marginal variability. In all the years, the peak frequency at T1 was found to be at the high magnitude follows by T2 and T3. The Gaussian distribution showed maximum occurrence of phosphate, at T1, for the year 2008, 2009, 2010, 2011 and 2012 and was 0 to 0.5, 4.5 to 5, 0.5 to

1.5, 0.5 to 1 and 3 to 3.5 respectively. At T2, the Gaussian distribution showed peak at 0 to 0.5, 0 to 0.5, 1 to 1.5, 0.5 to 1 and 0.5 to 1 µmol $l^{-1}$for the year from 2008 to 2012 respectively. At T3, the Gaussian distribution showed peak at 0 to 0.5, 0 to 0.5, 0 to 0.5, 0.5 to 1 and 0 to 0.5 µmol $l^{-1}$for the year from 2008 to 2012 respectively. Between the different years, maximum variability was seen during 2010 (T1: 0.537 to 4.5, T2: 0.115 to 4.48 and T3: 0.021 to 2.317µmol l^{-1}) whereas the minimum was observed during the year 2011 (T1: 00.516 to 4.59, T2: 0.105 to 2.59 and T3: 0.193 to 2.06µmol l^{-1}).

Silicate was found to be in the range of 0.307 to 82.96, 0.03 to 32.29 and 0.094 to 24.92 µmol l^{1} at T1, T2 and T3 respectively. In general, it was found that stations at T1 exhibit maximum variability. However, T2 and T3 showed similar trend with marginal variability. In all the years, the peak frequency at T1 was found to be at the high magnitude follows by T2 and T3. The Gaussian distribution showed maximum occurrence of silicate, at T1, for the year 2008, 2009, 2010, 2011 and 2012 and was 30 to 35, 0 to 5, 0 to 5, 0 to 5 and 0 to 15 µmol l^{1} respectively. At T2, the Gaussian distribution showed peak at 15 to 20 for the year 2008 0 to 5 for all the years from 2009 to 2012 respectively. At T3, the Gaussian distribution showed peak at 10 to 15 µmol l^{1} for the year 2008, 0 to 5 for all the years from 2009 to 2012. Between the different years, maximum variability was seen during 2010 (T1: 0.35 to 82.96 µmol l^{1}, T2: 0.27 to 29.76 µmol l^{1} and T3: 0.334 to 24.92 µmol l^{1}) whereas the minimum was observed during the year 2011 (T1: 0.307 to 12.41 µmol l^{1}, T2: 0.16 to 6.57 µmol l^{1} and T3: 0.094 to 5.57 µmol l^{1}).

Principal Component Analysis (PCA) was applied to the entire data set under two categories- monsoon and nonmonsoon period. Monthly averaged distribution of precipitation and distribution of mean magnitude and resultant current direction of the study area is shown in **figures 3.5 and 3.6.**

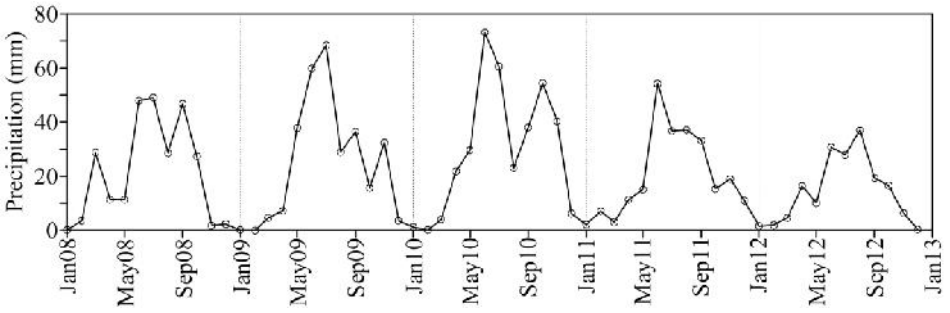

Figure 3.5: Monthly averaged distribution of precipitation in the study area (Data source: http://www.imd.gov.in/).

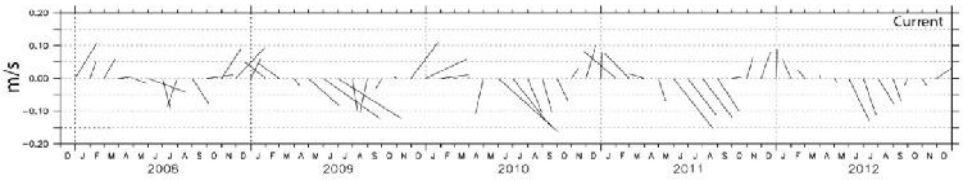

Figure 3.6: Distribution of mean magnitude and resultant current direction in the study area from year 2008 to 2012 (Date source: http://www.esrl.noaa.gov/psd/).

During the non-monsoon period, Fresh water influx was induced by low precipitation. Low oceanic current was also observed during the same period. During this period chl- *a* was also observed in close association with silicate, nitrite and phosphate. Combining the results from the pearson correlation matrices with PCA, it is signified that nitrite and silicate are the major environmental drivers for the phytoplankton growth during non-monsoon period. During this period the fresh water carrying with nutrient is the only source determining the productivity of the water column. PCA analysis also shows salinity and SST was in negative association with chl-*a*. Low saline water with low temperature favored the phytoplankton growth during non monsoon season.

3.3. Discussion

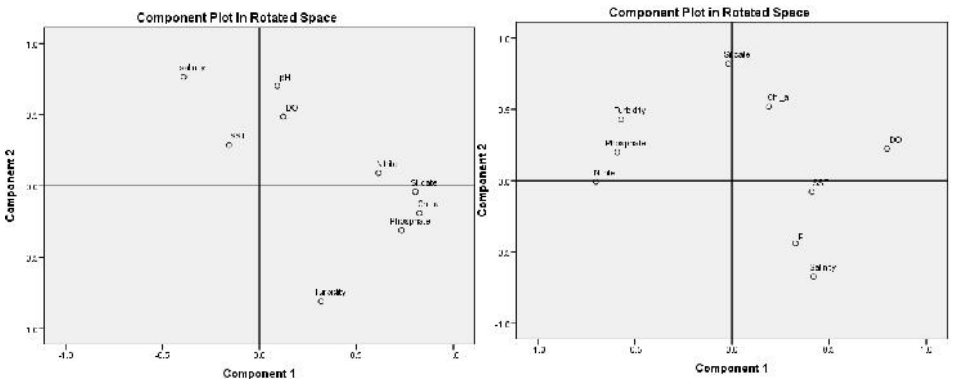

Figure 3.7: PCA analysis for the non monsoon and monsoon period of the different water parameters at the study area

During the monsoon, chl-*a* was not significantly influenced by any of the physical parameters measured. It shows that there is some other parameter which limit the production indexed by chlorophyll a concentration. It may be the combined effect of cloud, sky, turbidity due to upwelling, water column instability due to precipitation and fresh water influx.

Table 3.1. Non-monsoon correlation matrices

Correlations									
	Chl a	**SST**	**Salinity**	**DO**	**pH**	**Turbidity**	**Nitrite**	**Phosphate**	**Silicate**
Chl a	1								
SST	.076	1							
Salinity	-.259**	.115	1						
DO	.080	-.135	.090	1					
pH	-.031	-.171*	.235**	.129	1				
Turbidity	.173*	-.135	-.731**	-.074	-.254**	1			
Nitrite	.219**	.122	-.118	-.015	-.072	.125	1		
Silicate	.424**	.013	-.235**	-.138	-.053	.175*	.250**	.464**	1
**. Correlation is significant at the 0.01 level (2-tailed).									
*. Correlation is significant at the 0.05 level (2-tailed).									

Table 3.2. Monsoon correlation matrices

Correlations									
	Chl a	**SST**	**Salinity**	**DO**	**pH**	**Turbidity**	**Nitrite**	**Phosphate**	**Silicate**
Chl a	1								
SST	-.105	1							
Salinity	-.172	.119	1						
DO	.373**	.065	.093	1					
pH	.005	-.020	.123	-.045	1				
Turbidity	.295**	-.280**	-.264*	-.086	-.173*	1			
Nitrite	.103	-.186*	-.004	-.126	-.194*	.232**	1		
Phosphate	.212*	-.321**	-.221*	.089	-.204*	.331**	.285**	1	
Silicate	.234**	-.139	-.209*	.272**	-.242**	.251**	.004	.275**	1
**. Correlation is significant at the 0.01 level (2-tailed).									
*. Correlation is significant at the 0.05 level (2-tailed).									

Table 3.3: Range, average, standard deviation (in parenthesis) F and p values (using ANOVA) for the water parameters of monsoon and non- monsoon seasons at different tracks, T1, T2 and T3 of the study area.

Parameters	**Monsoon season**			**Non-monsoon season**			**Analysis of variation**	
	T1	**T2**	**T3**	**T1**	**T2**	**T3**	**Spatial**	**Seasonal**
Chl a	0.17-10.88 6.21 (2.52)	0.08-18.33 6.15(3.84)	0.09-11.19 4.71(2.55)	0.46-12.34 4.25(2.51)	0.089-14.16 1.07(1.67)	0.021-12.42 1.05(0.9)	F=5.03 p<0.001	F=5.39 p<0.001
SST	28-29.5 28.52(1.01)	27.31-32.32 28.72(1.46)	27.13-32.14 28.56(1.21)	25-31.3 28.51(1.61)	26.11-32.12 30.16(5.96	26.05-31.8 30.08(0.87)	F=3.46 P<0.05	F=24.61 p<0.001
Salinity	7.22-34.69 12.49(7.92)	8.27-35.72 30.29(5.33)	26.01-36.1 32.15(1.73)	2.25-33.49 24.75(6.78)	3.97-35.09 32.03(5.96)	29.18-35 34.1(0.8)	F=26.15 p<0.001	F=1.21 NS
DO	3.36-7.0 4.51(0.91)	3.14-7.9 5.69(1.34)	3.14-8.2 5.43(1.43)	2.68-6.99 4.02(0.93)	2.22-8.5 4.53(0.95)	3-7.48 4.48(0.98)	F=1.21 NS	F=11.13 p<0.001
pH	6.76-8.24 7.49(0.53)	7.44-8.94 8.01(0.27)	7.38-8.79 7.98(0.32)	6.78-8.78 7.77(0.49)	7.01-8.83 8.07(0.36)	7.07-8.81 8.13(0.37)	F=4.84 p<0.001	F=8.46 p<0.001
Turbidity	2.06-30.5 4.5(1.56)	0.75-9.42 4.06(2.11)	0.37-8.09 3.9(2.11)	0.87-37.6 6.66(4.65)	0.15-9.99 2.28(3.32)	0.097-8.51 1.39(0.92)	F=16.14 p<0.001	F=1.44 p<0.05
Nitrite	0.0704-4.24 2.4(1.2)	0.022-3.82 1.17(1.13)	0.022-4.69 1.53(1.47)	0.037-4.72 1.21(1.27)	0.018-2.84 0.64(0.87)	0.013-3.47 0.45(0.49)	F=1.87 NS	F=4.04 p<0.001
Phosphate	0.21-5.1 2.97(1.57)	0.112-3.62 2.07(1.17)	0.031-4.03 1.992(0.96)	0.021-4.59 2.28(1.47)	0.004-5.21 1.07(1.15)	0.021-6.3 0.77(0.76)	F=6.36 p<0.001	F=6.14 p<0.001
Silicate	3.17-82.96 26.25(8.2)	0.351-32.29 11.27(8.41)	0.412-24.92 8.83(6.62)	0.031-54.08 16.39(19.97)	0.03-24.1 4.71(5.97)	0.094-20.29 3.7(4.72)	F=10.47 p<0.001	F=6.34 p<0.001

A significant spatial and seasonal variation in all the physico-chemical and biological parameters observed during the study pointed that, monsoon and dry season periods were characterized by different physico-chemical and biological properties. The physico chemical variability at SEAS is influenced by circulation, and ocean atmosphere coupling. While there was evidence that physical factors as fresh water influx, precipitation and current pattern affected nutrient distribution along the salinity gradient, it was an interplay between nutrient availability, light and mixing that appeared to be important in regulating primary production, which is indexed as chlorophyll *a* concentration in this study. Primary production indicated by the chl-a, is high during monsoon period and during intra-monsoon high variability in chl-a was also measured and nutrients were not limiting factors of production as shown in the PCA analysis results. Higher variability in the abiotic condition implies a more unstable environment. This indicates that, in spite of strong seasonality, these coastal waters are highly productive during most of the time as compared to oceanic region supporting a large fishery. But the sustainability and precise prediction of this ecosystem can be explained only by continuing the long term time series analysis.

References

Balachandran, K.K. 2004. Does subterranean flow initiate mud banks off the southwest coast of India? Estuarine coastal and shelf science. 59: 589-598.

Basil, M. 1983. Studies on upwelling and sinking in the seas around India. *Ph.D. Thesis*, Cochin University of Science and Technology.

Bauer, J. E., Cai, W. J., Raymond, P. A., Bianchi,T. S., Hopkinson, C. S. and Regnier, P. A. G. 2013. The changing carbon cycle of the coastal ocean. Nature. 504: 61–70 doi:10.1038/nature12857

Chavez, F. P. 1989. Size distribution of phytoplankton in the Central and Eastern Tropical Pacific. Global Biogeochemical Cycles. 3: 27–35.

Cloern, J. E. 2001. Our evolving conceptual model of the coastal eutrophication problem. Marine ecology progressive series. 210: 223-253.

Gopinathan, C. K. and Qasim, S. Z. 1974. Mud Banks of Kerala – Their formation and characteristics. Indian Journal of Geo-Marine Science. 3: 105-114.

Grant, G. M., and Gross, E. 1996. Oceanography – a view of the earth. USA, Prentice-Hall.

Huot, Y., Babin, M., Bruyant, F., Grob, C., Twardowski, M. S., and Claustre, H. 2007. Relationship between photosynthetic parameters and different proxies of phytoplankton biomass in the subtropical ocean. Biogeosciences. 4(5): 853-868.

Legendre, L., & Le-Fevre, J. 1989. Hydrodynamical singularities as controls of recycled versus export production in oceans. In W. H Berger, V. S. Smetacek & G. Wefer (Eds.), Productivity of the oceans: present and past (pp.49–63).

Malone, T. C. 1980. Size-fractionated primary productivity of marine phytoplankton. In P. G. Falkowski (Ed.), Primary productivity in the sea (p. 319). New York: Plenum.

Nair, P. V. R., Samuel, S., Joseph, K. 1. and Balachandran, V. K. 1973. Primary production and potential fishery resources in the seas around India. In: Proc. Symp. Living Resources of Seas around India, 1960. ICAR Special publication, CMFRI, Cochin: 184-198.

Naqvi, S. W. A., D.A. Jayakumar. RV., Narvekar, H. Naik,V.V.S.S. Sarma, W. D'Souza, S. Joseph & M.D. George. 2000. Increased marine production of N_2O due to intensifying anoxia on the Indian continental shelf. Nature. 408:346-349.

Pankajakshan, T. and Rama, Raju., D. V. 1987. Intrusion of Bay of Bengal water into Arabian Sea along the west coast of India during northeast monsoon. In: Contibution *in Marine Sciences* - Dr. S.Z. Qasim felicitation volume. 237-244.

Platt, T. 1986. Primary production of the ocean water column as a function of surface light intensity, Algorithms for remote sensing. Deep-Sea Research. 31: 1-11.

Platt, T., Subba, Rao., D. V., and Irwin, B. 1983. Photosynthesis of picoplankton in the oligotrophic ocean. Nature. 301: 702–704.

Prasad, R.R., and Nair, P. V. R. 1960. A preliminary account of primary production and its relation to fisheries of the inshore waters of the Gulf of Mannar. Indian Journal of Geo-Marine. Science. 7: 165-168.

Ramamritham, C. P. and Rao, D. S. 1973. On upwelling along the west coast of India. Journal of Marine Biological Association of India. 15: 411-417.

Raymont, J. E. G. 1980. Plankton and productivity in the oceans. In Phytoplankton. (Vol.1). Pergamon.

Srinivas, K., Dineshkumar, P.K. 2006. Atmospheric forcing on the seasonal variability of sea level at Cochin, southwest coast of India. Continental Shelf Research. 26: 1113–1133.

Usha, B., Shaju, S.S., Ragesh, N., Meenakumari, B., Ashraf, P.M. 2014. Observation on bio-optical properties of a phytoplankton bloom in coastal waters off Cochin during the onset of southwest monsoon. India Journal of Geo-Marine Science. 43(2): 289-296.

Weyhenmeyer, G. A., Blenckner, T., and Pettersson, K. 1999. Changes of the plankton spring outburst related to the North Atlantic Oscillation. Limnology and Oceanography. 47: 1788–1792.

Wooster, W. S., Schaefer, M. B. and Robinson, M. K. 1967. Atlas of the Arabian Sea for Fishery' Oceanography. Institute of Marine Resources. University of California. 12-67.

Chapter 4

STUDIES ON PHYTOPLANKTON ABSORPTION COEFFICIENT AND DERIVATIVE ANALYSIS

4.1. Introduction

Phytoplankton modifies the optical properties of the seawater by altering the subsurface light field (Babin et al. 2003; Tzortziou et al. 2007; Bricaud 2012). This property of phytoplankton plays an important role in the remote estimation of aquatic biomass (Morel 1988). Knowledge of phytoplankton light absorption coefficients are used to predict the light energy absorbed by the phytoplankton and its utilization for photosynthesis (Bricaud et al. 2004). The variations in the optical properties of coastal waters are mainly attributed to the absorption by chlorophyll *a* (Chl-a) and other accessory pigments present in the phytoplankton. Coastal waters also receive dissolved and particulate materials from several sources that make them optically complex (IOCCG 2000). The process of light absorption by phytoplankton is a complex process and is a function of shape, size and optical properties of the cell (Ferreira 2013; Fujiki and Taguchi 2002). The important sources of variability in absorption come from the contributions of cellular pigment composition, accessory pigments, detritus absorption and pigment packaging effect (Bricaud et al. 2004 and Baird 2013).

The accessory pigments play an important role in the optical characteristics of most natural waters, especially in the 460 – 640 nm regions (Bidigare et al. 1989a). Different phytoplankton species have characteristic absorption peaks, which are related to the pigment composition (Mao et al.

2010). In addition, certain accessory pigments are found exclusively in certain phytoplankton groups and could be used as markers (Jeffry, Vesk 1997) to study the seasonal variation of phytoplankton in natural waters. Studying the phytoplankton biomass variability is essential for understanding the food web and its influence on the optical properties of aquatic ecosystem. Particulate detritus matter also makes large contributions to absorption especially in the blue and ultraviolet region of the spectrum (Stramski 2007; Kishino et al. 1986; Maske, Haardt 1987; Mitchell, Kiefer 1988).

The absorption spectra of phytoplankton are complex due to the mixtures of pigments and associated proteins; it is difficult to identify these components by optical analysis. The phytoplankton specific absorption coefficient (a^*_{ph} (λ)) spectra from coastal environment often lacks sharply defined peaks or shoulders due to the overlapping of pigment absorption bands. The derivative analysis was used as means of obtaining estimates of photosynthetic pigment concentrations in natural samples where absorption can be strongly influenced by detrital matter (Bidigare et al. 1989b). Recently Rosado-Torres (2008) used derivative analysis to study the phytoplankton dynamics and quantify the chlorophyll *a* in Mayagüez Bay. The utility of derivative analysis in highlighting the accessory pigment absorption during a bloom condition in a coastal bay was demonstrated by Vijayan and Somayajula, (2014). The 4^{th} derivative spectra computed for each *in vivo* absorption spectrum and amplitude of maxima obtained is often proportional to the concentration of the chromoprotein, which provides quantitative information on chlorophyll *a* and other accessory pigments.

The bio-optical data from the region are meager and this study is the first to report on the coastal waters of Southeastern Arabian Sea coast to characterize the absorption nature of the phytoplankton. Since information on accessory

pigments can help the differentiation into major phytoplankton classes or taxonomic groups (Hoepffner, Sathyendranath 1993, Coupel et al. 2014), it would be a great enhancement to ocean-color remote sensing if information regarding accessory pigments can also be retrieved from water color. For this purpose, one of our approaches in this paper is to retrieve dominant phytoplankton species and its characteristic accessory pigments from 4th derivative hyperspectral analysis of absorption by phytoplankton (a_{ph}) and thereby to study the variability in phytoplankton absorption in Arabian Sea.

4.2. Results

4.2.1. Variation in Phytoplankton Specific Absorption Coefficient

The **Figure 4.1.** shows the variation of phytoplankton specific absorption coefficient of different months during the study period and illustrates the spatial and temporal variation in spectral shape and magnitude.

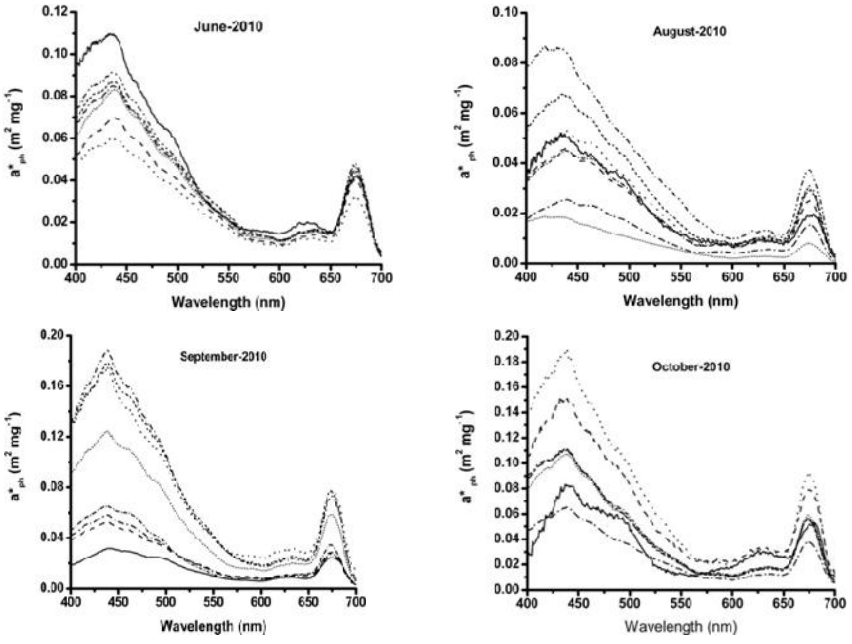

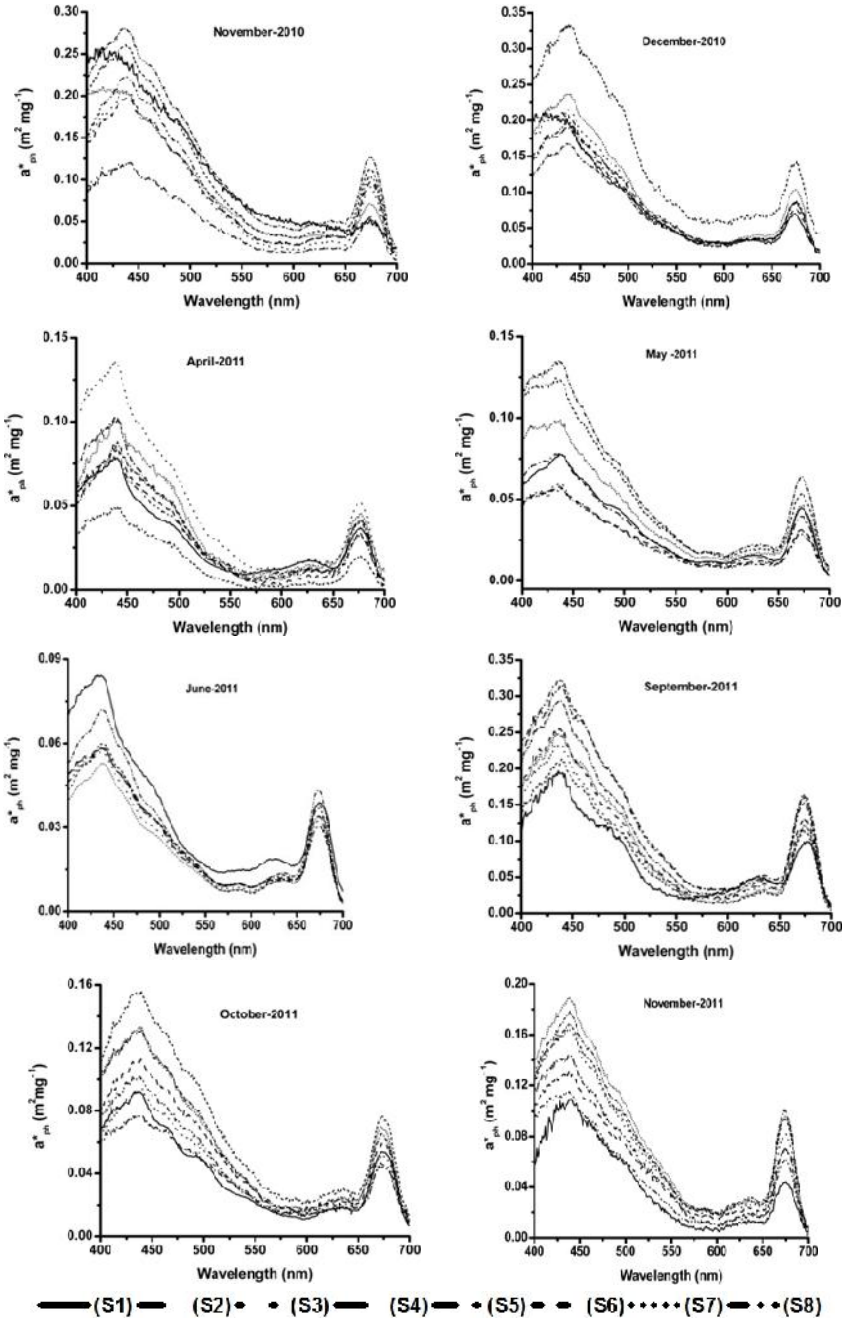

Figure 4.1. Plots showing the spectra of surface chlorophyll specific absorption by phytoplankton ($a^*_{ph}(\lambda)$) against wavelength (nm) for the study area covering Station 01 to Station 08 during 2010-2011.

Phytoplankton specific absorption coefficient, at 440 nm, ($a^*_{ph}(440)$) varied from 0.018 to 0.32 m^2 mg^{-1} with an average value of 0.12 during the study period. In the red region, a^*_{ph} (675) varied from 0.0005 to 0.16 m^2 mg^{-1} with an average value 0.054 m^2 mg^{-1}andChl- a concentration from 0.05 to 12.4 mg m^{-3} with an average value of 3.73 mg m^{-3}. During June, at the onset of south west monsoon for both the year 2010 and 2011, a^*_{ph} (440) exhibited a low value with an average of 0.0.015 m^2 $mg^{-1}$and 0.062 m^2 mg^{-1} with high Chl-a concentration 7.133±1.017 mg m^{-3} and 7.710±3.107 mg m^{-3} respectively. During November and December high a^*_{ph} (440) was measured. The scatter plot between a^*_{ph} at 440nm and 675nm with Chl-a are shown in **Figure 4.2**.

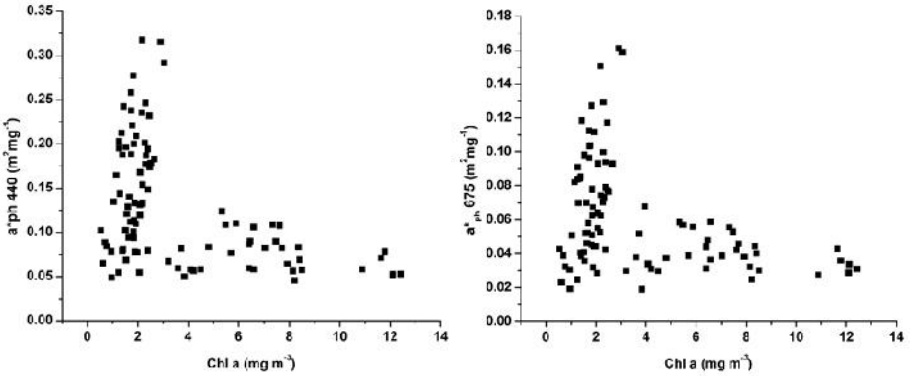

Fig 4.2. The variation in surface chlorophyll specific absorption by phytoplankton (a^*_{ph}) at 440nm and 675 nm (Y axis) as a function of Chlorophyll *a* concentration (X axis) during 2010-2011 in the study area

This shows that the absorption of Chl-a within algal cells is not a linear function of concentration, and specific absorption coefficient not constant. This might be due to either combined effect of packaging, where the Chl-a concentration per phytoplankton cell increases and their absorption efficiency decreases (Bricaud et al. 2012) or internal pigment variation due to change in the dominating phytoplankton species.

4.2.2. Spatial and Temporal Variation of Dominant Phytoplankton Species

The phytoplankton species which dominated in Southeastern coastal Arabian Sea during the study period was shown in **Table 4.1**.

Table 4.1 List of dominant species present in the study area during June 2010 to November 2011

Station	Jun-10	Aug-10	Sep-10	Oct-10	Nov-10	Dec-10	Apr-11	May-11	Jun-11	Sep-11	Oct-11	Nov-11
S1	C	Q	T	O	F	P	E	R	I	K	L	G
S2	E	C	K	C	M	S	U	B	C	B	I	S
S3	K	D	C	C	K	O	U	R	C	T	E	Q
S4	C	G	Q	S	T	S	A	B	C	K	I	K
S5	C	G	Q	S	K	L	C	C	C	S	L	K
S6	C	C	M	C	K	N	U	R	C	K	U	K
S7	C	G	Q	C	K	M	U	R	T	I	H	K
S8	C	G	K	C	K	B	U	R	R	K	I	L

A-*Anabaena* spp., B-*Asterionella* spp., C-*Chaetoceros* spp., D-*Corethron* spp., E-*Coscinodiscus* spp., F-*Cyclotella* spp., G-*Dinophysis* spp., H-*Eucampia* spp., I-*Gyrodinium* spp., J-*Gyrosigma* spp., K-*Leptocylindrus* spp., L-*Navicula* spp., M-*Nitzschia* spp., N-*Peridinium* spp., O-*Prorocentrum* spp., P-*Pseudonitzschia* spp, Q-*Rhizosolenia* spp., R-*Skeletonema* spp., S-*Thalasionema* spp., T-*Thalassiosira* spp., U-*Trichodesmium* spp

During 2010 monsoon, centric diatoms like *Chaetoceros* spp. dinoflagellates like *Dinophysis* spp. and pennate diatoms like *Rhizosolenia* spp. dominated. During October both the pennate and centric diatoms dominated in the study area. During November 2010, centric diatoms dominated while in December the dominance was by pennate diatoms and dinoflagellates. During April blue green algae like *Trichodesmium* spp. was abundant while in May it was centric and pennate diatoms. During June, September and November 2011, pennate and centric diatoms dominated in the study area. (Minu et al. 2014).

4.2.3. Derivative Analysis of Phytoplankton Absorption

Derivative analysis for the absorption data of a_p and a_{ph} (λ) of 1 nm resolution for the study area are shown in **Figure 4.3.** & 4.**4** respectively.

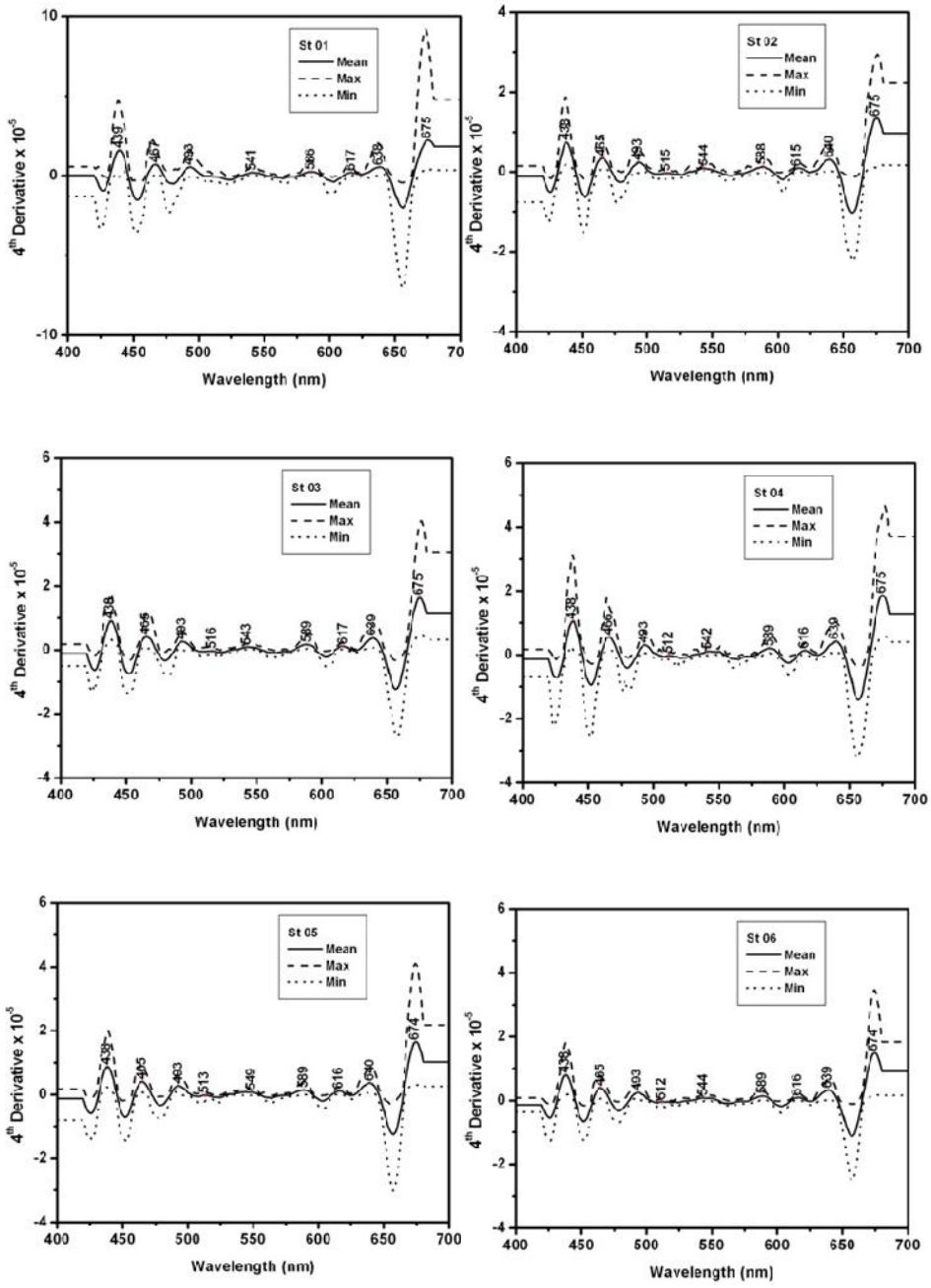
St 01
Mean
Max
Min
St 02
St 03
St 04
St 05
St 06
4th Derivative x 10-5
Wavelength (nm)

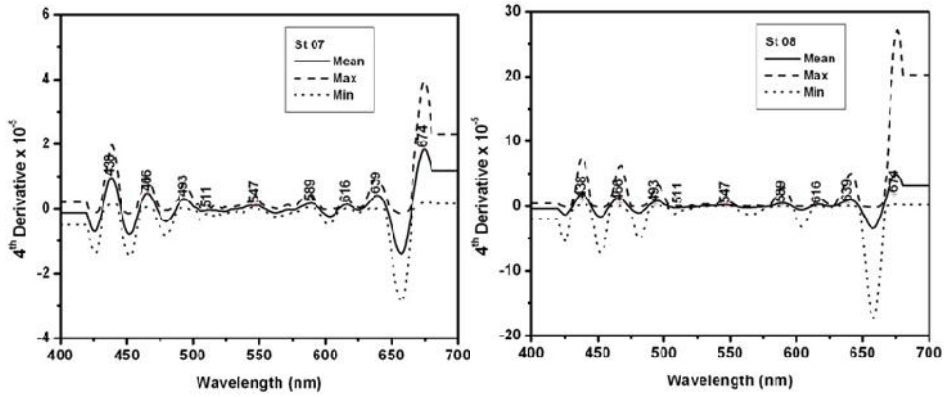

Fig 4.3. Spectra showing 4th derivative analysis of total particulate absorption ($a_p(\lambda)$) against wavelength (nm) in the study area

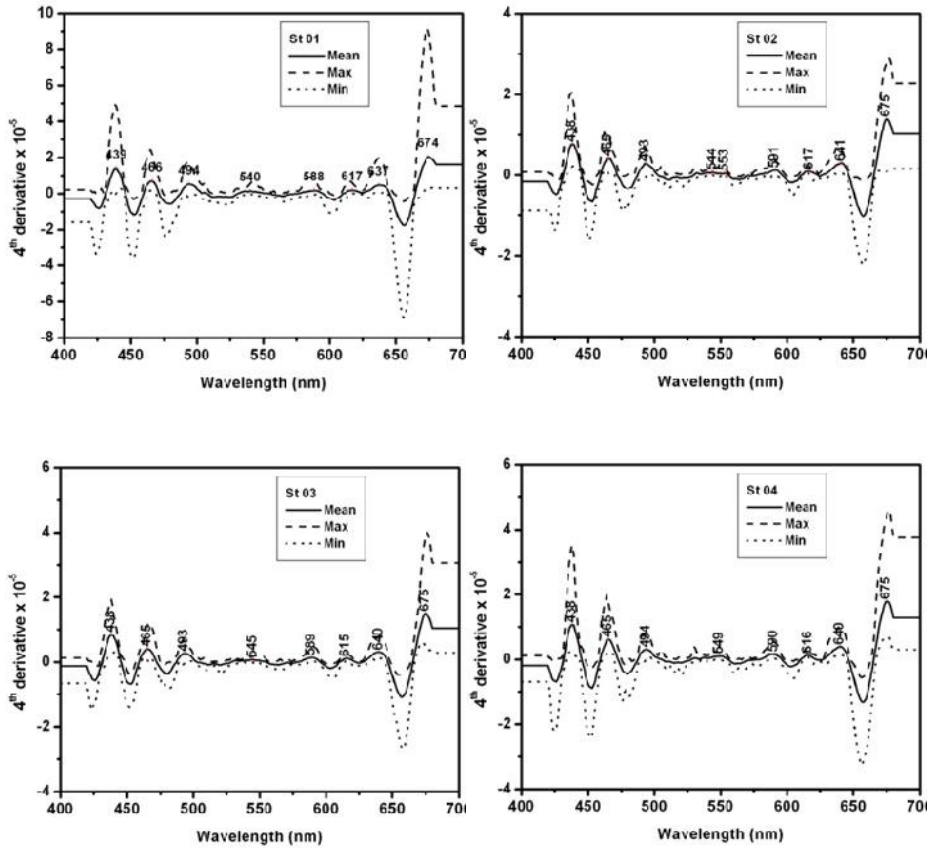

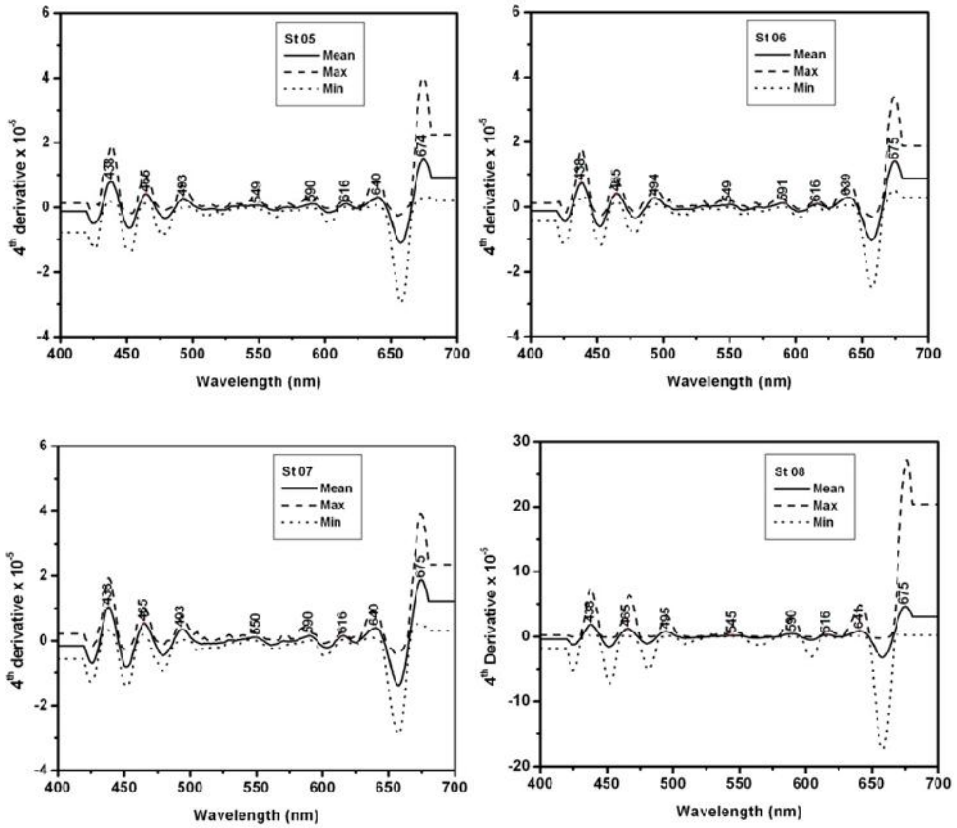

Fig4. 4. Spectra showing 4th derivative analysis of absorption by phytoplankton (a_{ph} (λ)) against wavelength (nm) in the study area

The maxima of the 4th derivative occur close to or at wavelengths where there are absorption peaks attributable to photosynthetic pigments. Since the magnitude of 2nd derivative does not provide a reliable measure of the concentration of photosynthetic pigments, due to the absorption contributed by overlapping pigments effect (Aguirre-Gomez et al. 2001), This study considered only 4th derivative analysis for the identification of absorption peaks. In order to identify the major contributing pigments of the *in vivo* absorption spectra of phytoplankton in coastal waters and compared the wavelength positions of the 4th derivative spectra of total absorption and

phytoplankton absorption with published values and were shown in Table 4.2. The identified positions and the corresponding pigments were also given in Table 4.2. Phytoplankton with pigments Chl-a, Chl-b, Chl-c, Fucoxanthin, Diadinoxanthin, and Phycoerythrobilin dominated in these waters. The comparison analysis of peak position of 4^{th} derivative of a_p and a_{ph} (λ) absorption indicated that the derivative analysis effectively filtered out the contribution of detritus absorption.

The value of the 4^{th} derivative for Chl-a was maximum at 675nm band. The phycoerythrin pigment was present and it was reflected at 495-499 nm peaks. Chl-a specific phytoplankton absorption $a^*_{ph}(\lambda)$ and their 4^{th} derivatives for the whole study in Arabian Sea showed the contribution by major phytoplankton groups from the different peaks identified.

4.3. Discussion

Derivative analysis is a powerful tool to study the phytoplankton dynamics, in the absence of microscopy data, especially in the coastal waters. Spectral derivative analysis has been applied successfully to optical data as a mean to produce wave crests at wavelengths where shoulders and peaks occur in spectroscopy curves (Millie et al., 1995). These wave crests correspond to the absorption peaks of accessory pigments, when derivative analysis is applied to phytoplankton absorption curves. The advantages of this method over solvent extraction and HPLC are that natural samples are processed rapidly with a high degree of precision, no extraction of pigments is needed, several pigments are determined at the same time, and errors due to pigment loss in extraction methods are minimized (Faust and Norris, 1985).

The spectral absorption coefficients obtained during different seasons and geographical regions, lack the sharply defined peaks and shoulders that

are apparent in spectra obtained from phytoplankton cultures. The plot showing the correlation coefficient analysis between Chlorophyll a concentration and coefficients of 4th derivative spectra of total particulate absorption, a_p (λ) and 4th derivative of absorption by phytoplankton, a_{ph}, is given in **Figure 4.5**.

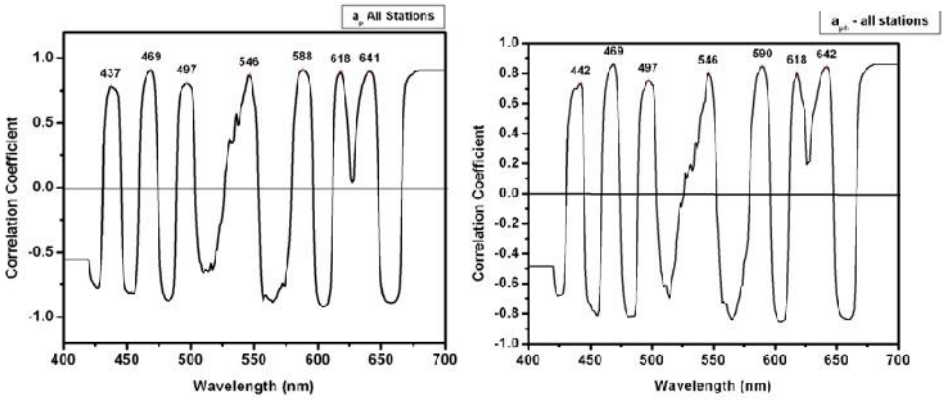

Fig 4.5. Plots showing the correlation coefficient analysis between surface Chlorophyll a concentration and coefficients of 4th derivative spectra of total particulate absorption, a_p (λ) and 4th derivative of absorption by phytoplankton, a_{ph} for the study area during 2010-2011.

The spectral shape and magnitude of the phytoplankton absorption curve reflects the pigment composition, dynamic variation of the species composition and packaging effect. Each species has its unique pigment signature and therefore contributes to the shape of the absorption spectrum. The diatoms which were found dominant phytoplankton group during the study period has marker pigments fucoxanthin and diadinoxanthin (Hsiu-Ping et al. 2002) which has absorption peak at 495, 512 and 541 nm. Phycobilin proteins, which are the light harvesting pigments found in cyanobacteria, rhodophytes and cryptophytes are evinced by peaks at 491-495 nm and at 544 nm especially at station S6, S7 and S8, where numerical abundance of *Trichodesmium* was more. Sometimes due to the overlapping of photosynthetic pigments with bands of absorption causes masking of spectral

absorption features of accessory pigments. This could also arise due to large contributions from detritus matter, which is generally in an oxidized state and lacks well-defined resonances (Babin et al. 2003), is the characteristic feature for coastal waters.

The accessory chlorophylls and carotenoid pigments have their absorption peaks in the 490-550 nm regions. Since Chl-a is the most abundant pigment found in phytoplankton whose absorption maxima is around 438-440 nm and 675-677 nm wavelengths, the accessory pigment's absorption peaks are relatively identified in the 450-550 nm spectral region applying 4^{th} derivative analysis. Other peaks found in the region from 560-618 nm may be accounted for degradation products and Chl-c.

Several works have identified the position of the absorption peaks of phytoplankton pigments with HPLC analysis. Bidigare et al. (1989b); and Coupel et al. (2014); reported absorption peaks for Chl-a at 675 nm, Chl-b at 650 nm and Chl-c at 467 nm. Absorption peaks at 438 and 677 nm were reported for Chl-a and at 466, 589 and 639 nm for Chl-c by Millie et al. (1995); and Chase et al.(2013). Carotenoids, especially fucoxanthin, diadinoxanthin and β-carotene, have peaks reported at 495 nm and in the case of fucoxanthin, at 550-555 nm (Chase et al 2013; Louchard et al. 2002, Gómez et al 2001.). Based on the literature, the peaks found with the 4^{th} derivative analysis in the study area are consistent of Chl- a (440 and 675 nm), Chl-b (465 nm), Chl-c (586 nm, 639 nm) and carotenoid pigments-fucoxanthin (495 and 547 nm) (Table 4.2).

Table 4.2. Summary of photosynthetic pigment absorption maxima determined by derivative analysis.

Pigment group	λ_{max} (Present study)	λ_{max} (Published)	Reference
Chlorophylls			
Chlorophyll *a*	438-440, 675 nm	438, 675 nm	Prezelin and Alberte (1978), Aguirre- Gomez et al (2001)
Chlorophyll b	465 -467 nm	470, 652 nm	Kan and Thornber (1976)
Chlorophyll c	465, 586, 639 nm	460, 640 nm	Mann and Myers (1968), Millie et al. (1997)
Carotenoids			
Fucoxanthin	495, 512, 541 nm	460 – 530 nm	Mann and Myers (1986)
Diadinoxanthin (+carotene)	495 ,512 nm	425 – 500 nm	Mann and Myers (1968)
Phycoerythrin			
Phycoerythrobilin	543,544 nm	543 nm	Ong et al. (1986)
Phycourobilin	491-495	492 nm	Ong et al. (1986), Louchard et al., (2002)

Chl-a is the principal photosynthetic pigment of phytoplankton and is common to all species. Chl-b and Chl-c are very common photosynthetic pigment, found in diatoms, dinoflagellates and other groups. The absorption peaks identified in coastal Arabian Sea are consistent with the dominance of these groups in the phytoplankton community (Table 4.1). Thus the 4th derivative analysis is found as simple and efficient tool for the monitoring of chemotaxonomic markers in phytoplankton assemblages. Some minor variations in the magnitude of the 4thderivative peaks and the appearance of new peaks in the study area suggest that they might be due to the spatial and temporal difference and the influence of rivers as all the stations in the study area is under riverine input, pigment packaging and photoadaption in the trophic condition (Shaw, Purdie 2001, Cleveland 1995, Jyothibabu et al. 2006, Roesler, Barnard 2014). The diatom abundance is high in the proximity of river mouths (Suzuki et al. 2014). Bigidare et al. (1989b) reported good correlation (R^2 = 0.89) between the 4th derivative of $a_{ph}(\lambda)$ at 467,650 and 675 nm vs. Chl-a concentration in the Sargasso Sea. In general, the 4th derivative analysis suggests that even though the relative composition of phytoplankton

community was stable throughout the year, the dominant taxa varied. Peaks identified in the 4th derivative of a_{ph} are by the contribution of all the taxa.

The spectral correlation analysis between the 4th derivative of $a_{ph}(\lambda)$ and Chl-a in the present study confirm such results. High correlation coefficients were also found for the wavelengths associated with carotenoid accessory pigments. In summary, 4th derivative of $a_{ph}(\lambda)$ appears to be a valuable alternative method for the quantification of Chl-a and other pigments in the SEAS from the absorption data. The result of this study would help in choosing spectral regions for Chl-a estimation where interference by accessory pigments is minimal.

4.4. Conclusions

From an optical point of view, the phytoplankton absorption in the coastal SEAS are highly scattering and absorbing, where the phytoplankton absorption in the water varies spatially and temporally with cell size, and taxonomic affiliations. Derivative analysis of the particulate absorption coefficients offers an alternative and efficient means of separating the absorption by specific photosynthetic pigments from that of detritus matter. This study suggests that the 4th derivative analysis appears to be efficient and simple tool for monitoring phytoplankton pigment.

The results obtained support that diatoms are the dominant phytoplankton group in Southeastern Arabian Sea. Phytoplankton communities are highly varying during the study period. Using fourth derivative plots of *in vivo* phytoplankton absorption spectra, ($d^4 a_{ph}(\lambda)$), it is possible to identify several maxima absorption values attributed to different pigments which can be further used for the study of the factors affecting the variation in phytoplankton absorption spectrum to develop the regional algorithm suitable for this region for various the remote sensing applications like prediction of harmful algal blooms.

References

Aguirre-Goméz, R., Weeks, A.R. and Boxall, S.R. 2001. The identification of phytoplankton pigments from absorption spectra. International Journal of Remote Sensing. 22 (2 & 3): 315 - 338.

Babin, M., Stramski, D., Ferrari, G.M., Claustre, H., Bricaud, A., Obolensky, G. and Hoepffner, N. 2003. Variations in the light absorption coefficients of phytoplankton, nonalgal particles, and dissolved organic matter in coastal waters around Europe. Journal of Geophysical Research. 108 (C7): 3211.

Baird, M. E., Ralph, P.J., Wild-Allen, K., Rizwi, F. and Steven, A. D. L. 2013. A dynamic model of the cellular carbon to chlorophyll ratio applied to a batch culture and a continental shelf ecosystem. Limnology and Oceanography. 58: 1215-1226.

Bigidare, R. R., Morrow, J.H., and Kiefer D. A. 1989a. Derivative analysis of spectral absorption by photosynthetic pigments in the Eastern Sargasso Sea. Journal of Marine Research. 47: 323 - 341.

Bidigare, R. R., Schofield, O. and Prezelin, B. B. 1989b. Influence of zeaxanthin on quantum yield of photosynthesis of Synechococcus clone WH7803 (DC2), Marine Ecology Progress Series. 56: 177-188.

Bricaud, A., Claustre, H., Ras, J. and Oubelkheir K. 2004. Natural variability of phytoplanktonic absorption in oceanic waters: Influence of the size structure of algal populations. Journal of Geophysical Research. 109: C11010 doi: 10.1029/2004JC002419.

Bricaud, A., Ciotti, A.M., and Gentili B. 2012. Spatial-temporal variations in phytoplankton size and colored detrital matter absorption at global and

regional scales, as derived from twelve years of SeaWiFS data (1998–2009). Global Biogeochemical Cycles. 26: GB1010, doi: 10.1029/2010GB003952.

Chase, A., Boss, E., Zanevel, R., Bricaud, A., Claustre, H., Ras, J., Dall'Olmo, G. and Westberry T.K. 2013. Decomposition of in situ particulate absorption spectra. Methods in Oceanography. 7: 110–124 doi: 10.1016/j.mio.2014.02.002.

Cleveland, J.B.S. and Weidemann A.D. 1993. Quantifying absorption by aquatic particles: A multiple scattering correction for glass-fiber filters, Limnology and Oceanography.38: 1321- 1327.

Cleveland, J.S. 1995. Regional models for phytoplankton absorption as a function of chlorophyll a concentration Journal of Geophysical Research. Oceans (1978–2012), 100(C7), 13333-13344.

Coupel, P., Matsuoka, A., Ruiz-Pino, D., Gosselin, M., Claustre, H., Marie, D., Tremblay, J.-É., and Babin, M. 2014. Pigment signatures of phytoplankton communities in the Beaufort Sea. Biogeosciences Discussion. 11:14489–14530. doi: 10.5194/bgd-11-14489-2014

Faust, M.A., and Norris, H.A. 1985. In vivo spectrophotometric analysis of photosynthetic pigments in natural populations of phytoplankton. Limnology and Oceanography. 30(6): 985 1316-1322.

Ferreira, A.D., Stramski, C.A.E., Garcia, V.M.T., Garcia, Á.M., Ciotti, and Mendes, C.R.B. 2013. Variability in light absorption and scattering of phytoplankton in Patagonian waters: Role of community size structure and pigment composition. Journal of Geophysical Research. *Oceans* 118: 698–71. doi:10.1002/jgrc.20082.

Fujiki, T, Taguchi, S. 2002. Variability in chlorophyll alpha specific absorption coefficient in marine phytoplankton as a function of cell size and irradiance. Journal of Plankton Research. 24: 859–874.

Hsiu-Ping, L., Gwo-Ching, G. and Tung-Ming, H. 2002. Phytoplankton pigment analysis by HPLC and its application in algal community investigations. Botanical Bulletin Academia Sinica.43: 283 - 290.

Hoepffner, N., and Sathyendranath, S. 1993. Determination of the major groups of phytoplankton pigments from the absorption spectra of total particulate matter. Journal of Geophysical Research. 98 (C12): 789-803.

IOCCG. (2000). Remote Sensing of Ocean Colour in Coastal, and Other Optically-Complex, Waters, In S. Sathyendranath [ed.], Reports of the International Ocean Colour Coordinating Group 3.

Jyothibabu, R., Madhu, N.V., Jayalakshmi, K.V., Balachandran, K.K., Shiyas, C.A., Martin, G.D. and Nair K.K.C. 2006. Impact of freshwater influx on microzooplankton mediated food web in a tropical estuary (Cochin backwaters – India).Estuarine Coastal Shelf Science. 69: 505 – 518.

Jeffrey, S.W. and Vesk, M. 1997. Introduction to marine phytoplankton and their pigment signatures. P37-84. In Phytoplankton Pigments in Oceanography, ed. By .S.W.Jeffrey, R.F.C.Mantoura and S.W.Wright, UNESCO, Paris.

Kan, K.S. and Thornber, J.P. 1976. The light-harvesting chlorophyll a/b-protein complex of *Chlamydomonas reinhardi*. *Plant Physiol*. 57: 47-52.

Kishino, M., Okami, N., Takahashi, M., Ichimura, S. 1986. Light utilization efficiency and quantum yield of phytoplankton in a thermally stratified sea. Limnology and Oceanography. 31: 557-566.

Louchard, E.M., Reid, R.P., Stephens, C.F., Davis, C.O., Leathers, R.A., Downes, T.V. and Maffione, R. 2002. Derivative analysis of absorption features in hyperspectral remote sensing data of carbonate sediments. Optics Express.10 (26): 1573 - 1584.

Mann, J.E. and Myers, J. 1986. On pigments, growth and photosynthesis of Phaeodactylum tricornutum. Journal of Phycology. 4: 349–355.

Maske, H. and Haardt, H. 1987. Quantitative *in vivo* absorption spectra of phytoplankton: Detrital absorption and comparison with fluorescence excitation spectra Limnology and Oceanography. 32: 620-633.

Mao, Z., Stuart, V., Pan, D., Chen, J., Gong, F., Huang, H. & Zhu, Q. 2010. Effects of phytoplankton species composition on absorption spectra and modeled hyperspectral reflectance. Ecological Informatics. 5: 359-366.

Millie, DF., Kirkpatrick GJ., Vinyard BT.1995. Relating photosynthetic pigments and *in vivo* optical density spectra to irradiance for the Florida red-tide dinoflagellate *Gymnodinium breve.* Marine Ecological. Progrmme. 120: 65 - 75.

Millie, D. F., Schofield, O., Kirkpatrick, G. J., Johnsen, G., Tester, P.A. and Vinyard, B.T. 1997. Phytoplankton pigments and absorption spectra as potential 'Biomarkers' for harmful algal blooms: a case study of the Florida red-tide dinoflagellate, *Gymnodinium breve*. Limnology and. Oceanography. 42: 1240–1251.

Minu, P, Shaju, S.S., Muhamed, A.P., and Meenakumari, B. 2014. Phytoplankton community characteristics in the coastal waters of southeastern Arabian Sea. Acta Oceanologica Sinica. 33(12): 170–179.

Mitchell, B.G. and Kiefer, D.A. 1988. Variability in pigment specific particulate fluorescence and absorption spectra in the northeastern Pacific Ocean. Deep-Sea Research. 35: 665-689.

Morel, A. 1988. Optical modeling of the upper ocean in relation to its biogenous matter content (case I waters). Journal of Geophysical. Research. 93(10): 749-768.

Morel, A & Bricard, A. 1981. Theoretical results concerning light absorption in discrete medium, and application to specific absorption of phytoplankton. Deep-Sea Research. Part A, 28A:1375-1393.

Ong, L.J., Glazer, A.N., and Waterbury, J.B. 1986. An unusual phycoerythrin from a marine cyanobacterium. Science: 224: 80- 83.

Prezelin, B.B. and Alberte, R.S. 1978. Photosynthetic characteristics and organization of chlorophyll in marine dinoflagellates. Proceedings of the National Academy of Sciences, USA 75: 1801-1804.

Roesler, C.S. and Barnard, A.H. 2014. Optical proxy for phytoplankton biomass in the absence of photophysiology: Rethinking the absorption line height. Methods in Oceanography.7:79–94 doi: 10.1016/j.mio. 2013.12.003.

Rosado-Torres, M.A. 2008 Evaluation and development of bio-optical algorithms for chlorophyll retrieval in western Puerto Rico. Ph.D thesis. University of Puerto Rico, 128 pp.

Savitzky, A., and Golay, M.J.E. 1964. Smoothing and differentiation of data by simplified least squares procedures. Analytical Chemistry.36: 1627 - 1639.

Shaw, P J. and Purdie, D.A. 2001. Phytoplankton photosynthesis-irradiance parameters in the near-shore UK coastal waters of the North Sea: temporal variation and environmental control. Marine Ecological Programme Series. 216: 83-94.

Stramski, D., Babin, M., and Woz´niak, S.B. 2007. Variations in the optical properties of terrigenous mineral-rich particulate matter suspended in seawater. Limnology and Oceanography. 52(6): 2418–2433.

Suzuki, K., Hattori-Saito, A., Sekiguchi, Y., Nishioka, J., Shigemitsu, M., Isada, T., Liu, H., and McKay, R.M.L. 2014. Spatial variability in iron nutritional status of large diatoms in the Sea of Okhotsk with special reference to the Amur River discharge. Biogeosciences. 11: 2503–2517. doi: 10.5194/bg-11-2503-2014

Tzortziou, M., Subramaniam, A., Herman, J., Gallegos, C., Neale, P., and Hardingjr, L. 2007. Remote sensing reflectance and inherent optical properties in the mid Chesapeake Bay. Estuarine Coastal Shelf Science. 72: 16-32.

Vijayan, A. K. and Somayajula, S.A. 2014. Effect of accessory pigment composition on the absorption characteristics of dinoflagellate bloom in a coastal embayment. Oceanologia. 56(1): 107–124.

Chapter 5

STUDIES ON THE APPARENT OPTICAL PROPERTIES

5.1. Introduction

Ocean color algorithms developed to estimate biological variables such as Chl a have been used in both case I and case II waters (O'Reilly et al., 1998) and are based on the premise that other in-water constituents such as colored dissolved organic matter (CDOM) and detrital material covary with Chl a, the primary pigment used to represent phytoplankton concentrations. However, the ability of these algorithms to accurately estimate bio-optical variables in coastal waters is not very clear as in-water constituents such as CDOM and suspended sediments may not co-vary with Chl a (Carder et al., 1991; Tassan, 1994), although still influencing the water leaving radiance. The contribution of particulate and dissolved constituents to the variability of optical properties and ocean color in coastal waters requires a better understanding of the linkages between the concentration of these constituents, the inherent optical properties (IOPs) of absorption and scattering coefficients, and the apparent optical properties (AOPs) such as the spectral attenuation for downward irradiance Kd(λ) and remote sensing reflectance Rrs(λ). Knowledge of these relationships is important for characterizing the marine optical environment and developing remote sensing ocean color algorithms for coastal waters.

Remote sensing of the colour of the ocean is effective for monitoring water quality, including phytoplankton blooms and river plume from the cochin backwaters. Remote sensing of ocean color relies on detecting the light signal that leaves the water surface and reaches a sensor onboard a satellite, carrying with it information on IOPs of the water. Ocean remote sensing reflectance, Rrs, is related to backscattering, which redirects downwelling photons to travel upward and eventually leave the water surface, and absorption, which converts photons to heat or chemical energy. (Austin 1974, Lee et al 1974) several researchers studied the variations in diffuse attenuation coefficient and its vertical distribution of chlorophyll a concentration (Parsons et al. 1984). To optically characterize the water column, the diffuse attenuation coefficient needs to be determined precisely (Mobley 1994). The lack of information on the optical properties like attenuation in the SEAS area characterized by the seasonally reversing monsoon currents (Srinivas and Dineshkumar, 2006) makes this study important for increasing the efficiency of ocean colour algorithms and understanding of water column properties from the satellite platform.

The properties of the two main AOPs of importance to remote sensing, Kd(λ) and Rrs(λ), are discussed and analyzed in relation to absorption and scattering in an attempt to examine closure between the AOPs and IOPs based on field data. Some bio optical properties like Kd (λ) depends on both the composition of the medium and directional structure of the ambient light field; hence it is classified as an apparent optical property of the water. To characterize the water column, the diffuse attenuation coefficient, needs to be determined precisely. It is a quasi apparent optical property, that is influenced by the angular distribution of light field as well as the nature and quantity of substances present in the medium, is of particular interest because it quantifies the presence of light, the nature of particles present in it and the depth of the euphotic zone. Kd is an

indicator of the penetrating component of solar radiation. For most waters Kd (λ) is largely determined by absorption properties of water.

5.2. Result

5.2.1. Variability in the Remote sensing reflectance

The Spatial and temporal variblity in the remote sensing reflectance Spectra (Rrs) measured during the study period is shown in the **figure 5.1.** The remote sensing reflectance showed different patterns, depending on the seasons each station having a unique spectral shape. At station S1, the remote sensing reflectance increased sharply in the blue and green regions of the spectrum up to a wavelength of 570 nm and then decreased in the red region with a fluorescence peak at 670 nm. The shape of the spectrum is similar to that shown in (IOCCG report 2000) for waters with very high sediment and CDOM concentration. At station S2, S5, S6 and S7, R_{rs} increased in the blue region and showed a wider maximum from 500 to 560 nm and a very small but identifiable fluorescence peak. This remote sensing reflectance spectrum represents the suspended particular matter dominated by mineral fraction and a much lower Chl-*a* concentration. At station S3, S8 and S6 R_{rs} spectrum was similar to that of S4 except for the fluorescence peak. No fluorescence peak was detected at the stations during premonsoon and postmonsoon seasons, indicating minimal chlorophyll concentration. At station S4 and S8, R_{rs} spectrum showed a very unique peak showing minimum reflectance in the green region and high reflectance in blue and red region. At bar mouth region even high chl-a is present the Rrs spectra is masking the absorption by phytoplankton. This is due to the high concentration of the sediment and CDOM.

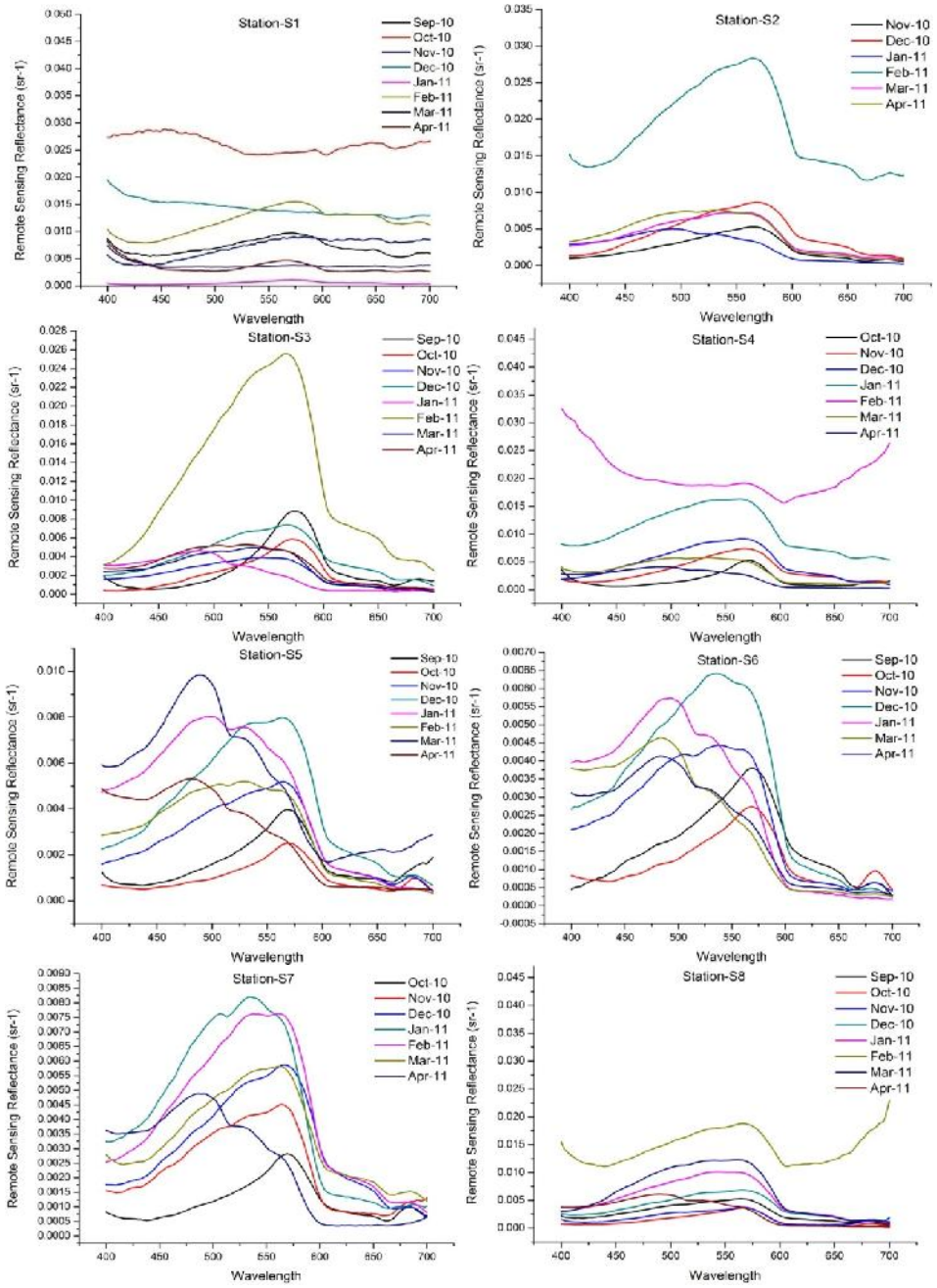

Figure 5.1. Temporal variations of the remote sending reflectance(Rrs) (Sr-1) spectra in the visible wavelength region of the coastal waters of the South Eastern Arabian Seas (SEAS) of the stations S1, S2, S3, S4, S5, S6 S7, S7 and S8

5.2.2. Variability of attenuation coefficient

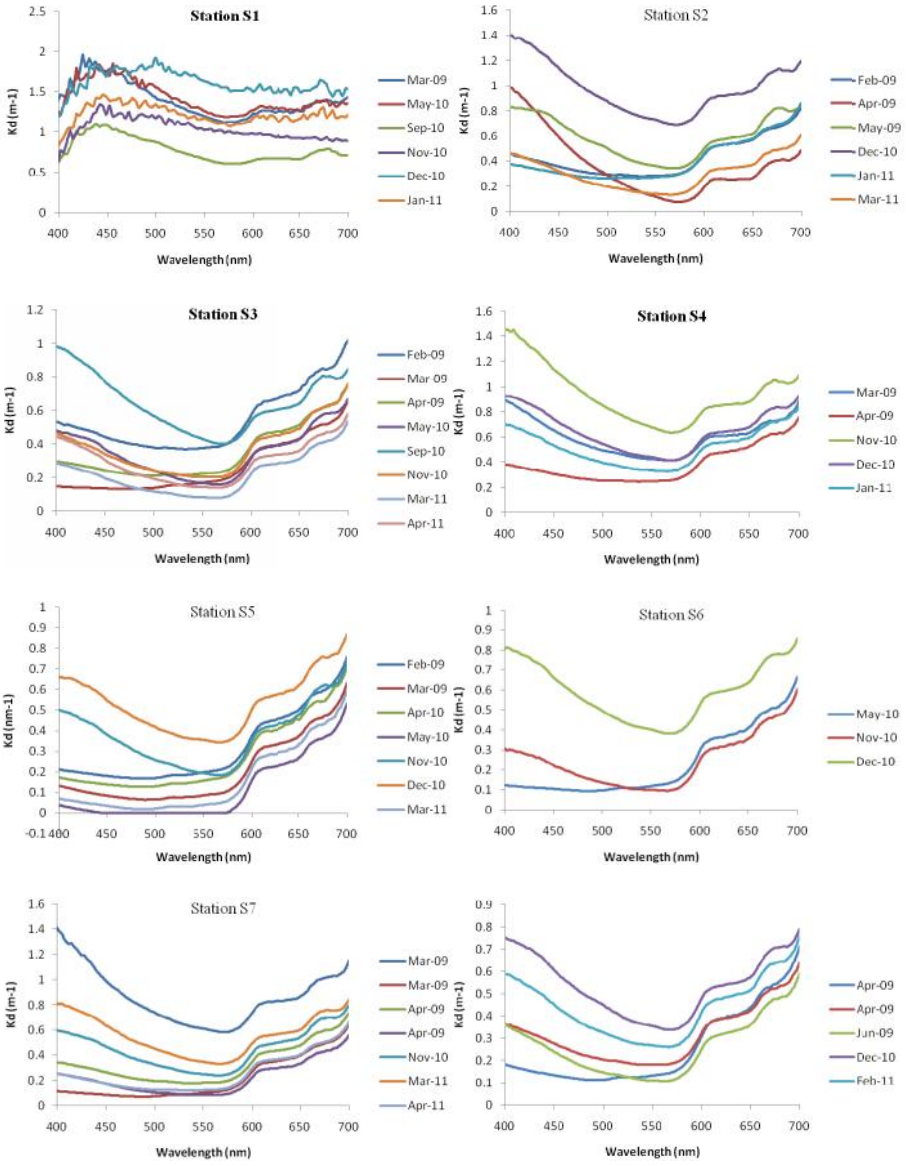

Figure 5.2. Temporal variations of the Downwelling Diffuse attenuation coefficient (Kd) (m^{-1}) spectra in the visible wavelength region of the coastal waters of the South Eastern Arabian Seas (SEAS) of the stations S1, S2, S3, S4, S5, S6 S7, S7 and S8.

The temporal variations of the Downwelling Diffuse attenuation coefficient (Kd) (m^{-1}) spectra in the visible wavelength region of the coastal waters of the South Eastern Arabian Seas (SEAS) of the stations S1, S2, S3, S4, S5, S6 S7, S7 and S8 is shown in the **figure 5.2.** It exhibited a high variability in the shape and magnitude making the water column optically very complex and a high variability in attenuation coefficient was found in post-monsoon period. In addition to the variation in magnitude k_d (λ) spectra showed very high variability in the shape also. At station 2 and 4 mostly influenced by freshwater inputs from the Cochin estuary carried with high detritus and CDOM and nutrients is showing much variability in magnitude and shape. The highest attenuation is shown in December 2010 at S2 with a corresponding chl-a concentration of 1.839 mgm^{-3} and a high turbidity of 4.06 NTU. At station S4, highest attenuation is shown in November 2009 with a corresponding chlorophyll_a concentration of 2.629 mgm^{-3} and turbidity 2.1 NTU and at station S3 high attenuation is found at September 2010 with a chl-a concentration 2.474 mgm^{-3} and turbidity 2.7 NTU. During May 2009 at S2 showed very different attenuation spectra with a sharp decline in attenuation value from 440 nm with a corresponding chl-a concentration of 2.7 mgm^{-3} and turbidity 4.6 NTU indicating the extend of optical components alters the attenuation coefficient in the coastal waters. At S5, except during December and November the attenuation is lesser in the blue region with corresponding lower chl-a concentration. This indicates near to the shore water column is optically more complex than the offshore stations and also there exist a strong seasonal influence in the optical components also have to be considered for the retrieval algorithms.

5.2.3. Spectral Model of Diffuse Attenuation Coefficient

Large spatial and temporal variation was observed in the surface chl-a values and the histogram is shown in **figure 3.1.** The relationship between Downwelling Diffuse attenuation coefficient (Kd) (m-1) at 412nm, 443nm and 676nm against Chlorophyll a (mg/m-3) concentration and CDOM is shown in the **figure 5.3 and 5.4** respectively**.** The determination coefficient at blue wavelength were higher but the values were small and insignificant in the red wavelength due to the inelastic scattering and high absorption capability of pure seawater plays a significant role. Also at 412nm R2 values were low may be due to high sediment particle in the water. The relationship between *Kd(λ)and* Chl-a, CDOM at short wavebands can be well described with a power law function, which shows that phytoplankton and associated CDOM is an important factor causing variability in *Kd(λ)*. At longer wavelength, seawater has strong absorption capability due to quick attenuation of downwelling irradiance and the suspended sediment makes uncertainties in *Kd(λ)* calculation, which blurred the relations between *Kd(λ) and* Chl-*a*

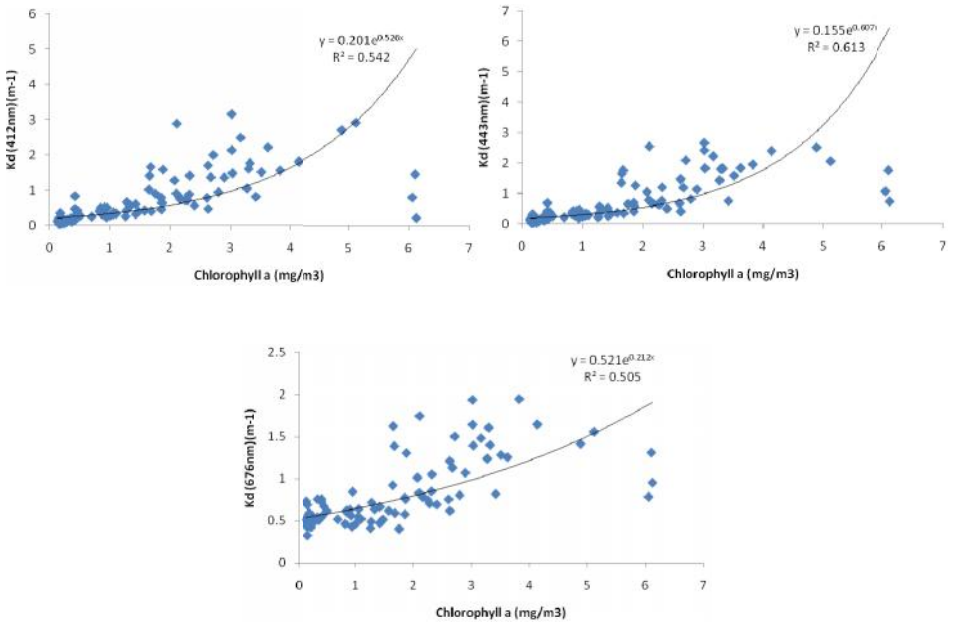

Figure 5.3. Exponential relationship between Downwelling Diffuse attenuation coefficient (Kd) (m^{-1}) at 412nm, 443nm and 676nm against Chlorophyll a (mg/m^{-3}) concentration.

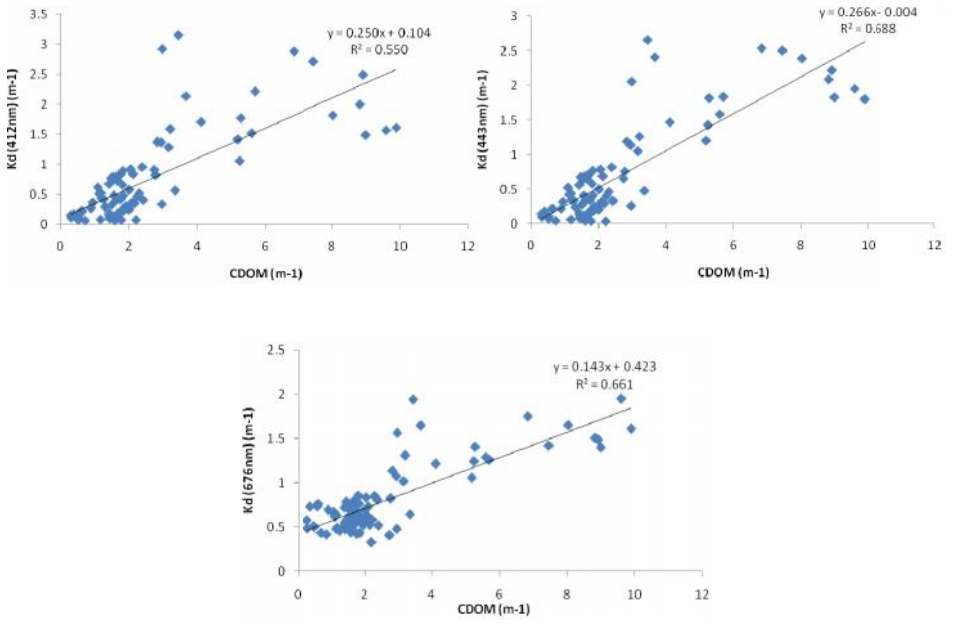

Figure 5.4. Exponential relationship between Downwelling Diffuse attenuation coefficient (Kd) (m^{-1}) at 412nm, 443nm and 676nm against CDOM (m^{-1}) concentration.

The linear relationship between Downwelling Diffuse attenuation coefficient (Kd) (m-1) at 490nm against Downwelling Diffuse attenuation coefficient (Kd) (m-1) at 440nm, and 665nm were shown in **figure 5.5.**

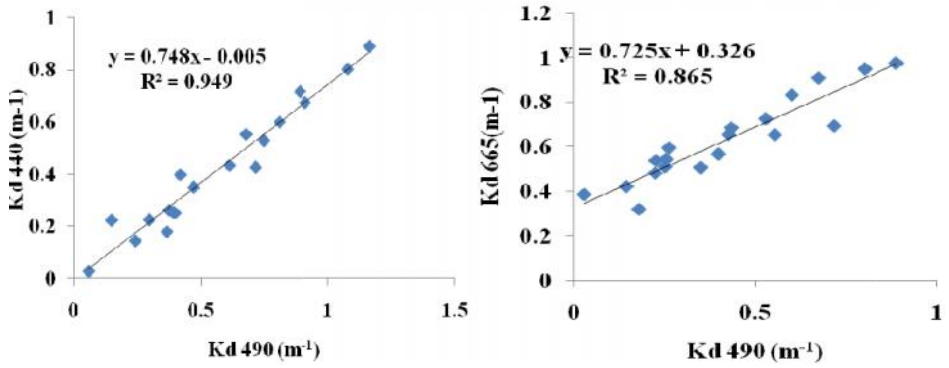

Figure 5.5. The linear relationship between Downwelling Diffuse attenuation coefficient (Kd) (m-1) at 490nm against Downwelling Diffuse attenuation coefficient (Kd) (m-1) at 440nm, and 665nm.

- A good linear relation is found during the period between Kd 440 with Kd 490 with the determination coefficient (R^2) above 0.94
- In the longer wavelength a linear relation exists but with lesser R^2 (0.86) compared to the shorter wavelength
- As the diffuse attenuation coefficient depends on wavelength, Kd(λ) at shorter wavelengths can be well regressed linearly with Kd (490), with higher determination coefficients at shorter wavebands than those at longer wavebands

5.3. Discussion

Observed variability in water IOPs resulted in large spatial and temporal variability in the magnitude of measured Rrs spectra. However, in most of the cases, maximum values of Rrs occurred in the green because of the

large pure-water absorption in the red and the large CDOM and non-algal particulate absorption in the blue region of the spectrum.

Because of the strong interference from CDOM and nonalgal particulate absorption in the blue-green, regionally specific algorithms based on the strong chlorophyll-a fluorescence signal at around 685 nm or the chlorophyll-a absorption feature at 676 nm have been proposed for improving chlorophyll retrievals in highly turbid, coastal and inland waters (e.g. Ruddick et al., 2001; Dall'Olmo et al., 2005).

5.4. Conclusion

Despite the consistency in $R_{rs,}$ other absorption and reflectance data could not be used for establishing general relationships for the specific coastal region for the entire year because of significant seasonal variability and differences in the optically active substance composition. A true synthesis of the optical component variability in coastal waters is difficult to achieve based on the existing data, because studies were mostly conducted at limited regional scale. The data necessary for future ocean color remote sensing applications, seasonal variability and regional algorithms for the retrieval of bio-optical components are rare in the SEAS coastal waters. Seasonal fresh influenced coastal waters such as the SEAS are highly dynamic regions where the use of global ocean color algorithms may not be appropriate for accurate retrieval of bio-optical variables such as phytoplankton biomass. In developing local ocean colour remote sensing algorithms or parameterizations of bio-optical models, there is a need to understand the processes and mechanisms that influence the ocean color or the remote sensing signal.

References

Austin, R.W., 1974. The remote sensing of spectral radiance from below the ocean surface. In: Jerlov, N.G., Steemann-Nielsen, E. (Eds.), Optical Aspects of Oceanography. Academic Press, London, New York, pp. 317e344.

Carder, K. L., Hawes, S. K., Baker, K. A., Smith, R. C., Steward, R. G., & Mitchell, B. G. 1991. Reflectance model for quantifying chlorophyll a in the presence of productivity degradation products. Journal of Geophysical Research. 96: 20599–20611.

Dall'Olmo, G., Gitelson, A.A., Rundquist, D.C., Leavitt, B., Barrow, T., Holz, J.C., 2005. Assessing the potential of SeaWiFS and MODIS for estimating chlorophyll concentration in turbid productive waters using red and near-infrared bands. Remote Sensing of Environment. 96 (2): 176e187.

IOCCG. 2000. Remote Sensing of Ocean Colour in Coastal, and Other Optically-Complex, Waters. In S. Sathyendranath [ed.], Reports of the International Ocean Colour Coordinating Group 3.

Lee, Z.P., Carder, K.L., Hawes, S.H., Steward, R.G., Peacock, T.G., Davis, C.O., 1994. A model for interpretation of hyperspectral remote sensing reflectance. Applied Optics. 33: 5721-5732.

O'Reilly, J. E., Maritorena, S., Mitchell, G. G., Siegel, D. A., Carder, K. L., Garver, S. A., Kahru, M., & McClain, C. 1998. Ocean color algorithms for SeaWiFS. Journal of Geophysical Research. 103: 24937– 24953

Parsons, T. R., Maita, Y., and Lalli, C. M. 1984. A manual of chemical and biological methods for seawater analysis. Oxford: Pergamon Press

Ruddick, K.G., Gons, H.J., Rijkeboer, M., Tilstone, G. 2001. Optical remote sensing of chlorophyll a in case 2 waters by use of an adaptive two-band algorithm with optimal error properties. Applied Optics. 40 (21): 3575e3585.

Srinivas, K., and P. K. Dineshkumar. 2006. Atmospheric Forcing on the Seasonal Variability of Sea Level at Cochin, Southwest Coast of India. Continental Shelf Research. 26: 1113–1133. doi:10.1016/ j.csr.2006.03.010.

Tassan, S. 1994. Local algorithms using SeaWiFS data for the retrieval of phytoplankton, pigments, suspended sediment, and yellow substance in coastal waters. Applied Optics. 33: 2369– 2377.

Chapter 6

VALIDATION OF SATELLITE DERIVED Chlorophyll *a* AND REMOTE SENSING REFLECTANCE

6.1. Introduction

The spectrum of radiation emerging from the sea surface is significantly influenced by the presence of subsurface optically active substances (OAS). The major OAS encountered in the world oceans are phytoplankton pigment, chlorophyll (chl-a), coloured dissolved organic matter (CDOM), and total suspended matter (TSM). Chlorophyll absorbs in the blue and red parts of the electromagnetic spectrum whereas CDOM has a strong absorption in shorter wavelengths. TSM contributes more towards scattering at longer wavelengths.

In the perspective of ocean colour remote sensing, the ratio of water-leaving radiance to downwelling radiance, known as remote-sensing reflectance (Rrs), is used to estimate the concentration of various OAS present within the water column. O'Reilly et al. (1998, 2000) established an empirical algorithm for satellite estimation of chl-a using Rrs. However, such bio-optical algorithms were primarily developed for case 1 waters where phytoplankton is solely responsible for the variation in Rrs (Gordon and Morel 1983; Morel and Prieur 1977; Siegel and Michaels 1996; Stramski and Tegowski 2001; Terrill, Melville, and Stramski 2001; O'Reilly et al. 1998, 2000). These types of algorithm based on single models of chl-a are inadequate for optically

complex coastal and inland case 2 waters where substances other than phytoplankton, including TSM and CDOM, have a significant effect on Rrs (Bukata et al. 1995; IOCCG 2000). In case 2 waters, where Rrs is influenced by signals from both CDOM and TSM, chl-a often acquires a bias when estimated using such empirical algorithms (Ruddick, Ovidio, and Rijkeboer 2000; Siegel et al. 2000; Wang and Shi 2005). On the other hand, such empirical algorithms are computationally less intensive and easier for operational implementation. Moreover, advances in ocean colour satellite sensors with more spectral bands, improved bio-optical algorithms, and novel atmospheric correction models now provide more accurate ocean colour products, even in case 2 waters (Zibordi, Mélin, and Berthon 2006).

The accurate retrieval of chl-a in case 2 waters also requires the selection of a suitable atmospheric correction scheme. In turbid waters, sensor-derived Rrs at blue wavelengths is often biased downward and sometimes even negative. This problem often results from assumptions that water-leaving radiance is negligible at near-infrared (NIR) bands (Siegel et al. 2000). For the ocean–atmosphere system, top-of-atmosphere (TOA) reflectance, $\rho t(\lambda)$, as measured by the satellite sensor, can be written as a linear sum from various contributions (ignoring whitecaps and sun glint):

$$\rho t(\lambda) = \rho r(\lambda) + \rho a(\lambda) + t(\lambda)\rho w(\lambda)$$

where $\rho r(\lambda)$, $\rho a(\lambda)$, and $\rho w(\lambda)$ are the reflectance contributions from molecules (Rayleigh scattering), aerosols (including Rayleigh-aerosol interactions), and ocean waters, respectively, and $t(\lambda)$ is the diffuse transmittance of the atmosphere. The goal of ocean colour remote sensing is accurate retrieval of water-leaving reflectance, $\rho w(\lambda)$, by eliminating the contribution from atmospheric radiance ($\rho r(\lambda)$ and $\rho a(\lambda)$) and ocean surface

effects. The contribution of atmospheric radiance to the total signal received by the visible satellite sensor is approximately 85%. In the default iterative atmospheric correction scheme used by many sensors, ocean is assumed to be dark at NIR bands (748 and 869 nm). This black pixel assumption (BPA) is used for initial iteration and relaxed progressively. However, the initial BPA in the NIR region is invalid for turbid waters, leading to significant errors in retrieval of chl-a (Siegel et al. 2000; Ruddick, Ovidio, and Rijkeboer 2000).

The quality of the data products derived from ocean colour satellites largely depends on an accurate atmospheric correction scheme and a suitable bio-optical algorithm. Hence the chapter is on with these objectives: (1) to understand the effect of OASs on Rrs; (2) to validate an operational bio-optical algorithm (OC3M) for retrieval of chl-a; and (3) to understand the effect of atmospheric correction schemes on retrieval of Rrs and chl-a.

6.2. Results

6.2.1. Distribution of OASs

The preliminary analysis of the study includes understanding the variability in distribution of OASs, such as chl-a, aCDOM440, and TSM. The distribution of OASs for the entire sampling period was analysed using frequency distribution plots (Figure 6.1). The results showed a large variability in the distribution of chl-a and TSM: chl-a ranged between 0.006 and 25.85 mg m^{-3} whereas the concentration of TSM ranged from 0.005 to 33.44mg l–1 and aCDOM440 ranged between 0.002 and 0.31 m–1. The distribution of chl-a did not show any specific trend in terms of magnitude. The maximum in the distribution of aCDOM440 was seen at the median frequency, ranging from 0.1 to 0.15 m–1, with lower values occurring more frequently as compared

with higher. The distribution of TSM showed a higher frequency at lower concentrations (<4.0 mg l^{-1}).

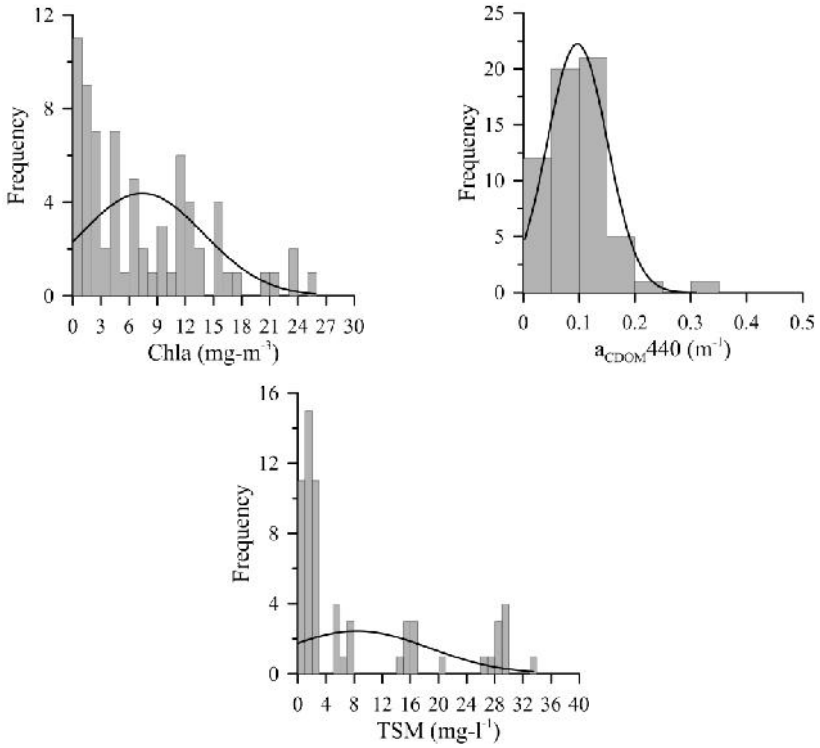

Fig 6.1: Frequency distribution of Chlorophyll_a (Chla), absorption due to Chromophoric Dissolved Organic Matter (CDOM) at 440 nm ($a_{CDOM}440$) and Total Suspended Sediment (TSM) in the study area for the entire sampling period. The curve indicates the normal distribution.

The analysis carried out using frequency distribution plots gave an insight into overall distribution of OASs sampled during the study period. However, it is also important to understand the variability of these OASs on the temporal scale. To achieve this, the variability in the distribution of OASs was analysed on a monthly scale. All spatial data corresponding to one month were averaged and are shown in Figure 6.2, along with the standard deviation.

The monthly mean chl-a concentration was found to vary between 3.85 and 12.49 mg m^{-3}. The highest concentration was observed during the end of

the southwest monsoon and prior to the onset of the northeast monsoon (i.e. from August to November).

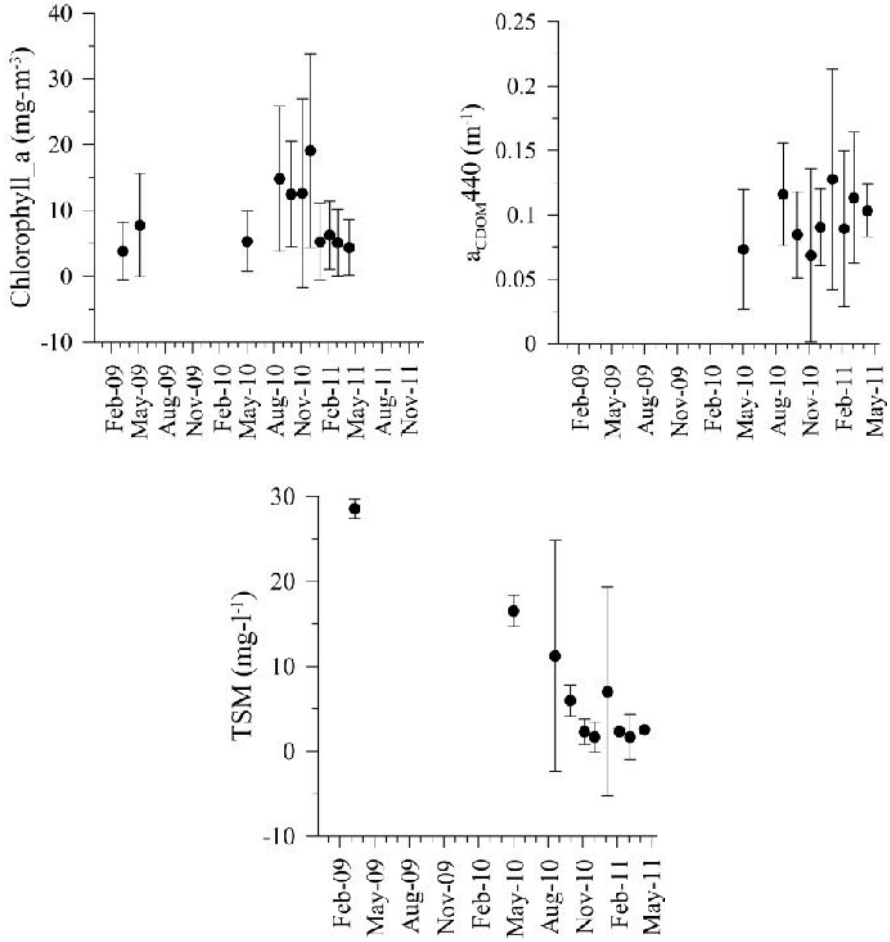

Fig 6.2: Monthly variability in spatial mean of Chlorophyll_a (Chla), absorption due to Chromophoric Dissolved Organic Matter (CDOM) at 440 nm ($a_{CDOM}440$) and Total Suspended Sediment (TSM) in the study area. The vertical bars indicate standard deviation.

The concentration of chl-a was significantly lower between February and May, corresponding to the later phase of the northeast monsoon. In addition, a high standard deviation was observed throughout the study period. The spatial mean of aCDOM440 did not show any significant trend at the

monthly scale. The values encountered in the were also on the lower side of the global mean as reported by Siegel et al. (2002); aCDOM440 reached a peak during the northeast monsoon (i.e January), with a mean value of 0.13 ± 0.08 m^{-1}. The TSM concentration showed a large variability at the temporal scale, with a maximum of 28.58 ± 1.14 mg l^{-1} for the month of March 2009. The overall trend showed that TSM was high prior to the onset of the southwest monsoon while the standard deviation was very low except for two months (September and January 2011).

6.2.2. Effect of chl-a on Rrs

This section analyses the effect of OASs on spectral Rrs. Furthermore, the variability in Rrs is derived using two different atmospheric correction schemes (A1, multi-scattering with two-band model selection NIR correction; and A2, multi-scattering with multi-scattering with Management Unit of North sea Mathematical Model (MUMM) correction and MUMM NIR calculation). The spectral variability of in situ (solid line) and satellite-derived Rrs using A1 (triangles) and A2 (circles) is presented in Figure 6.3. Although we amassed a total of 63 data points, only those stations where satellite match-up was available are presented here. The plots were arranged with increasing concentrations of chl-a. Even though the magnitude of satellite-derived spectral Rrs does not match, in most cases, the shape of the spectra seems to be in good agreement with that in situ. At a lower concentration of chl-a, maximum Rrs was at the shorter wavelength and decreased exponentially towards a longer wavelength. Furthermore, it was also observed that with increasing concentration of chl-a, peak Rrs shifted towards a longer wavelength.

While investigating satellite-derived spectral Rrs using A1 and A2, it was observed that A1 was higher than A2 in all cases. In addition, spectral Rrs

derived using the atmospheric correction scheme A1 was found to be in better agreement with in situ measurements. Furthermore, spectral Rrs derived using the atmospheric correction scheme A2 was found to be underestimated in all cases. The Rrs spectra are appropriately fitted at chl-a concentrations of less than 5 mg m–3, whereas at concentrations of greater than 5 mg m–3 they seemed to be slightly overestimated. In cases where chl-a concentration was greater than 12 mg m–3, satellite-derived Rrs spectra were underestimated. However, no trend was observed in spectral Rrs with respect to variability of TSM and aCDOM440.

6.2.3 Validation of chl-a

In this section an attempt has been made to evaluate the effect of two atmospheric correction schemes on retrieval of chl-a using a default bio-optical algorithm. Prior to this the biooptical algorithm was also validated. To do this, in situ Rrs measured using a radiometer was used in order to ignore the effect of atmospheric contribution. Chl-a estimated using radiometric Rrs by applying the OC3M algorithm (chl-a_R) was validated against that estimated from water sample analysis (chl-a_F), and the results are shown in Figure 6.4(a). The validation statistics are given in Table 1. The results show that both are closely matched with good correlation (correlation coefficient, R2 = 0.64) and $\log_{10}$(RMSE) was 0.43. The absolute and relative percentage error was on the high side (absolute percentage difference (APD) = 43.6% and relative percentage difference (RPD) = 42.33%).

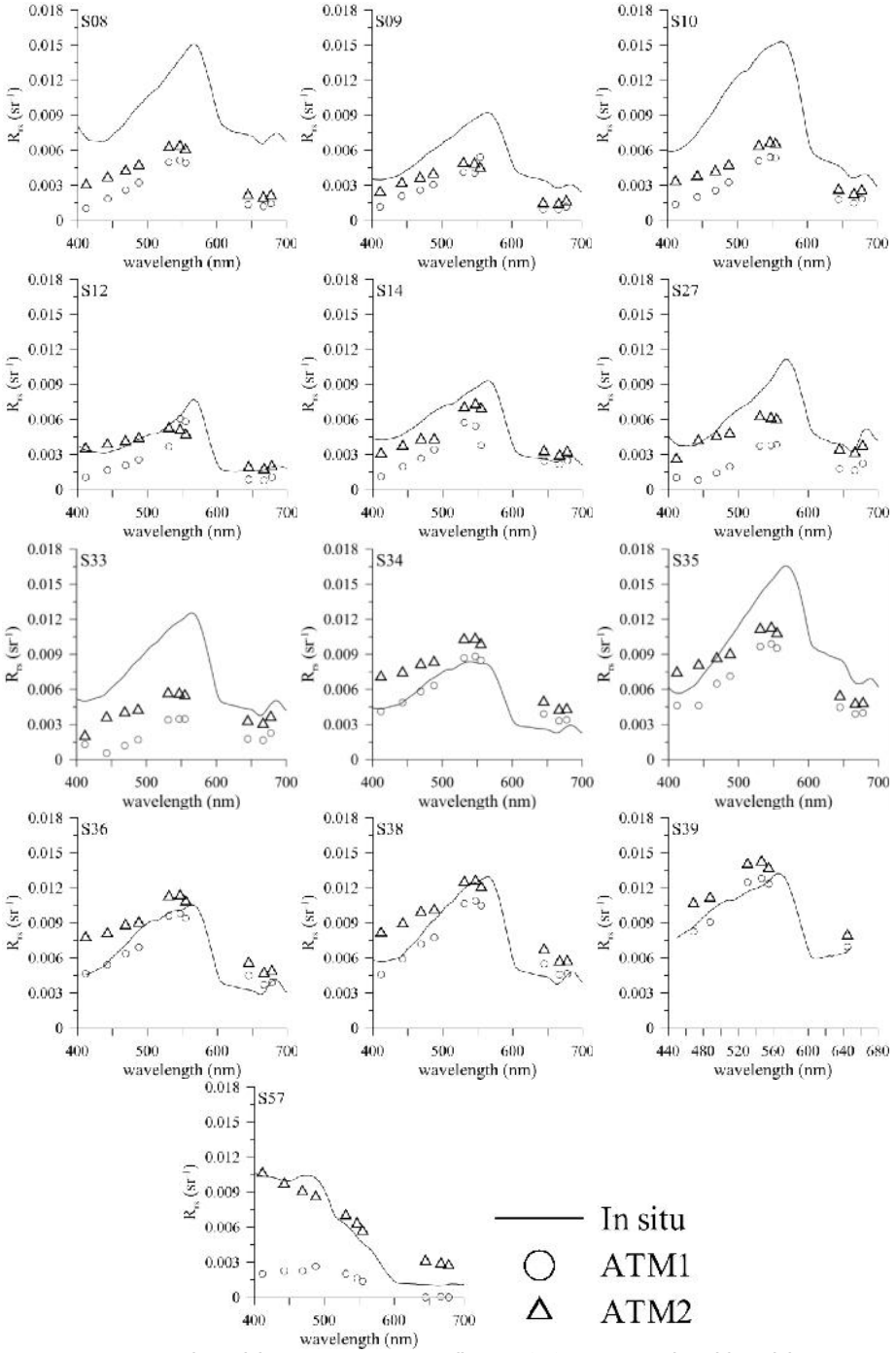

Fig 6.3: Spectral variability in remote sensing reflectance (R_{rs}) at stations selected for validation

Figures 6.4(b) and (c) show the correlation between in situ measured chl-a (chl-a_F) and that derived from MODIS-Aqua using A1 (chl-a_A1) and A2 (chl-a_A2) atmospheric correction schemes.

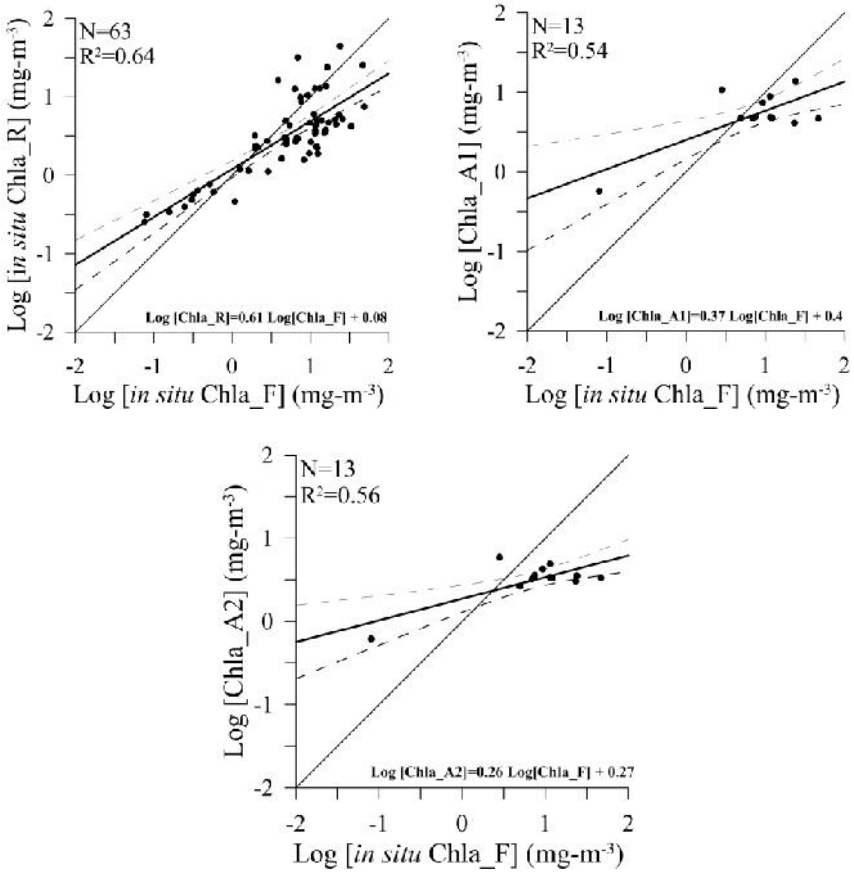

Fig 6.4: Correlation between *in situ* measured fluorometric Chla, and a) Chla estimated using R_{rs} from radiometer data, b) Chla generated from satellite data using 2-band model selection and iterative NIR correction, c) 2-band model selection and MUMM NIR correction. In all cases OC3M algorithm was used to estimate Chla. The thin solid line represents perfect linear fit. The thick solid line represents the linear data trend. The dotted line represents the 95% confidence limit.

In general, 77% of the data points were within a 95% confidence limit. The statistical indicators (Table 1) showed comparable correlation coefficients of 0.54 and 0.56 for A1 and A2, respectively.

Table 6.1 Statistical analysis of in-situ derived Chl a with OC3M generated chl a and chl a derived after two atmospheric correction schemes.

	N	R^2	SLOPE	INTERCEPT	r	Log RMSE	APD	RPD
Chl Radiometer	63	0.64	0.61	0.077	1.806	0.434	43.601	42.334
Chl Atm1	13	0.536	0.366	0.399	1.611	0.488	25.464	17.574
Chl Atm2	13	0.561	0.26	0.272	2.176	0.625	40.007	41.426

The intercept was low in the case of A2 (0.27) as compared with that of A1 (0.4). Chl-a derived using A1 showed a low value of mean ratio of measured to estimated chl-a ('r' = 1.6) as compared with that from A2 (2.18). Furthermore, APD and RPD were lower in the case of chl-a derived using A1. The overall statistical indicators showed better 'r', RMSE, APD, and RPD in the case of A1 as compared with A2, whereas in the case of A2, R2, slope, and intercept were better as compared with A1.

6.3. Discussion

This chapter focused on two major objectives, the first being to understand the variability of OAS in an area subjected to strong monsoonal forcing. The second was to evaluate the effect of the atmospheric scheme on retrieval of Rrs and chl-a from satellite data. The first objective was addressed by analysing the frequency distribution of OAS throughout the period of the study and also by understanding its spatial and temporal variability on a monthly scale. The results of analysis showed a large variability in the distribution of chl-a, with aCDOM440 being lower than the global mean as reported by Siegel et al. (2002). Furthermore, the maximum frequency for TSM was observed at the lower concentration. This clearly indicates that chl-a is the primary matter that can affect the distribution of light – and hence Rrs. Furthermore, a high concentration of chl-a was encountered during the end of the southwest monsoon and prior to the onset of the northeast monsoon.

Previous studies carried out by Lévy et al. (2007) clearly show chl-a peaks during August–September along the southwestern coast of India, which was attributed to the intense coastal upwelling occurring during the southwest monsoon. During the southwest monsoon the West Indian Coastal Currents (WICC) change direction towards the south, resulting in the coastal upwelling (Shankar, Vinayachandran, and Unnikrishnan 2002). Furthermore, the upwelling process also results in a high primary production ranging between 40.0 and 1225.0 mg C m^{-2} day^{-1} (Joshi and Rao 2012).

Distribution of aCDOM440 and TSM was highly variable at the temporal scale but the average value of aCDOM440 was found to be on the lower side of the global mean. The distribution of CDOM and TSM was further analysed by correlating with salinity at a seasonal scale. During the southwest monsoon season a strong negative correlation ($R = –0.6$) was observed between aCDOM440 and salinity, but in other months no significant correlation was found. River discharge is the major contributor of CDOM in coastal waters, but resuspension and in situ degradation can also enhance CDOM (Menon et al. 2011). Similarly, the potential source of TSM is either from rivers or due to resuspension in shallow waters. The coastal waters off Kochi are subjected to upwelling and heavy fresh water discharge from the adjacent estuary during the southwest monsoon period, which enhances nutrient upload resulting in increased biological production (Nair, Devassy, and Madhupratap 1992; Jyothibabu et al. 2006). This indicates that much of the CDOM during the southwest monsoon is derived from river discharge, and there was no significant relationship between aCDOM440 and TSM. Furthermore, a lag in the elevation of chl-a concentration and aCDOM440, during nonmonsoon months, indicates that during these months the presence of CDOM could be principally due to the in situ degradation of phytoplankton.

Although TSM distribution showed a higher frequency at lower concentrations, the maximum concentration was during the southwest monsoon. Furthermore, TSM did not show any significant relation with salinity. Previous studies by Thomas et al. (2004), Srinivas et al. (2003), and Jyothibabu et al. (2006) reported that a continuous dredging process occurring throughout the year in the study area had increased the nutrient and sediment load in the estuary, which had drained into the coastal waters.

Spectral Rrs is the basis for the empirical bio-optical algorithm (O'Reilly et al. 1998, 2000). The spectral Rrs was found to be strongly linked to variability in chl-a concentration. It was observed that with the increase in chl-a concentration, peak Rrs was shifted to a longer wavelength. This is analogous to previous studies that formed the basis for the development of an empirical band ratio algorithm for the retrieval of chl-a from satellite data (O'Reilly et al. 1998, 2000). While analysing Rrs derived using two atmospheric correction schemes (A1 and A2), A1 was closer to the measured Rrs. In the case of A1, Gordon and Wang (1994) showed that the assumption of zero water-leaving radiance (Lw) in the NIR channel of SeaWiFS was better justified. Moreover, the concept of BPA at NIR does not hold true in turbid coastal waters. Wang, Son, and Shi (2009) showed that shifting BP to SWIR reduces the bias error but increases noise error significantly. In the A2 correction scheme, these assumptions were replaced by the assumption of spatial homogeneity of the 765 and 865 ratios for aerosol reflectance, and for water-leaving reflectance. Ruddick, Ovidio, and Rijkeboer (2000) reported that the A1 scheme failed in the area of high TSM and CDOM. His theoretical analysis showed an error in the estimation of normalized water-leaving radiance (Lwn) and was of the order of ± 0.01 for turbid water with turbid atmosphere. It was found that there is no significant difference between

spectral Rrs derived using A1 and A2. This was probably due to the fact that the study area was dominated more by chl-a, with a lesser impact of TSM and CDOM. The variability in spectral Rrs depends upon both variability in OASs and accurate computation of atmospheric radiance. This chapter has addressed both these issues. An earlier study carried out by Menon, Lotliker, and Nayak (2005) showed that higher concentrations of chl-a and CDOM significantly decrease Lw at shorter wavelengths. In their study, Gordon and Wang (1994) estimated the effect of errors induced in atmospheric correction using single- and multi-scattering approximation. In the case of chl-a derived using the algorithm of Gordon (1998), an error of more than ±20% was found in all cases. Siegel et al. (2000) showed that this error that was due to BPA for any arbitrary band ratio corresponding to SeaWiFS bands. Their results showed that for chl-a values less than 1 mg m–3, differences due to the application of NIR correction are less than 2%. However for chl-a greater than 2 mg m^{-3}, band ratio error increases dramatically.

The validation of the MODIS default bio-optical algorithm (OC3M) showed significant validation statistics. Although the statistical indicators showed moderate values, the accuracy of the algorithm was still within acceptable limits. The OC3M algorithm was initially developed for case 1 waters, eliminating the effect of OASs other than chl-a. Its predicted accuracy was 70% in the open ocean (O'Reilly et al. 1998). Thirteen points were used for the validation. Furthermore, these match-up points cover the entire range of OAS encountered within the study area. These points were associated with a range of chl-a concentration from 0.15 to 13.89 mg m–3, aCDOM440 between 0.015 and 0.14 m–1, and TSM between 1.26 and 28.32 mg l–1. Statistical analysis indicated that the default atmospheric correction scheme (A1) performed better. This was probably due to the fact that the concentration

of TSM and CDOM was lower, to overcome the impact of chl-a. Earlier studies carried out by Zhang et al. (2011) also showed that the default algorithm for MODIS performs well in the high-chl-a and -TSM waters of the Perl River Estuary where both OAS were closely associated.

6.4. Conclusion

This chapter is focused on the effect of OASs and atmospheric correction schemes on retrieval of spectral Rrs and chl-a from MODIS data. The variability of OASs in the study area was attributed to coastal upwelling and freshwater discharge, especially during the southwest monsoon. Chl-a was the major light-absorbing component in the study area. The distribution of OASs was highly variable, with maxima during the southwest monsoon. The average value of aCDOM440 was found to be on the lower side of the global mean. A significant negative relationship between aCDOM440 and salinity during the southwest monsoon indicates that much of the CDOM during this season was from river discharge. The spectral Rrs was found to be strongly linked to the variability in chl-a concentration. With an increase in chl-a concentration, peak Rrs was shifted to the longer wavelength. The validation of chl-a, derived from in situ Rrs, showed moderate performance. However, the accuracy of the algorithm was still within acceptable limits. Spectral Rrs derived using the atmospheric correction scheme A1 was found to be in better agreement with in situ results. Further chl-a retrieved using A1 and A2 did not show any significant difference, probably be due to the fact that the study area was dominated by chl-a with lower concentrations of CDOM and TSM. The statistical analysis indicates that the default atmospheric correction scheme (A1) performs better. Furthermore, the variability in Rrs and chl-a retrieved using different atmospheric correction schemes has been fully addressed.

References

Bukata, R. P., J. H. Jerome, K. Y. Kondratyev, and D. V. Pozdnyakov. 1995. Optical Properties and Remote Sensing of Inland and Coastal Waters. New York: CRC Press.

Gordon, H. R., and A. Y. Morel. 1983. Remote Assessment of Ocean Colour for Interpretation of Satellite Visible Imagery: A Review, 114 pp. New York: Springer-Verlag.

Gordon, H. R., and M. Wang. 1994. Retrieval of Water-Leaving Radiance and Aerosol Optical Thickness over the Oceans with Seawifs: A Preliminary Algorithm. Applied Optics 33 (3): 443–452. doi:10. 1364/AO.33.000443

Gordon, H. R. 1998. In-Orbit Calibration Strategy for Ocean Color Sensors 1998. Remote Sensing of Environment 63 (3): 265–278. doi:10.1016/S0034-4257(97)00163-6

IOCCG. 2000. Remote Sensing of Ocean Colour in Coastal, and Other Optically-Complex, Waters. In Reports of the International Ocean-Colour Coordinating Group, edited by S. Sathyendranath, No. 3. Dartmouth: IOCCG.

Joshi, M., and A. D. Rao. 2012. Response of Southwest Monsoon Winds on Shelf Circulation off Kerala Coast, India. Continental Shelf Research 32: 62–70. doi:10.1016/j.csr.2011.10.015

Jyothibabu, R., N. V. Madhu, K. V. Jayalakshmi, K. K. Balachandran, C. A. Shiyas, G. D. Martin, and K. K. C. Nair. 2006. Impact of Fresh Water Influx on Microzooplankton Mediated Food Web in a Tropical Estuary (Cochin Backwaters – India). Estuarine, Coastal and Shelf Science. 69: 505–518. doi:10.1016/j.ecss.2006.05.013

Lévy, M., D. Shankar, J.-M. André, S. S. C. Shenoi, F. Durand, and C. de Boyer Montégut. 2007. Basin-Wide Seasonal Evolution of the Indian Ocean's Phytoplankton Blooms. Journal of Geophysical Research (C): Oceans 112: C12014. doi: 10.1029/2007JC004090.

Menon, H. B., A. Lotliker, and S. R. Nayak. 2005. Pre-Monsoon Bio-Optical Properties in Estuarine, Coastal and Lakshadweep Waters. Estuarine, Coastal and Shelf Science. 63 (1–2): 211–223. doi:10.1016/ j.ecss.2004.11.015

Menon, H. B., N. P. Sangekar, A. A. Lotliker, and P. Vethamony. 2011. Dynamics of Chromophoric Dissolved Organic Matter in Mandovi and Zuari Estuaries – A Study Through In Situ and Satellite Data. ISPRS Journal of Photogrammetry and Remote Sensing. 66 (4): 545–552. doi:10.1016/j.isprsjprs.2011.02.011

Morel, A., and L. Prieur. 1977. Analysis of Variations in Ocean Color. Limnology and Oceanography. 22 (4): 709–722. doi: 10.4319/ lo.1977.22.4.0709

Nair, S. S., V. P. Devassy, and M. Madhupratap. 1992. Blooms of Phytoplankton along the West Coast of India Associated with Nutrient Enrichment and the Response of Zooplankton. Science of the Total Environment. 26: 819–828.

O'Reilly, J. E., S. Maritorena, B. G. Mitchell, D. A. Siegel, K. L. Carder, S. A. Garver, M. Kahru, and C. R. McClain. 1998. Ocean Color Chlorophyll Algorithms for Seawifs. Journal of Geophysical Research. 103: 24937–24953. doi:10.1029/98JC02160

O'Reilly, J. E., S. Maritorena, D. Siegel, M. C. O'brien, D. Toole, B. G. Mitchell, M. Kahru, F. P. Chavez, P. Strutton, G. Cota, S. B. Hooker, C. R. McClain, K. L. Carder, F. Muller-Karger, L. Harding, A.

Magnuson, D. Phinney, G. F. Moore, J. Aiken, K. R. Arrigo, R. Letelier, and M. Culver. 2000. Ocean Color Chlorophyll a Algorithms for Seawifs, OC2, and OC4: Version 4. In Seawifs Postlaunch Technical Report Series, Seawifs Post-Launch Calibration and Validation Analyses, edited by S. B. Hooker and E. R. Firestone, Vol, 11, Part 3, 9–23. Greenbelt, MA: NASA Goddard Space Flight Center.

Ruddick, K. G., F. Ovidio, and M. Rijkeboer. 2000. Atmospheric Correction of Seawifs Imagery for Turbid Coastal and Inland Waters. Applied Optics. 39: 897–912. doi:10.1364/ AO.39.000897

Shankar, D., P. N. Vinayachandran, and A. S. Unnikrishnan. 2002. The Monsoon Currents in the North Indian Ocean. Progress in Oceanography. 52: 63–120. doi:10.1016/S0079- 611(02)00024-1

Siegel, D., and A. Michaels. 1996. Quantification of Non-Algal Light Attenuation in the Sargasso Sea: Implications for Biogeochemistry and Remote Sensing. Deep Sea Research Part II: Topical Studies in Oceanography. 43: 321–345. doi:10.1016/0967-0645(96)00088-4

Siegel, D. A., M. Wang, S. Maritorena, and W. Robinson. 2000. Atmospheric Correction of Satellite Ocean Color Imagery: The Black Pixel Assumption. Applied Optics. 39: 3582−3591. doi:10.1364/ AO.39.003582

Siegel, D. A., S. Maritorena, N. B. Nelson, D. A. Hansell, and M. Lorenzi-Kayser. 2002. Global Distribution and Dynamics of Colored Dissolved and Detrital Organic Materials. Journal of Geophysical Research Oceans. 107 (C12). doi:10.1029/2001JC000965

Srinivas, K., C. Revichandran, P. A. Maheswaran, M. T. T. Ashraf, and N. Murukesh. 2003. Propagation of Tides in the Cochin Estuarine

System South West Coast of India. Indian Journal of Geo-Marine Sciences. 32 (1): 14–24.

Stramski, D., and J. Tegowski. 2001. Effects of Intermittent Entrainment of Air Bubbles by Breaking Wind Waves on Ocean Reflectance and Underwater Light Field. Journal of Geophysical Research. 106: 31345–31360. doi:10.1029/2000JC000461

Terrill, E. J., W. K. Melville, and D. Stramski. 2001. Bubble Entrainment by Breaking Waves and Their Influence on Optical Scattering in the Upper Ocean. Journal of Geophysical Research. 106: 16815–16823. doi:10.1029/2000JC000496

Thomas, J. V., P. Premlal, C. Sreedevi, and M. B. Kurup. 2004. Immediate Effect of Bottom Trawling on the Physicochemical Parameters in the Inshore Waters (Cochin-Munambum) of Kerala. Indian Journal of Fisheries. 51 (3): 277–286.

Wang, M., and W. Shi. 2005. Estimation of Ocean Contribution at the MODIS Near-Infrared Wavelengths along the East Coast of the US: Two Case Studies. Geophysical Research Letters. 32: L13606. doi:10.1029/2005GL022917

Wang, M., S. Son, and W. Shi. 2009. Evaluation of MODIS SWIR and NIR–SWIR atmospheric Correction Algorithms Using Seabass Data. Remote Sensing of Environment. 113: 635−644. doi:10.1016/ j.rse.2008.11.005

Zhang, Y., H. Lin, C. Chen, L. Chen, B. Zhang, and A. A. Gitelson. 2011. Estimation of Chlorophyll-A Concentration in Estuarine Waters: Case Study of the Pearl River Estuary, South China Sea. Environmental Research Letters. 6. doi:10.1088/1748-9326/6/2/024016

Zibordi, G., F. Mélin, and J. F. Berthon. 2006. Comparison of Seawifs, MODIS and MERIS Radiometric Products at a Coastal Site. Geophysical Research Letters. 33 (6). doi:10.1029/ 2006GL025778

Chapter 7

SUMMARY AND CONCLUSION

A significant spatial and seasonal variation in all the physico-chemical and biological parameters observed during the study pointed that, monsoon and dry season periods were characterized by different physico-chemical and biological properties. While there was evidence that physical factors as fresh water influx, precipitation and current pattern affected nutrient distribution along the salinity gradient, it was an interplay between nutrient availability, light and mixing that appeared to be important in regulating primary production. Primary production is high during monsoon period and during intra-monsoon high variability of production was also measured and nutrients were not limiting factors of production. Higher variability in the abiotic condition implies a more unstable environment. This indicates that, in spite of strong seasonality, these coastal waters are highly productive during most of the time as compared to oceanic region supporting a large fishery. But the sustainability and precise prediction of this ecosystem can be explained only by continuing the long term time series analysis.

Chl-a is the principal photosynthetic pigment of phytoplankton and is common to all species. Chl-b and Chl-c are very common photosynthetic pigment, found in diatoms, dinoflagellates and other groups. The absorption peaks identified in coastal Arabian Sea are consistent with the dominance of these groups in the phytoplankton community. Thus the 4^{th} derivative analysis is found as simple and efficient tool for the monitoring of chemotaxonomic markers in phytoplankton assemblages. Some minor variations in the magnitude of the 4^{th}derivative peaks and the appearance of new peaks in the

study area suggest that they might be due to the spatial and temporal difference and the influence of rivers as all the stations in the study area is under riverine input, pigment packaging and photoadaption in the trophic condition. The diatom abundance is high in the proximity of river mouths. Many studies has been reported that good correlation ($R^2 = 0.89$) between the 4^{th} derivative of $a_{ph}(\lambda)$ at 467,650 and 675 nm vs. Chl-a concentration. In general, the 4^{th} derivative analysis suggests that even though the relative composition of phytoplankton community was stable throughout the year, the dominant taxa varied. Peaks identified in the 4^{th} derivative of a_{ph} are by the contribution of all the taxa.

The spectral correlation analysis between the 4^{th} derivative of $a_{ph}(\lambda)$ and Chl-a in the present study confirm such results. High correlation coefficients were also found for the wavelengths associated with carotenoid accessory pigments. In summary, 4^{th} derivative of $a_{ph}(\lambda)$ appears to be a valuable alternative method for the quantification of Chl-a in the Arabian Sea. The result of this study would help in choosing spectral regions for Chl-a estimation where interference by accessory pigments is minimal.

From an optical point of view, the phytoplankton absorption in the coastal Arabian Sea varies spatially and temporally with cell size, and taxonomic affiliations. Derivative analysis of the particulate absorption coefficients offers an alternative and efficient means of separating the absorption by specific photosynthetic pigments from that of detritus matter. This study suggests that the 4^{th} derivative analysis appears to be efficient and simple tool for monitoring phytoplankton pigment.

The results obtained support that diatoms are the dominant phytoplankton group in Southeastern Arabian Sea. Phytoplankton communities

are highly varying during the study period. Using fourth derivative plots of *in vivo* phytoplankton absorption spectra, ($d^4 a_{ph}(\lambda)$), it is possible to identify several maxima absorption values attributed to different pigments which can be further used for the study of the factors affecting the variation in phytoplankton absorption spectrum to develop regional algorithm suitable for this region for various remote sensing applications like prediction of harmful algal blooms.

Seasonal fresh water influenced coastal waters such as the SEAS are highly dynamic regions where the use of global ocean color algorithms may not be appropriate for accurate retrieval of bio-optical variables such as phytoplankton biomass. In developing local ocean colour remote sensing algorithms or parameterizations of bio-optical models, there is a need to understand the processes and mechanisms that influence the ocean color or the remote sensing signal. This study put forward background information for the spectral variability of the remote sensing reflectance and attenuation coefficient in the SEAS.

The study alsofocused on the effect of OAS and atmospheric correction schemes on retrieval of spectral Rrs and chl-a from MODIS data. The variability of OASs in the study area was attributed to coastal upwelling and freshwater discharge, especially during the southwest monsoon. Chl-a was the major light-absorbing component in the study area. The distribution of OASs was highly variable, with maxima during the southwest monsoon. The average value of aCDOM440 was found to be on the lower side of the global mean. A significant negative relationship between aCDOM440 and salinity during the southwest monsoon indicates that much of the CDOM during this season was from river discharge. The spectral Rrs was found to be strongly linked to the variability in chl-a concentration. With an increase in chl-a concentration, peak

Rrs was shifted to the longer wavelength. The validation of chl-a, derived from in situ Rrs, showed moderate performance. However, the accuracy of the algorithm was still within acceptable limits. Spectral Rrs derived using the atmospheric correction scheme A1 was found to be in better agreement with in situ results. Further chl-a retrieved using A1 and A2 did not show any significant difference, probably be due to the fact that the study area was dominated by chl-a with lower concentrations of CDOM and TSM. The statistical analysis indicates that the default atmospheric correction scheme (A1) performs better. Furthermore, the variability in Rrs and chl-a retrieved using different atmospheric correction schemes has been fully addressed.

.....ꕥ.....

RESEARCH PAPERS PUBLISHED

Papers Published

1. **Shaju, S. S.**, P. Minu, A. S. Srikanth, P. Muhamed Ashraf, Anil Kumar Vijayan, B. Meenakumari . (2015). Decomposition study of in vivo phytoplankton absorption spectra to identify the pigments and phytoplankton group in complex case 2 waters of coastal Arabian Sea Oceanological and Hydrobiological Studies. Volume 44, Issue 3, Pages 282–293, September 2015. DOI: 10.1515/ohs-2015-0027

2. Ashraf,P. M., **S. S. Shaju**, D. Gayatri, P. Minu, B. Meenakumari. (2013).In Situ Time Series Estimation of Downwelling Diffuse Attenuation Coefficient at Southern Bay of Bengal Journal of the Indian Society of Remote Sensing. 41(3):725–730. DOI 10.1007/s12524-012-0244-1

3. Bhagirathan, U., **Shaju S.S.**, Ragesh N., B. Meenakumari and P. M. Ashraf.(2014). Observations on bio-optical properties of a phytoplankton bloom in coastal waters off Cochin during the onset of southwest monsoon" Journal Indian Journal of Geo-Marine Sciences (IJMS) Vol.43(2) 289-296.

4. Minu P, A. Lotliker, **S.S. Shaju**, B. S. Kumar, P. M. Ashraf, B. Meenakumari. (2014). A paper entitled "Effect of optically active substances and atmospheric correction schemes on remote sensing reflectance at a coastal site off Kochi" authored by published in the International Journal of Remote Sensing Vol. 35, No. 14, 5434–5447, http://dx.doi.org/10.1080/01431161.2014.926420

5. Minu P., **Shaju S. S.**, M. Ashraf P., Meenakumari B. (2014). Phytoplankton community characteristics in the coastal waters of the southeastern Arabian Sea. Acta Oceanolgica Sinica, Vol. 33, No. 12, P. 170–179. DOI: 10.1007/s13131-014-0571-x
6. Minu P. A. Lotliker, **Shaju**, **S.S.** P. M. Ashraf, T. S. Kumar, B. Meenakumari, Performance of operational satellite bio-optical algorithms in different water types in southeastern Arabian Sea. Oceanologia manuscript number OCEANO-D-15-00116.(accepted)
7. Ashamol Antony, T.V. A. Mercy and **Shaju S.S.** (2014). Effect of Rotational Pokkali cultivation and Shrimp farming on the Soil Characteristics of two different Pokkali field at Chellanam and Kadamakudi, Kochi, Kerala, INDIA. International Research Journal of Environment Sciences Vol. 3(9), 61-64.
8. Minu P., S S Shaju, V P Souda, B Usha, P M.Ashraf, B Meenakumari 2015. Hyperspectral Variability of Phytoplankton Blooms in Coastal Waters off Kochi, South-eastern Arabian Sea. Fishery Technolgy Vol 52, 218 – 222

Technical Report Published

1. **Shaju S. S.**, P. Minu, P. M. Ashraf and B. Meenakumari Measurements of Bio-optical Parameters of Southern Ocean. (2011). Southern Ocean Expedition Technical Report 2011, National Centre for Antarctic & Ocean Research (NCAOR). P.34-40.

Symposium and Seminar

1. **Shaju S S.**, Muhamed Ashraf P., Minu P., Archana G., and Meenakuamri B. (2011). Seasonal variation of inherent bio-optical properties of Cochin coastal waters. XXXV Optical Society of India

Symposium on 'Contemporary trends in Optics and Optoelectronics.' 17th to 19th January, 2011 at Indian Institute of Space Science and Technology, Trivandrum

2. **Shaju, S.S.**, Ragesh, N., Usha Bhagirathan, Ashraf, P.M. and B. Meenakumari. (2009). Pre-monsoon Bio-optical Properties of Estuarine and Coastal Waters of Cochin' authored by at National Seminar on Aquatic Chemistry (Aquasem '09) held at Cochin University of Science and Technology (CUSAT) conducted during 26th to 28th March 2009.
3. U. Bhagirathan, **S. S. Shaju**, N. Ragesh , M. Ashraf and B. Meenakumari (2010). 'Bio optical properties of a phytoplankton bloom in the coastal waters off cochin during the onset of the south west monsoon. International Symposium on Remote Sensing & Fisheries (SAFARI). 15th-17th February 2010.
4. Ashraf P. M., **S.S. Shaju**, D. Gayatri, U. Bhagirathan, and B. Meenakumari (2010). In-situ estimation of underwater light field during the northwest monsoon in the Bay of Bengal., International Symposium On Remote Sensing & Fisheries (SAFARI). 15th-17th February 2010.
5. **Shaju S. S.**, U. Bhagirathan, N.Ragesh , M. Ashraf, N. Perur and B. Meenakumari. (2010). A Comparative Study on Pre-Monsoon Inherent Bio optical Properties of Estuarine and Coastal Waters of Cochin. International Symposium on Remote Sensing & Fisheries (SAFARI) conducted during 15th-17th February 2010.
6. Dhiju Das P.H., Minu P., **Shaju S.S.,** kumar B. S., Archan G., P. M. Ashraf, B. Meenakumari, M. Raman. (2012). Seasonal effect of Physico-chemical paramters in distribution of chlorophyll-a concentration in sardine shoal sited areas of South eastern Arabian Sea,

Kerala., Pan Ocean Remote sensing conference - PORSEC 2012. 5 -9 November , 2012.

7. Minu P., **Shaju S.S.**, Muhamed Ashraf P., B. S. kumar, A. Lotliker., Meenakumari B. (2012). Effect of optically active substances and atmospheric correction scheme on remote sensing reflectance at a coastal site off Kochi Pan Ocean Remote sensing conference - PORSEC 2012. 5 -9 November , 2012.

8. **Shaju S.S**., A. Lotliker., S. K. Baliarsingh, P. Minu, P.M. Ashraf and Meenakumari (2015). Long term time-series study on the environmental control on phytoplankton biomass in coastal waters off southeastern Arabian Sea. World Ocean Science Congress 2015. 5-8 February, 2015.

9. Soman A., **S.S.Shaju,** Raman N. N., T. N. Babu and B. Bhaskaran. (2015). Studies on the primary productivity and nutrient abundance at two sites Vembanad and Kumbalm region at Cochin estuary World Ocean Science Congress 2015. 5-8 February, 2015.

10. Minu P, **S.S. Shaju**, G. Archana, P. Muhamed Asharaf, B. Meenukamari. (2011). Studies on effects of Photo synthetically active radiation in Chlorophyll a during Post monsoon season off Cochin waters. National conference on 'Technologies for ocean Exploration' OSICON. 13-15th July 2011.

11. Minu P., **Shaju S.S.**, Souda V.P., P.M. Ashraf, and B. Meenakumari. (2013). Optical properties of phytoplankton bloom observed in coastal waters off Kochi, South Eastern Arabian Sea. National conference on Roll of Ocean in the Earth System - OSICON 13, 26-28 November 2013.

12. Minu P., Souda V.P., **Shaju S.S.**, Mishra R. K., Anilkumar N., P.M. Ashraf, and B. Meenakumari. (2015). Bio-optical studies in the Indian Ocean Sector of Southern Ocean.World Ocean Science Congress 2015. 5-8 February, 2015.

13. **Shaju S.S.**, P Minu, M. Ashraf, N. Menon, A. Samuelsen, B. Meenakumari. (2016). Influence of phytoplankton and abiotic factors on herbivore fishery in the coastal waters off southeastern Arabian Sea. International conference on 'towards a Sustainable Blue Economy: Production, strategies and policies' 2016. 4-6, February 2016.

Oceanological and Hydrobiological Studies

International Journal of Oceanography and Hydrobiology

Volume 44, Issue 3, September 2015
pages (282-293)

ISSN 1730-413X
eISSN 1897-3191

Decomposition study of in vivo phytoplankton absorption spectra aimed at identifying the pigments and the phytoplankton group in complex case 2 coastal waters of the Arabian Sea

by

S. S. Shaju[1], P. Minu[1], A. S. Srikanth[2], P. Muhamed Ashraf[1,*], A. K. Vijayan[3], B. Meenakumari[4]

DOI: 10.1515/ohs-2015-0027
Category: Original research paper
Received: November 20, 2014
Accepted: March 18, 2015

[1]*Fishing Technology Division, Central Institute of Fisheries Technology, Matsyapuri PO, Cochin 682 029, Kerala, India*

[2]*Takuvik Joint UL/CNRS Laboratory, Department of Biology, Laval University, Quebec G1V 0A6, Canada*

[3]*Centre of Marine and Living Resources and Ecology, Ministry of Earth Sciences, Govt. of India, Kendriya Bhavan, Kakkanad, P.B.NO.5415, P.O.CSEZ, Kochi, Kerala-682037, India*

[4]*Indian Council of Agricultural Research, Pusa, New Delhi 110 012, India*

* Corresponding author: *ashrafp2008@gmail.com*

Abstract

Phytoplankton modify the optical properties of the seawater by altering the subsurface light field. Information on the accessory pigments present in the phytoplankton helps to differentiate major phytoplankton classes or taxonomic groups. The variability in the absorption spectra of phytoplankton and particulate matter of case 2 coastal waters of the Southeastern Arabian Sea were studied from June 2010 to November 2011. The phytoplankton specific absorption coefficient, at 440 nm and 675 nm, a^*_{ph} (440) and a^*_{ph} (675) varied from 0.018 to 0.32 m^2 mg^{-1} and from 0.0005 to 0.16 m^2 mg^{-1}, respectively. The 4th derivative spectra computed for each *in vivo* absorption spectrum showed that the amplitude of maxima obtained is proportional to the concentration of the chromoprotein which absorbed that wavelength. Regression of pigment concentration against the 4th derivative spectral coefficient showed that the measurements of particulate absorption could provide quantitative information on chlorophyll *a* and other accessory pigment concentrations. Fucoxanthin and diadinoxanthin, the carotenoid pigments found in the diatoms were identified from the derivatives peaks. The study demonstrates the utility of using the 4th derivative analysis as a tool to identify the dominating phytoplankton group and its pigment composition.

Key words: Total particulate absorption, phytoplankton specific absorption coefficient, packaging effect, derivative analysis

DE GRUYTER

The *Oceanological and Hydrobiological Studies* is online at oandhs.ocean.ug.edu.pl

Acta Oceanol. Sin., 2014, Vol. 33, No. 12, P. 170–179
DOI: 10.1007/s13131-014-0571-x
http://www.hyxb.org.cn
E-mail: hyxbe@263.net

Phytoplankton community characteristics in the coastal waters of the southeastern Arabian Sea

MINU P.[1], SHAJU S. S[1], MUHAMED ASHRAF P.[1]*, MEENAKUMARI B.[2]

[1] Central Institute of Fisheries Technology, Indian Council of Agricultural Research (ICAR), Matsyapuri P.O., Cochin 682029, India
[2] Indian Council of Agricultural Research (ICAR), Krishi Anusandhan Bhavan–II, Pusa, New Delhi 110012, India

Received 3 July 2013; accepted 3 May 2014

Abstract

Remote sensing applications are important in the fisheries sector and efforts were on to improve the predictions of potential fishing zones using ocean color. The present study was aimed to investigate the phytoplankton dynamics and their absorption properties in the coastal waters of the southeastern Arabian Sea in different seasons during the year 2010 to 2011. The region exhibited 73 genera of phytoplankton from 19 orders and 41 families. The numerical abundance of phytoplankton varied from 14.235×10^3 to 55.075×10^6 cells/L. Centric diatoms dominated in the region and the largest family identified was Thalassiosiraceae with main genera as *Skeletonema* spp., *Planktionella* spp. and *Thalassiosira* spp. Annual variations in abundance of phytoplankton showed a typical one-peak cycle, with the highest recorded during premonsoon season and the lowest during monsoon season. The species diversity index of phytoplankton exhibited low diversity during monsoon season. Phytoplankton with pigments Chlorophyll *a*, Chlorophyll *b*, Chlorophyll *c*, peridinin, diadinoxanthin, fucoxanthin, *β*-carotene and phycoerythrobilin dominated in these waters. The knowledge on phytoplankton dynamics in coastal waters of the southeastern Arabian Sea forms a key parameter in bio-optical models of pigments and productivity and for the interpretation of remotely sensed ocean color data.

Key words: phytoplankton, diversity, community structure, ocean color, southeastern Arabian Sea

Citation: Minu P, Shaju S S, Muhamed Ashraf P, Meenakumari B. 2014. Phytoplankton community characteristics in the coastal waters of the southeastern Arabian Sea. Acta Oceanologica Sinica, 33(12): 170–179, doi: 10.1007/s13131-014-0571-x

1 Introduction

The chlorophyll concentration, considered as an indicator of phytoplankton biomass, determines the optically active constituents altering the underwater light field. Hence *in-situ* measurements of phytoplankton and their optical characteristics in the coastal areas can provide the database required to develop bio-optical algorithms useful in retrieving chlorophyll from space (Carder et al., 1991; Tassan, 1994; Le et al., 2011). Chlorophyll *a* (Chl *a*) is the major pigment in phytoplankton which absorbs blue and red light in the visible spectrum and results in the blue-green color of ocean. Also the regional, seasonal and inter-annual variations of the ocean color products and its retrieval depend on the types of dominant phytoplankton that contribute to the ocean color. Hence understanding the variations in phytoplankton community structure helps to know its own inherent optical properties and dynamics of complex coastal waters in which they inhabit, thereby to get a clear idea about the water leaving signal reaching the sensor (IOCCG report No.9). Phytoplankton taxonomic studies provide basic information on the phytoplankton species which can be used in pigment marker studies. The contribution of various marker pigments is used for the development of algorithms to determine the contribution of these pigments to the total Chl *a* concentration.

Few studies have been carried out in the coastal waters off Kochi, in the eastern Arabian Sea to know the phytoplankton community characteristics, even though the Kochi backwaters and Arabian Sea were investigated in detail. Previous studies in the area were mainly focused on physical and chemical characteristics of phytoplankton blooms (Padmakumar et al., 2010, 2012). A latest study on identification of the major phytoplankton confirmed nanoplankton as the major contributor to the total Chl *a* and primary production in the region. Nanoplankton is found to have maximum photosynthetic efficiency in coastal waters (Madhu et al., 2010). The present study examines the phytoplankton community structure, its diversity and the variation in absorption properties in relation to its diversity index.

2 Methodology

The study area is situated between 9°54′28″N, 76°12′47″E and 10°02′37″N, 76°09′15″E which is in the eastern coast of Arabian Sea. The area being in the tropics experiences an annual rainfall of 4000 mm per year and is subjected to seasonally reversing monsoonal wind system, which drives the near surface currents and affects the development of mixed layer, thereby the nutrient availability in the upper water column which favours the phytoplankton growth. Based on these diverse features and prevailing monsoon, three distinct seasons exists in this region-

Foundation item: The Indian National Centre for Ocean Information Services (INCOIS), Ministry of Earth Sciences under Satellite Coastal Oceanographic Research (SATCORE) programme.
*Corresponding author, E-mail: ashrafp2008@gmail.com

International Journal of Remote Sensing, 2014
Vol. 35, No. 14, 5434–5447, http://dx.doi.org/10.1080/01431161.2014.926420

Taylor & Francis
Taylor & Francis Group

Effect of optically active substances and atmospheric correction schemes on remote-sensing reflectance at a coastal site off Kochi

P. Minu[a], Aneesh A. Lotliker[b]*, S. S. Shaju[a], B. SanthoshKumar[a], P. Muhamed Ashraf[a], and B. Meenakumari[c]

[a]*Central Institute of Fisheries Technology, ICAR, Kochi 682 029, India;* [b]*Indian National Centre for Ocean Information Services (INCOIS), Hyderabad 500 090, India;* [c]*Indian Council of Agricultural Research (ICAR), New Delhi 110 012, India*

(*Received 15 January 2013; accepted 9 January 2014*)

The present study focused on understanding the variability of optically active substances (OASs) and their effect on spectral remote-sensing reflectance (R_{rs}). Furthermore, the effect of atmospheric correction schemes on the retrieval of chlorophyll-*a* (chl-*a*) from satellite data was also analysed. The OASs considered here are chl-*a*, coloured dissolved organic matter (CDOM), and total suspended matter (TSM). Satellite data from the Moderate Resolution Imaging Spectroradiometer (MODIS) on the Aqua satellite was used for this study. The two atmospheric correction schemes considered were: multi-scattering with two-band model selection NIR correction (hereon referred as 'A1') and Management Unit of the North Sea Mathematical Models (MUMM) correction and MUMM NIR calculation (hereafter referred as 'A2'). The default MODIS bio-optical algorithm (OC3M) was used for the retrieval of chl-*a*. Analysis of OASs showed that chl-*a* was the major light-absorbing component, with highly variable distribution (0.006–25.85 mg m^{-3}). Absorption due to CDOM at 440 nm ($a_{CDOM}440$) varied from 0.002 to 0.31 m^{-1} whereas TSM varied from 0.005 to 33.44 mg l^{-1}. The highest concentration of chl-*a* was observed from August to November (i.e. end of the southwest monsoon and beginning of the northeast monsoon), which was attributed to coastal upwelling. The average value of $a_{CDOM}440$ was found to be lower than the global mean. A significant negative relationship between $a_{CDOM}440$ and salinity during the southwest monsoon indicated that much of the CDOM during this season was derived from river discharge. Spectral R_{rs} was found to be strongly linked to the variability in chl-*a* concentration, indicating that chl-*a* was the major light-absorbing component. Satellite-derived spectral R_{rs} was in good agreement with that *in situ* when chl-*a* concentration was lower than 5 mg m^{-3}. The validation of chl-*a*, derived from *in situ* R_{rs}, showed moderate performance (correlation coefficient, R^2 = 0.64; $\log_{10}$(RMSE) = 0.434; absolute percentage difference (APD) = 43.6% and relative percentage difference (RPD) = 42.33%). However the accuracy of the algorithm was still within acceptable limits. The statistical analysis for atmospheric correction schemes showed improved mean ratio of measured to estimated chl-*a* ('*r*' = 1.6), $\log_{10}$(RMSE) (0.49), APD (25.46%), and RPD (17.57%) in the case of A1 as compared with A2, whereas in the case of A2, R^2 (0.56), slope (0.26), and intercept (0.27) were better as compared with A1. The two atmospheric correction schemes did not show any significant statistical difference. However the default atmospheric correction scheme (A1) was found to be performing comparatively better probably due to the fact that the concentration of TSM and CDOM was much lower to overcome the impact of chl-*a*.

*Corresponding author. Email: aneesh@incois.gov.in

Indian Journal of Geo-Marine Sciences
Vol. 43(2), February 2014, pp. 289-296

Observations on bio-optical properties of a phytoplankton bloom in coastal waters off Cochin during the onset of southwest monsoon

Usha Bhagirathan*, Shaju S.S., Ragesh N., Meenakumari B.[1] & Muhamed Ashraf,P.

Central Institute of Fisheries Technology (ICAR), Matsyapuri P.O., Kochi- 682 029, India

[E-mail: ushasreenath@yahoo.co.in]

Received 3 April 2013; revised 30 May 2013

A phytoplankton bloom dominated by *Chaetoceros* spp. was detected in the Arabian Sea, off Cochin coast during May 2009 coinciding the onset of southwest monsoon with an average chlorophyll *a* concentration of 8.42 mg m^{-3} at four stations (A, C, D & E) of total 7 stations studied in coastal waters situated between latitudes 9°54'-10°02' N and longitudes 76°05'-76°12' E. All the stations were resampled after seven days and found that the average chlorophyll *a* concentration at the bloom stations has decreased to 2.91 mg m^{-3}. The inherent optical properties (chlorophyll *a*, specific phytoplankton absorption coefficient, chlorophyll scattering coefficient) of water were analyzed from the study area. The physico-chemical parameters like dissolved oxygen, pH, turbidity and nutrients were estimated for surface waters in these stations using standard methods. The phytoplankton of the study area was identified and their density was recorded. The phytoplankton community composed primarily of diatom *Chaetoceros* sp. in all the stations, with a percentage composition greater than 55 at the bloom. The highest phytoplankton density recorded was 4,89,578 cell no./l at station D. Samples from the bloom showed higher specific phytoplankton absorption coefficient [$a^*_c(\lambda)$] than other stations. $a^*_c(435)$ varied from 4.11 to 5.68 m^2mg^{-1} and a^*_c (665) from 1.45 to 1.80 m^2mg^{-1}. A survey on purse seine fishery showed a higher pelagic catch in close proximity to the bloom area during this period. Further investigation of absorption properties of blooms using remote sensing at complex case II waters is needed to interpret bio-optical properties as well as fisheries. The present study is the first attempt of this kind off Cochin coast.

Keywords: bloom, phytoplankton, specific absorption coefficient, Cochin coast

Introduction

The phytoplankton blooms are incidence of proliferation of microalgae in an aquatic environment. They can be quick events that begin and end within a few days or they may stay for several weeks; they can occur on a relatively small scale or cover hundreds of square kilometres of the ocean's surface[1]. Blooms are events of rapid production and accumulation of phytoplankton biomass that are usually responses to changing physical forcing originating in the coastal ocean (tides), the atmosphere (wind) or on the land surface (precipitation and river runoff)[2]. The excessive growth of an alga during a bloom usually causes water discolouration, depending on the predominant species.

The Arabian Sea is highly influenced by monsoon systems like south west monsoon (June – September) and north east monsoon (December-February). This affects availability of nutrients, distribution pattern of phytoplankton and also the fishery along the coast of India. The reports of algal blooms indicate their predominance along the west coast of India especially the southern part[3]. Several studies have reported the occurrence of phytoplankton bloom along Kerala coast[3,4,5,6]. Event of blooms along Cochin coast is also very prevalent[7,8,9]. The influence of bloom on the fishery of Kerala coast has been studied[5,10].

The present study reports observations and findings of an algal bloom observed during May 2009 in the Arabian sea, off Cochin coast. Analysis of *in-situ* water column measurements contributes to our knowledge of the optical characteristics of the phytoplankton community involved. The possible effect of bloom on pelagic fishery of the close by area has been studied.

*Corresponding author Email: ushasreenath@yahoo.co.in (Usha Bhagirathan)
[1]Indian Council of Agricultural Research (ICAR), Krishi Anusandhan Bhawan- II, New Delhi – 110 012, India

J Indian Soc Remote Sens (September 2013) 41(3):725–730
DOI 10.1007/s12524-012-0244-1

SHORT NOTE

ISRS

In Situ Time Series Estimation of Downwelling Diffuse Attenuation Coefficient at Southern Bay of Bengal

P. Muhamed Ashraf · S. S. Shaju · D. Gayatri · P. Minu · B. Meenakumari

Received: 8 July 2012 / Accepted: 17 October 2012 / Published online: 27 November 2012

Abstract The present study is aimed to determine the bio-optical characteristics of oceanic waters during South west monsoon in Bay of Bengal using hyperspectral radiometer. The variability of diffuse attenuation coefficient, $K_d(\lambda)$, with chlorophyll *a* showed a good relation at shorter wavelengths, indicating the effect of phytoplankton on $K_d(\lambda)$. The determination coefficient, R^2 at 412, 443, 490 and 555 nm were greater than 0.931. A good linear relation between $K_d(490)$ and $K_d(\lambda)$ was observed at shorter wavelengths. These relationships of $K_d(\lambda)$ provides a platform to study the underwater light field during Southwest monsoon in Bay of Bengal.

Keywords Diffuse attenuation coefficient · Chlorophyll *a* · Photosynthetically active radiation · Tropical convergence zone · Bay of Bengal

P. M. Ashraf (✉) · S. S. Shaju · P. Minu
Central Institute of Fisheries Technology,
Matsyapuri P.O,
Cochin 682 029 Kerala, India
e-mail: ashrafp2008@gmail.com

D. Gayatri
Indian National Centre for Ocean Information Services,
Hyderabad, India

B. Meenakumari
Indian Council for Agricultural Research,
New Delhi, India

Introduction

During South-west monsoon, the west India coastal current merges with the eastward flowing Equatorial Counter Current and the part of this whole eastward flowing South-west Monsoon Current, flows northward into Bay of Bengal. This region experiences very turbulent environment with higher levels of waves and winds because of the Inter Tropical Convergence Zone located over the warmest surface waters that are associated with eastward oceanic currents (Philander et al. 1995; Pickard and Emery 2003; Francis and Gadgil 2010).

Inside and outside of the intercontinental tropical convergence zone, the fluxes of heat, moisture, momentum and radiation through the surface of the ocean and in the atmosphere itself differ dramatically and the absorption properties of the water column have significance. One of the important water column property to study the characteristics of the water and light availability is diffuse attenuation coefficient for downwelling irradiance, $K_d(\lambda)$. It is a quasi apparent optical property, that is influenced by the angular distribution of light field as well as the nature and quantity of substances present in the medium, is of particular interest because it quantifies the presence of light, the nature of particles present in it and the depth of the euphotic zone. K_d is an indicator of the penetrating component of solar radiation. For most waters $K_d(\lambda)$ is largely determined by absorption

International Research Journal of Environment Sciences ISSN 2319–1414
Vol. **3(9),** 61-64, September **(2014)** *Int. Res. J. Environment Sci.*

Effect of Rotational Pokkali cultivation and Shrimp farming on the Soil Characteristics of two different Pokkali field at Chellanam and Kadamakudi, Kochi, Kerala, INDIA

Ashamol Antony, T.V.Anna Mercy and Shaju S.S.
Kerala University of Fisheries and Ocean Studies, Kochi – 682506, Kerala, INDIA

Available online at: www.isca.in, www.isca.me
Received 19th July 2014, revised 30th August 2014, accepted 19th September 2014

Abstract

Pokkali field is prevalent in the coastal saline tracts of Kerala. Pokkali fields are able to produce paddy and shrimp rotationally in an organic way. The sediment characteristics were studied in two Pokkali fields, Chellanam and Kadamakudi, Ernakulam District, Kerala, India during April to June 2013. The soil pH varied highly acidic to7.15 slightly alkaline in Chellanam and alkaline in Kadamakudi. The least value of conductivity and salinity were occurred on the first half of the June.The highest value of total organic carbon was 1.05%in Chellanam and 6.225% in Kadamakudi observed on the second half of April. The highest value of phosphate was 0.1578 mg/g in Chellanam and 0.2125 mg/g in Kadamakudi with a mean and standard deviation of 6.87 ± 7.67 and 0.14 ± 0.05 respectively on the first half of the May. The nitrogen content of the soil also showed the same trend as phosphate. The carbon content of the soil showed a slight increasing trend. The sulphur content of the soil is negligible except last half of may showed 0.18% . In Chellanam and Kadamakudi, the sulphur content of the soil showed a decreasing trend from April to June.C – N ratio was in the range of 6.3: 1 to 8.1: 1. C- N ratio in Chellanam and in Kadamakudi was in the range of 9: 1 to 10.2: 1. The sediment characteristics in this area was completely depends on the south west monsoon and the tides of the Vembanad estuary.

Keywords: Pokkali, soil conductivity, pH nitrogen, phosphate, sulphur, carbon nitrogen ratio.

Introduction

The Vembanad wetland complex provide a means of livelihoods for local who are dependent on fishing and related industries, an important tourist destination and also supports an agricultural system including the 'rice bowl of Kerala'[1]. A variety of rice which are salt resistant locally called Pokkali are cultivated in the coastal regions of Ernakulam, Alappuzha and Thrissur districts of Kerala state, India has been upgraded into the the status of registered Geographical Indication (GI) by the Geographical Indications Registry Office, Chennai, Tamil Nadu[2]. The pokkali fields adjacent to the Vembanad lake below sea level and having acid saline soils[3]. Traditionally natural available prawns and fish seeds collected by trapping of natural saline waters from the Vembanad estuary, which enters to the field during the high tides is collected for the farming on a seasonal basis are traditionally known as pokkali fields. It is a unique ecosystem situated adjacent to Vembanad lake having with rich biodiversity and capacity to produce rotational paddy and shrimp organically[2]. It is a classic example of sustainable agri – aqua integration providing a means of rural livelihood. The rice seedling grows in the natural way without addition of any fertilizers. These fields are waterlogged throughout the year. The crop that can grow upto 2m can survive in this area[4]. The rice produced from this area is purely organic[5]. In Kerala, traditional and extensive shrimp culture is in practice and the total area under traditional farming system is 12,986.6 ha, of which 84% is under *pokkali* fields[6]. There are about 4000 hectares of paddy fields under pokkali cultivation in Ernakulam district, while in Alappuzha and Thrissur the extent of paddy cultivation is in about 3000 hectares and 2000 hectare respectively[2]. The Pokkali fields of Kerala has been declining from 25,000 hectares to 9000 hectares[3]. The Pokkali fields which are marshy situated close to the sea and the mouth of the rivers. Therefore, they are prone to flooding and salinity. The successful growth, propagation, survival, reproduction and harvest of shrimps are heavily dependent upon the quality of the field soil and water, degradation of which often limits the production in aquaculture systems[7,8]. Keeping in view, the benefits of farm organic agriculture and shrimp farming and also the declining of pokkali farms, a study was taken to estimate the soil quality parameters after shrimp farming and before pokkali farming.

Material and Methods

Study area: The coastal saline soils along the Ernakulam district are referred to as *pokkali* fields. The traditional paddy cultivation involving a salt-resistant and tall *pokkali* variety of paddy, which used to cultivate from May-June to September-October is followed by shrimp filtration[9]. According to Pillai[10] during high tides, the water entered into the pokkali fields through the sluice in twice daily. During night, the mouth of the sluice was fitted with bulbs/ hurricanes/ petromaxes etc for

Fishery Technology 52 (2015) : 218 - 222

Hyperspectral Variability of Phytoplankton Blooms in Coastal Waters off Kochi, South-eastern Arabian Sea

P. Minu[1], S. S. Shaju[1, 3], V. P. Souda[1], B. Usha[1,4], P. Muhamed Ashraf[1]* and B. Meenakumari[2]
[1] *ICAR- Central Institute of Fisheries Technology, P. O. Matsyapuri, Cochin - 682 029, India*
[2] *Indian Council of Agricultural Research (ICAR), Krishi Anusandhan Bhavan–II, Pusa, New Delhi - 110 012*

Abstract

Ocean colour radiometry offers cost-effective, frequently acquired synoptic data pertaining to phytoplankton biomass in surface waters and is of considerable value in monitoring and better understanding of algal blooms. Algal blooms have occur frequently in coastal waters resulting in severe negative impacts to local marine ecosystems and communities. Remote sensing reflectance [$R_{rs}(\lambda)$] and absorption coefficients of phytoplankton blooms were measured in coastal waters off Kochi, South-eastern Arabian Sea, to investigate differences in the absorption and reflectance of different types of blooms. Peaks of the $R_{rs}(\lambda)$ spectra of *Trichodesmium* spp. bloom were at 490 nm, while those of non-bloom areas were 482, 560 and 570 nm. The absorption maximam of phytoplankton were at 435, 437, 438 and 439 nm in the blue region and 632, 674, 675 and 635 nm in the red region respectively for *Trichodesmium* spp., *Chaetoceros* spp., *Dinophysis* spp. and *Prorocentrum* spp. blooms. The study showed that the variation of $a_{ph}(\lambda)$ with Chl a dominates the behavior of the $R_{rs}(\lambda)$ peak in these blooms.

Keywords: Phytoplankton absorption, remote sensing reflectance, bloom, bio-optics, Arabian Sea

Introduction

Marine phytoplankton influences the thermodynamic processes by air-sea exchange of gases like carbon dioxide and inorganic sulfur compounds affecting the global climate system. There is an increase in the frequency of occurrence of harmful algal blooms (HABs) worldwide (León et al., 2006). Blooms are caused by changes in tide patterns, wind direction and speed, precipitation and river runoff (Cloern, 1996). The reversal of monsoon winds and increase in anthropogenic enrichment and eutrophication has led to increased number of harmful algal blooms (Dwivedi et al., 2006; Padmakumar et al., 2010). Diatom or dinoflagellate blooms in coastal waters are usually caused by upwelling (Padmakumar et al., 2010). The necessity for close monitoring of hydrology of the west coast of India was pointed out, but *in-situ* data of apparent and inherent optical properties of blooms in the Arabian Sea is limited (Usha et al., 2013). Hydrology along with the inherent and apparent optical properties of phytoplankton blooms can be used as an effective tool in detecting HABs from space. This is a preliminary study which measured the apparent and inherent optical properties of four phytoplankton blooms observed off Kochi, south-west coast of India with an objective to determine the variation in absorption properties of different bloom causing phytoplankton.

Received 14 August 2015; Revised 25 September 2015; Accepted 03 October 2015

* *E-mail: ashrafp2008@gmail.com*

[3] *Present Address: NansenEnvoronmental Research Centre (India,) 6A, Oxford Business Centre (6th Floor) Sreekandath Road, Ravipuram, Cochin - 682 016, India*

[4] *Present Address: Department of Zoology, Sree Kerala Varma College, P.O. Kanattukara, Thrissur - 680 01, India*

Materials and Methods

Data was measured for three different blooms along latitudes 10°00'02"N, 10°02'58"N and 9°56'256"N and longitudes 76°06'05"E, 76°09'15"E and 75°52'216"E respectively during May 2009, August 2010, December 2010 and March 2011 (Fig. 1). During August 2010 and December 2010, blooms occurred in the same location. Surface sea water samples from the bloom sites were collected onboard using Niskin plastic water sampler Hydro-Bios™ of 2.5L capacity. Samples were stored in clean polyethylene bottles in ice and transported to laboratory for further analysis. The samples were